SYNTHESIS, PHOTO- AND ELECTRO- OPTICAL PROPERTIES OF LUMINESCENT π-CONJUGATED POLYMERS

by

George Vamvounis

B.Sc. (Hons.), St. Francis Xavier University, 1998

THESIS SUBMITTED IN PARTIAL FULFILLMENT OF
THE REQUIREMENTS FOR THE DEGREE OF

DOCTOR OF PHILOSOPHY

in the Department

of

Chemistry

SIMON FRASER UNIVERSITY

Fall 2004

APPROVAL

Name: George Vamvounis

Degree: Doctor of Philosophy

Title of Thesis: Synthesis, Photo- and Electro- Optical Properties of Luminescent π-Conjugated Polymers

Examining Committee:

Chair: Dr. N.R. Branda (Professor)

Dr. S. Holdcroft (Professor)
Senior Supervisor

Dr. G.W. Leach (Associate Professor)
Committee Member

Dr. P.D. Wilson (Assistant Professor)
Committee Member

Dr. V.E. Williams (Assistant Professor)
Internal Examiner

Dr. David M. Collard (Professor)
External Examiner
Chemistry and Biochemistry Department
Georgia Institute of Technology

Date Approved: NOV 3. 2004

SIMON FRASER UNIVERSITY

Partial Copyright Licence

Abstract

The focus of this work is the synthesis, structure, and luminescent properties of π-conjugated polymers. The polymer properties may be tailored with various functional groups, resulting in an increase of emission efficiency and colour tunability. These polymers are important since polymer light emitting diodes (PLEDs) may be used in the production of next generation displays. For this reason, it is important understand the structure-property relationships of luminescent π-conjugated polymers, and their spatial controlled deposition.

Three classes of luminescent π-conjugated polymers are investigated herein – poly(3-alkylthiophene)s (P3ATs), poly(phenylenevinylene) (PPVs), and poly(fluorene-*co*-thiophene) (PFTs). Their structure-property relationships were studied by post-functionalization and host-guest type methodologies.

Post-functionalization - via electrophilic aromatic substitution - of P3AT and PPV was efficient, and provided a precise method to control the effective conjugation length. Further post-functionalization of the P3AT system *via* Pd-catalyzed cross coupling proved effective for obtaining a plethora of 3,4-disubstituted P3ATs. It was found that sterically encumbered groups increased the luminescence efficiency by increasing the interlayer distance between the polymer chains.

Alternating poly(fluorene-*co*-thiophene)s were prepared with 2,5-, 2,4- and 3,4-thiophene linkages. The type of thiophene linkage had a dramatic effect on the emission colour - from UV emitting to green – while little effect was observed for the emission efficiency. Since the strong spectral overlap between the

emission of the 3,4-linked PFT with the absorption of 2,5-linked PFT, and the molecular similarity, host-guest systems *via* blending and copolymerization was investigated. In an effort to obtain high energy emission, a PFT with 2,7-linked fluorene as the guest in a 3,4-linked PFT host were also investigated.

Tetrahydropyan (THP) bearing conjugated polymers have proven useful for obtaining spatial controlled deposition. Since these polymers are important for high resolution displays, the photo-physics of these polymers were investigated. Two classes of THP-containing conjugated polymers were studied; namely, P3ATs and PFTs. For P3ATs, it was found that shorter alkyl chain spacers enhanced the emission efficiency and tuned the emission colour. Upon thermolytic cleavage of the THP group, the luminescence efficiency decreased dramatically. Since PFTs are inherently more luminescent than P3ATs, PFTs bearing THP-groups were also investigated.

Dedication

For my parents and family who encouraged and supported me throughout my studies

Acknowledgments

To: Dr. Steven Holdcroft, my senior supervisor, who gave me his supervision, endless patience, words of wisdom, scientific freedom, many research assistantships, and the opportunity to work in his laboratory.

My committee members: Drs. Gary Leach and Peter Wilson who have helped me many times beyond the call of duty, and my examining committee, Drs. David Collard and Vance Williams, for taking the time to read my thesis.

Drs. Yuning Li and Jianfei Yu, who have provided polymer samples and shared my excitement towards science as well as for interesting discussions.

Drs. Hany Aziz and Zoran Popovic, for an excellent adventure into LED device fabrication and testing.

Xerox Research Centre of Canada for funding my NSERC industrial fellowship and for the use of their LED device fabrication equipment.

My proof readers: Ms. Ana Siu, Mr. Frank Orfino, Ms. Gisela Schulz, Dr. Jimmy Lowe, Mr. Terry Gordon and Mr. Jusroop Mattu for their timely and constructive criticisms.

Past and current group members who have taught me many lifelong skills and cultural capital. It has been a great adventure!

Natural Science and Engineering Research Council (NSERC) for funding my industrial fellowship.

Table of Contents

List of Figures

List of Schemes

List of Tables

List of Abbreviations

COD	1,3-Cyclooctadiene
3-HT	3-Hexylthiophene
Alq_3	Tris(8-hydoxyquinoline)aluminum
Ar-PHT	Poly(3-aryl-4-hexyl-thiophene)
Br-PHT	Poly(3-bromo-4-hexyl-thiophene)
CIE	Commission internationale de l'eclairage
Cl-PHT	Poly(3-chloro-4-hexylthiophene)
DCJTB	4-(Dicyanomethylene)-2-tert-butyl-6-(1,1,7,7-tetramethyljulolidyl-9-enyl)-4H-pyran
DHF	Dihexylfluorene
DHO-PPV	Poly(p-2,5-dihexylox-phenlenevinyelene)
dppe	Diphenylphosphinoethane
dppp	Diphenylphosphinopropane
EL	Electroluminescence
FETs	Field effect transistors
GPC	Gel permeation chromatography
GRIM	Grignard metathesis
HOMO	Highest occupied molecular orbital
ITO	Indium-tin oxide
LDA	Lithium diisopropylamine
LEDs	Light emitting diodes
LPPP	Ladder-type poly(*p*-phenylene)
LUMO	Lowest unoccupied molecular orbital
NBS	*N*-bromosuccinimide
NCS	*N*-chlorosuccinimide

NMR	Nuclear magnetic resonance
OLEDs	Molecular light emitting diodes
P3HT	Poly(3-hexylthiophene)
PA	Poly(acetylene)
PAF	Poly(9,9-dialkylfluorene)
PAPV	Poly(2,5-dialkoxy-1,4-phenylenevinylene)s
PATs	Poly(3-alkylthiophene)s
PDHF	Poly(9,9-dihexylfluorene)
PEDOT	Poly-3,4-ethylenedioxythiophene polystyrenesulfonate
PF	Poly(fluorene)
PFT	Poly(fluorene-*co*-thiophene)
PFT-C_{11}THP	Poly(9,9-dihexylfluorene-alt-3-(11-(2-tetrahydropyranyloxy)undecyl)thiophene)
PFT-C_2THP	Poly(9,9-dihexylfluorene-alt-2-(2-thiophene-3-ethoxy)tetrahydropyran)
PFT-HT	Poly(9,9-dihexyfluorene-alt-3-hexylthiophene)
PFTT	Poly(9,9-dihexylfluorene-alt-2,2'-bithiophene)
PFT-THP-HG	Poly(9,9-dihexylfluorene-alt-2-(2-thiophen-3-ethoxy)tetrahydropyran)-co-(9,9-dihexylfluorene-alt-bithiophene)
PFT-THP-HG-D	Deprotected poly(9,9-dihexylfluorene-alt-2-(2-thiophen-3-ethoxy)tetrahydropyran)-co-(9,9-dihexylfluorene-alt-bithiophene)
PL	Photoluminescence
PLEDs	Polymer light emitting diodes
PMMA	Poly(methylmethacrylate)
PPDB	poly(perylene-*co*-diethynylbenzene)
PPh_3	Triphenylphosphine
PPP	Poly(*p*-phenylene)
PPV	Poly(*p*-phenylenevinylene)

PPy	Poly(pyrrole)
PT	Poly(thiophene)
PTFE	Poly(tetrafluoroethylene)
PTHPET	Poly[3-(2-(2-tetrahydropyranyloxy)ethyl)thiophene)]
PTHPUDT	Poly[3-(11-(2-tetrahydropyranyloxy)undecyl)thiophene]
RGB	Red, green, blue
TGA	Thermal gravimetric analysis
THP	Tetrahydropyran
TPT	Triphenyltriazine
UV-vis	Ultraviolet - visible

Chapter 1.

Synthesis and Properties of Conjugated Polymers

1.1 Overview of π-conjugated polymers

Conjugated polymers are macromolecules that possess alternating single and double bonds along the main chain. Some common conjugated polymers are poly(acetylene) (PA), poly(thiophene) (PT), poly(pyrrole) (PPy), poly(*p*-phenylene) (PPP), poly(*p*-phenylenevinylene) (PPV) and poly(fluorene) (PF), which are illustrated in Figure 1.1.

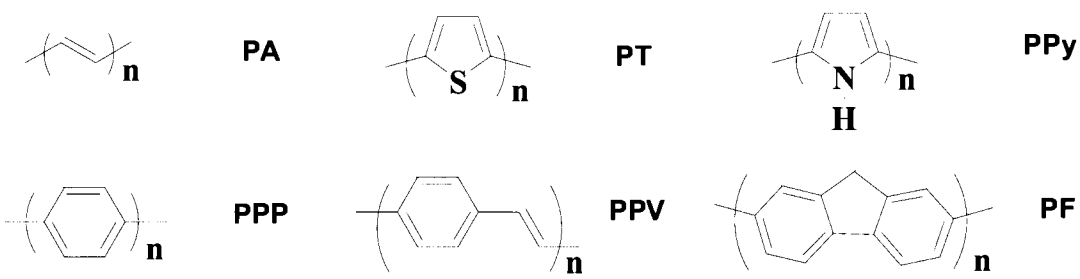

Figure 1.1: Structures of several common conjugated polymers

The potential use of conjugated polymers in electronic devices was realized in the late 1970s when electrically conductive polymers were discovered; i.e. PA doped with iodine.[1] In recognition of this extraordinary discovery, the scientists (Shirakawa, MacDiramid, and Heeger) were jointly awarded the 2000 Nobel Prize in Chemistry.

Many conjugated polymers that were studied in the early 1980s were based on heterocyclic compounds which were synthesized using chemical and electrochemical means.[2-3] Chemically synthesized conjugated polymers resulted in powders which were insoluble and uncharacterizable using conventional analytical techniques.[2] The primary interest in these powders was their electrical conductivity and their corresponding electronic structure. Alternatively,

electrochemical synthesis of conjugated polymers was a more attractive approach because films were formed on the electrode.[3] Significant research on these polymer films was therefore performed to understand their spectro-electrochemical properties. In the mid 1980s, Elsenbaumer reported the ground-breaking synthesis of soluble conjugated polymers by attaching an alkyl side chain on PT. The solubility of the polymers allowed structural characterization and polymer processing using spin or drop cast methods.[4-5]

To date, a surge of research on soluble conjugated polymers has been performed, due to their potential use as components in electronic applications, such as field effect transistors (FETs),[6] light emitting diodes (LEDs),[7] actuators,[8] and solar cells.[9] The development of these soluble conjugated polymers has lead to significant improvement in their properties, including their high electrical conductivity (up to 2000 S/cm),[10] high field effect mobility (~0.12 $cm^2 V^{-1} s^{-1}$) with excellent on/off ratios in FETs (10^7),[6f] high solid state photoluminescent[11] and LED[7e] efficiencies (10% photons/electrons, external), and significant solar energy conversion efficiencies (4.2%).[9b]

1.2 Polymer Light Emitting Diodes

Polymer light emitting diodes (PLEDs) are excellent candidates in the next generation of portable displays. The advantages of these devices include mechanical flexibility, high brightness, viewing angle independence, fast video response, low operating voltage, simple device structures, and ultra thin architectures.

LEDs fabricated with a light emitting polymer were first reported by

Partridge in 1983 with the use of poly(vinylcarbazole).[7f] These devices were inefficient, required high voltages, and had a low operational lifetime. For these reasons, there was minimal research in this field since the devices could not compete with incandescent lights and inorganic LEDs. In 1989, efficient light emission from PPV based polymers was discovered at Cambridge University.[7g] This discovery was pivotal and lead to a flash flood of research on the design and synthesis of new polymers for use as potential "plastic" displays. The three primary classes of conjugated polymers commonly used in PLEDs are PPVs, PFs, and PTs.

1.3 Synthesis of Conjugated Polymers

The first challenge in studying conjugated polymers is their synthesis. The two methods for obtaining conjugated polymers are by electrochemical and chemical polymerization means. Electrochemical polymerization is usually carried out in oxidative anodic conditions and yields a polymer film.[12] This method allows a facile route to prepare conducting polymers but yields a limited amount of the desired polymer and, as a consequence, chemical synthesis appears more desirable. There are several chemical synthesis approaches to obtain luminescent conjugated polymers, and they will be highlighted in the next section.

1.3.1 Chemical Synthesis of Luminescent Conjugated Polymers

1.3.1.1 Oxidative Coupling

Oxidative coupling is a straightforward and versatile method to synthesize conjugated polymers. It was developed by Yoshino and co-workers[13] to synthesize poly(9,9-dialkylflourene)s (PAFs)[13a] and poly(3-alkylthiophene)s (PATs).[13b] In this method, the monomer is dissolved and oxidatively polymerized with $FeCl_3$. Ferric chloride oxidizes the 3-alkylthiophene monomer to produce radical cations with spin-density, predominantly in the 2 and 5- positions of the thiophene, which then couple to form a polymer. This procedure yields polymers with reasonably high molecular weights; however, they contain many structural defects that may lead to undesirable properties.[14a] It has been reported that these defects can be minimized by performing the reactions at lower temperatures or by using vanadium based oxidants.[14b-c] However, the inability to completely remove the oxidant from the final product can still dramatically influence its performance in devices such as FETs[15a] and LEDs.[15b]

1.3.1.2 Yamamoto Coupling

The Yamamoto coupling method, shown in Scheme 1.1, is an effective route to synthesize conjugated polymers. This route has been successful in polymerizing several classes of conjugated polymers which include thiophene, fluorene, thiazole and phenylene. The use of a large quantity of $Ni(COD)_2$ (COD = 1,3-cyclooctadiene) and the instability of the nickel complex, however, makes

this reaction undesirable.

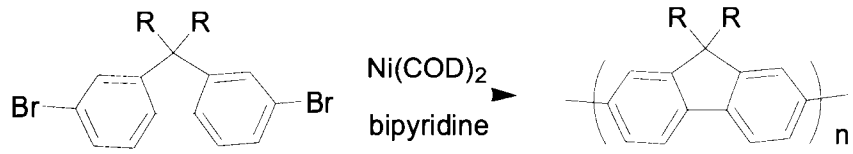

Scheme 1.1: Synthesis of poly(9,9-dialkylfluorene) via Yamamoto coupling

1.3.1.3 Metal-Catalyzed Cross Coupling

Metal-catalyzed cross coupling has been proven a versatile route to synthesize conjugated polymers. The catalyzed reaction mechanisms are essentially the same regardless of the reaction type, and follows three key steps: (i) oxidative addition of an aryl halide to the metal catalyst, (ii) transmetallation between the aforementioned catalyst complex and the organometallic reagent to form a diorganometallic, (iii) reductive elimination to give an aryl-aryl bond and a regenerated catalyst, as illustrated in Scheme 1.2. The use of this method - with several different catalysts - is discussed in the next subsection.

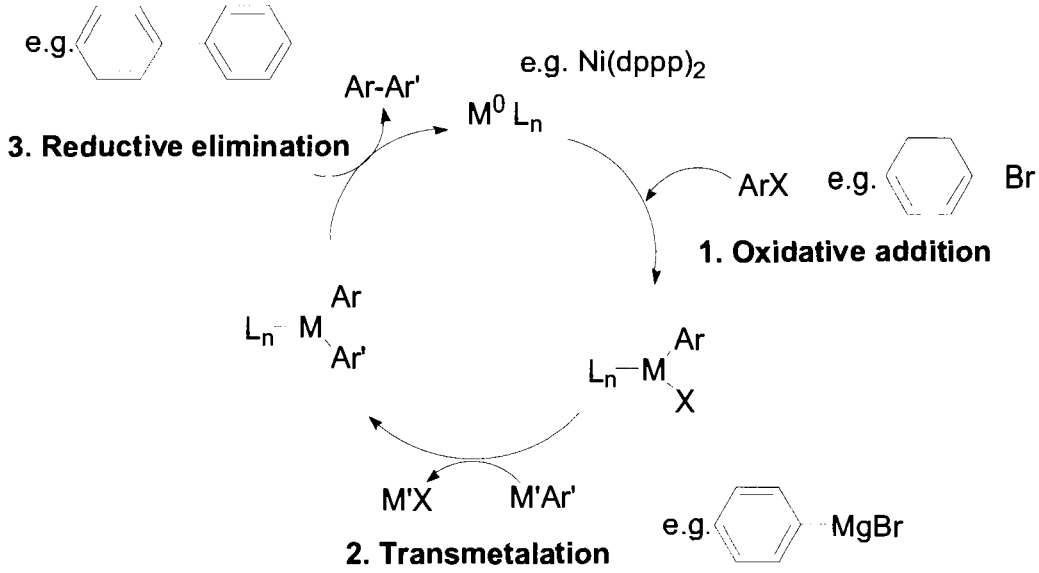

Scheme 1.2: Metal-catalyzed cross coupling mechanism

1.3.1.3.1 Kumada Coupling

Kumada cross coupling, illustrated in Scheme 1.3, was first used to prepare soluble and processable poly(3-alkylthiophene)s (when alkyl chains are greater than propyl) by Elsenbaumer and co-workers.[4] In this method, 2,5-diiodo-3-alkylthiophene was treated with one mole equivalent of magnesium to form the Grignard species. When $Ni(dppp)Br_2$ (dppp = diphenylphosphinopropane) catalyst was introduced, a polymer formed.

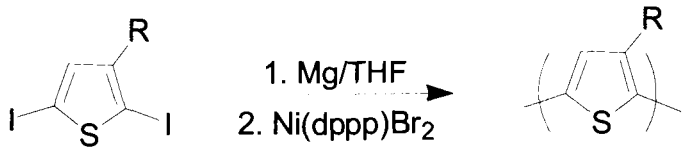

Scheme 1.3: Grignard synthesis of poly(3-alkylthiophene)

Since poly(3-alkylthiophene)s are non-centrosymmetric, regio-regularity is a factor. PATs may couple as: head-to-head, head-to-tail, and tail-to-tail; as illustrated in Figure 1.2. These linkages have a pronounced effect on their

properties and will be discussed in Section 1.4. The PATs synthesized by Elsenbaumer and co-workers were regio-random.[4]

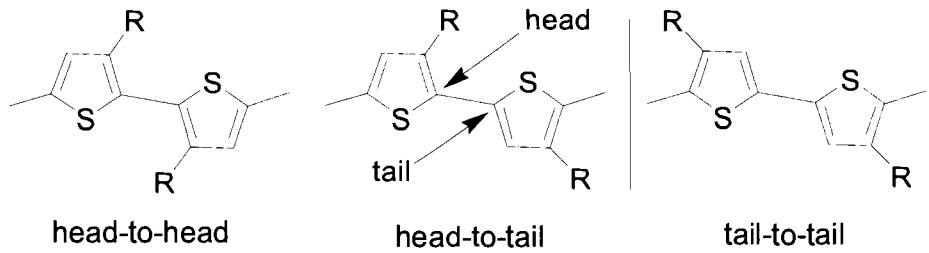

Figure 1.2: Possible diad linkages for 3-alkylthiophene

McCullough and co-workers discovered two methods to produce regio-regular (>98% head-to-tail coupling) P3ATs: The McCullough [17a-b] and the Grignard Metathesis (GRIM) methods.[17c-d] These methods are illustrated in Scheme 1.4 and are both based on the Kumada cross coupling of 2-bromo-5-(magnesiobromo)-3-alkylthiophene.

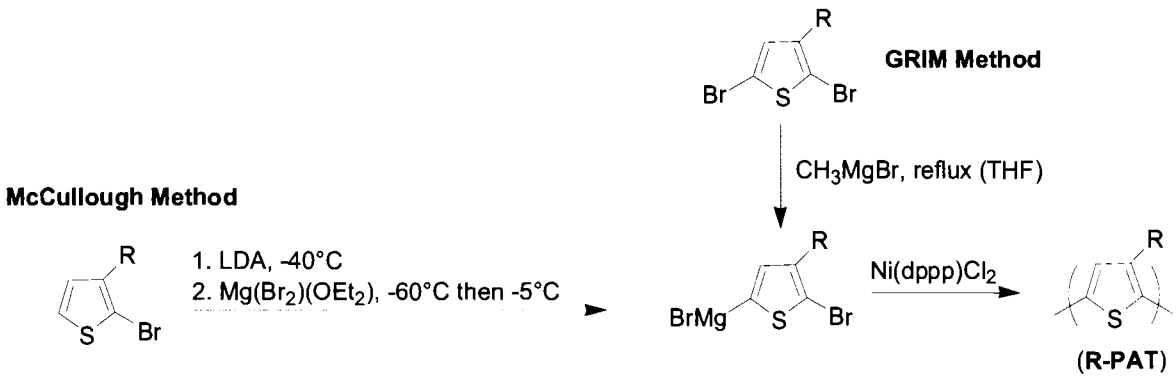

Scheme 1.4: Regio-regular P3AT synthesis

In the McCullough method, high purity 2-bromo-3-alkylthiophene (free from the 2-bromo-4-alkylthiophene isomer) is selectively lithiated at the 5-position with lithium diisopropylamine (LDA) at low temperatures (-40 °C) to afford 2-bromo-3-

alkyl-5-lithiothiophene. This organolithium intermediate is converted to a Grignard reagent by reacting with $MgBr_2 \cdot Et_2O$ to yield 2-bromo-5-(magnesiobromo)-3-alkylthiophene. With the addition of $Ni(dppp)Cl_2$ catalyst, reaction of the Grignard with 2-bromo-3-alkylthiophene results in regio-regular poly(3-alkylthiophene).

The GRIM method is a facile route to make regio-regular P3ATs. In this method, 2,5-dibromo-3-alkythiophene monomer is used, rather than 2-bromo-3-alkylthiophene. The former is easier to purify due to the large differences in volatility of the reactants and the side products.[18] The 2-bromo-5-(magnesio-bromo)-3-alkylthiophene is easily formed by reacting 2,5-dibromo-3-alkythio-phene with methylmagnesium bromide, followed by introduction of the nickel catalyst to yield a regio-regular poly(3-alkylthiophene) in high yields (60-70%).

1.3.1.3.2 Reike Method

Reike and co-workers discovered a method to produce regio-regular PATs.[19] This method is illustrated in Scheme 1.5. This polymerization method is a one pot reaction in which reactive Reike zinc undergoes a regio-selective oxidative addition on the 5-position of 2,5-dibromo-3-alkylthiophene to form 2-bromo-5-bromozincio-3-alkylthiophene. With the addition of $Ni(dppe)Cl_2$ (dppe = diphenylphosphinoethane), regio-regular PAT (R-PAT) is formed. Alternatively, with the addition of $Pd(PPh_3)_4$ (PPh_3 = triphenylphosphine), a regio-random polymer is obtained. It is rationalized that the size of the catalyst (both metal and ligands) controls the regio-specificity of the resulting polymer. [18d, 19a]

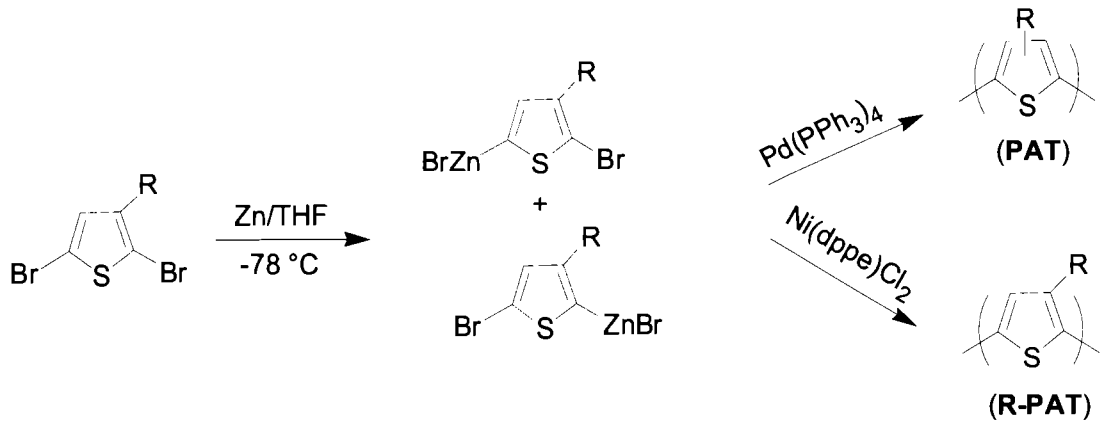

Scheme 1.5: Reike synthesis of PATs and catalyst specificity.

1.3.1.3.3 Suzuki and Stille Polycondensation

Pd-Catalyzed cross coupling is a convenient method for aryl-aryl coupling[20] and provides a route to synthesize a wide variety of conjugated polymers, and copolymers. Two common Pd-catalyzed cross coupling methods are Suzuki[21] and Stille[22] type reactions. The advantages of these methods are water insensitivity, commercial availability of many monomers (and precursors), and the yield of high molecular weight polymers.[23]

In Suzuki coupling, a diboronic acid (or ester) is coupled with a dibrominated aryl group in the presence of a base (e.g. K_2CO_3), as illustrated in Scheme 1.6. This procedure was first reported in 1989 by Wegner and co-workers, for the synthesis of well-defined processable poly(*p*-phenylene)s.[21a] This method is quite versatile, especially for the synthesis of alternating copolymers, and can tolerate a large number of functional groups. Fluorene type polymers are commonly synthesized by this method.[21b-d]

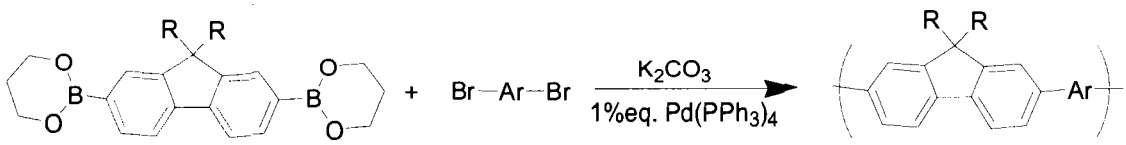

Scheme 1.6: Suzuki coupling of conjugated polymers, where Ar is an aromatic group

Stille coupling is also a versatile, polycondensation reaction to form conjugated polymers. The primary drawback of this method is the use of toxic tin compounds.

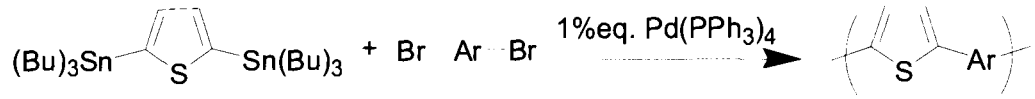

Scheme 1.7: Stille polycondensation of conjugated polymers, where Ar is an aromatic group

1.3.1.4 PPV polymerization methods

Reports on PPV synthesis are based on either (a) direct or (b) precursor approaches. These two methods are addressed in the following section.

1.3.1.4.1 Direct Synthesis

Gilch and coworkers were the first to report the synthesis of PPV; hence it has been coined the Gilch route.[24] In this method, PPV was formed directly by adding excess potassium *tert*-butoxide to *p*-xylylenedichloride, as depicted in Scheme 1.8.

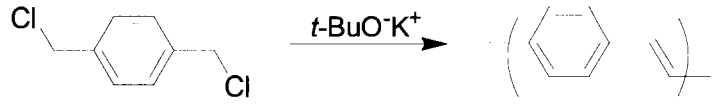

Scheme 1.8: Gilch synthetic route for PPV

Although this route is a facile method to synthesize PPV, it produces polymers which are insoluble and difficult to process into thin films. The addition of alkoxy groups aided in circumventing this issue, however micro-gel formation still occured.[25] This synthetic method was improved by adding 4-*tert*-butylbenzylchloride, to achieve a fully soluble polymer.[26]

1.3.1.4.2 Precursor approach

Several precursor methods were developed for the synthesis of PPVs. The two most common methods are halo[27] and Wessling's[28] precursor routes, which are described below. These methods are desirable because insoluble target films can be made from soluble precursor polymers.

1.3.1.4.2.1 Halo precursor route

The halo precursor route is commonly referred to as a modified Gilch method, in which one equivalent of a strong base is added to a *p*-xylylene-dichloride derivative, to obtain a halo precursor polymer. This polymer may be solution cast to form a film, where upon elimination of HCl with heat (220-250°C), gives PPV[27a] and derivatives.[27b]

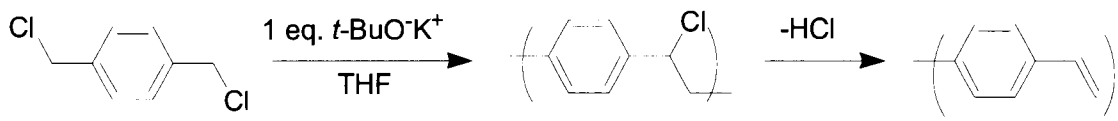

Scheme 1.9: Halo precursor method

1.3.1.4.2.2 Wessling precursor route

The Wessling precursor route to make PPVs is illustrated in Scheme 1.10.[28] In this method, polymerization of the 1,4-xylylenebis-(dialkylsulfonium)-dichloride was achieved in the presence of NaOH to form the precursor polymer. With heating, elimination of the tetrahydrothiophene and HCl affords the corresponding PPV polymer.

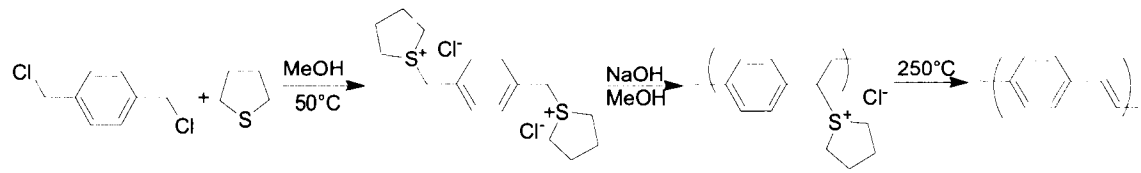

Scheme 1.10: Wessling precursor method

1.4 Characterization of Luminescent Conjugated Polymers

Characterization techniques discussed in the following sections are those used to examine the optical properties of conjugated polymers. These characterization tools are important for understanding the role of the chemical structure on the properties of these materials.

1.4.1 Absorption, Photo- & Electro-luminescence Spectroscopy

1.4.1.1 Theory

Generally, the observed transitions in absorption spectroscopy of conjugated polymers are attributed to electronic excitation from π to π^* states and π^* to π states for emission spectroscopy. Upon electronic excitation of the polymer, a number of photo-physical processes, shown in Figure 1.3, may occur:

fluorescence, phosphorescence, or radiationless decay.[29] Fluorescence is observed after singlet relaxation from the first excited state. If intersystem crossing occurs, a triplet excited state is generated whose relaxation will result in phosphorescence. If emission does not occur, then a non-radiative pathway is dominant and the electronic excitation is converted into rotational or vibrational motion within the polymer and its surroundings. The difference between the absorption and emission maxima of the spectra is called the Stokes shift, and it occurs when emission from the lowest vibrational excited state relaxes to various vibrational levels of the electronic ground state.

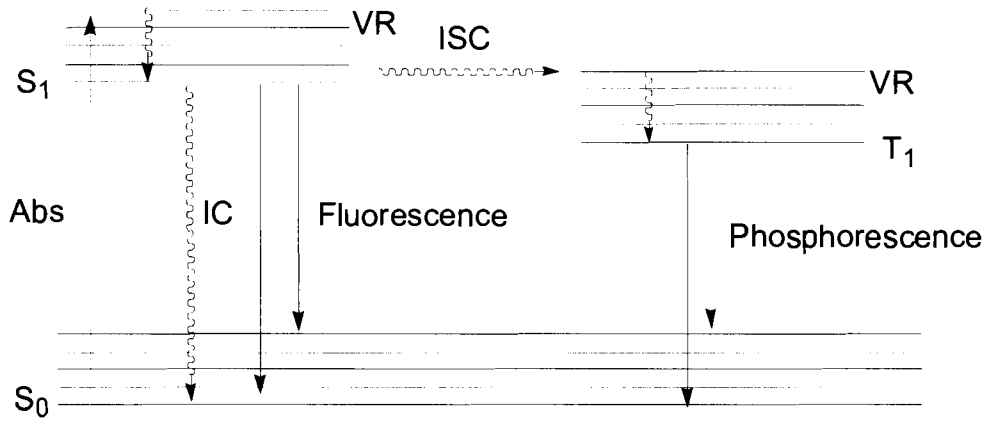

Figure 1.3: Jablonski diagram. Abs = absorption, VR = vibrational relaxation, ISC = intersystem crossing, IC = internal conversion, S_0 = ground state singlet, S_1 = first excited state, T_1 = first triplet excited state.

Quantitative analysis of the emission efficiency of the polymer is characterized by its quantum yield of luminescence (Φ_{pl}). The Φ_{pl} is the ratio of the number of photons emitted to the number of photons absorbed, as shown in Equation 1.1.

$$\Phi_{PL} = \frac{Photons_{EM}}{Photons_{ABS}}$$

Equation 1.1: Quantum yield of photo-luminescence. $Photons_{EM}$ = photons emitted, $Photons_{ABS}$ = photons absorbed.

According to the law of conservation of energy, the maximum Φ_{pl} must be 1. The value of Φ_{pl} is related to the rates of radiative (τ_r) and non-radiative (τ_{nr}) decays, as described in Equation 1.2.[30]

$$\Phi_{PL} = \frac{\tau_r}{\tau_r + \tau_{nr}}$$

Equation 1.2: Quantum yield of luminescence with respect to rates of radiative (τ_r) and non-radiative relaxation (τ_{nr}).

As τ_{nr} approaches 0, the quantum yield of luminescence approaches unity. Generally, Φ_{pl} is highest in dilute solutions, where the emitting species are isolated from each other. In most cases, increasing the concentration of the polymer in solution decreases the quantum yield of luminescence due to concentration quenching, which follows the Stern-Volmer relationship[29] shown in Figure 1.4.

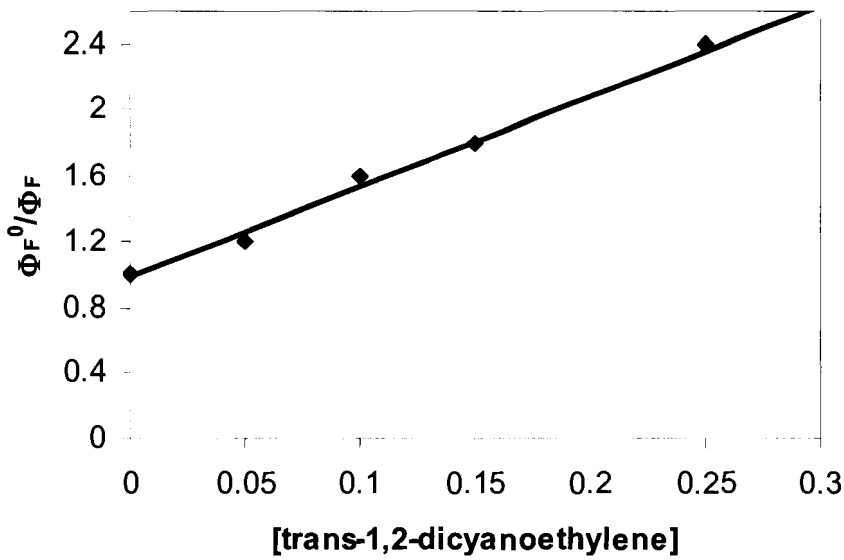

Figure 1.4: Stern-Volmer plot; where the quantum yields are normalized to that of dilute solution (Φ_F^0).

The quantum yield of luminescence can be determined either by secondary or primary methods.[31] In the secondary method, the quantum yield is related to that of a known standard as shown in Equation 1.3. In this equation, Φ represents quantum yield of luminescence, A is the absorbance at the excitation wavelength, F is the integrated emission area under the peak, and n is the refractive index of the solvent. The *u* subscript represents an unknown and the *s* subscript represents a standard. Typical standards are 9,10-diphenylanthracene in cyclohexane (Φ_{pl} = 0.90),[32a-b] quinine sulfate in 1 N H_2SO_4 (Φ_{pl} = 0.546),[32b-c] and rhodamine 101 in ethanol (Φ_{pl} = 1).[32d] This method assumes that the emission from the sample is isotropic (equal in all directions), as is the case in dilute solutions. Measuring the Φ_{pl} of an anisotropic sample, such as a film, is quite difficult since its emission intensity has an angular dependence.

$$\Phi_u = \left(\frac{n_u^{\,2} \times A_s \times F_u}{n_s^{\,2} \times A_u \times F_s} \right) \Phi_s$$

Equation 1.3: Secondary method for quantum yield of luminescence calculation.

In the primary method, measurement of the Φ_{pl} does not rely on standards, but rather on quantifying the number of photons absorbed and emitted in the sample with an integrating sphere.[33] An integrating sphere is a hollow sphere which has its inner surface coated with a reflective material. The sphere allows one to accurately measure the luminescent efficiency of films by collecting light in all directions.[33] That is, the large index of refraction of polymeric semiconductor films could result in substantial waveguiding of the polymer's luminescence, which leads to anisotropic distribution of the emission.

An example of results from a Φ_{pl} experiment using an integrating sphere is illustrated in Figure 1.5. Two spectra are needed to obtain the Φ_{pl} of an unknown sample. The first spectrum involves scanning the emission over the entire range, which includes the excitation line (400 nm in this case) *without* the polymer film. A second measurement is performed afterwards (with the same parameters), *with* the unknown polymer film in the integrating sphere. The number of photons absorbed is measured by integrating under the excitation line (e.g. 390 nm – 410 nm) with and without the sample. The difference between the areas under the excitation lines is the related to the number of photons absorbed. The number of photons emitted is related to the area under the emission peak.

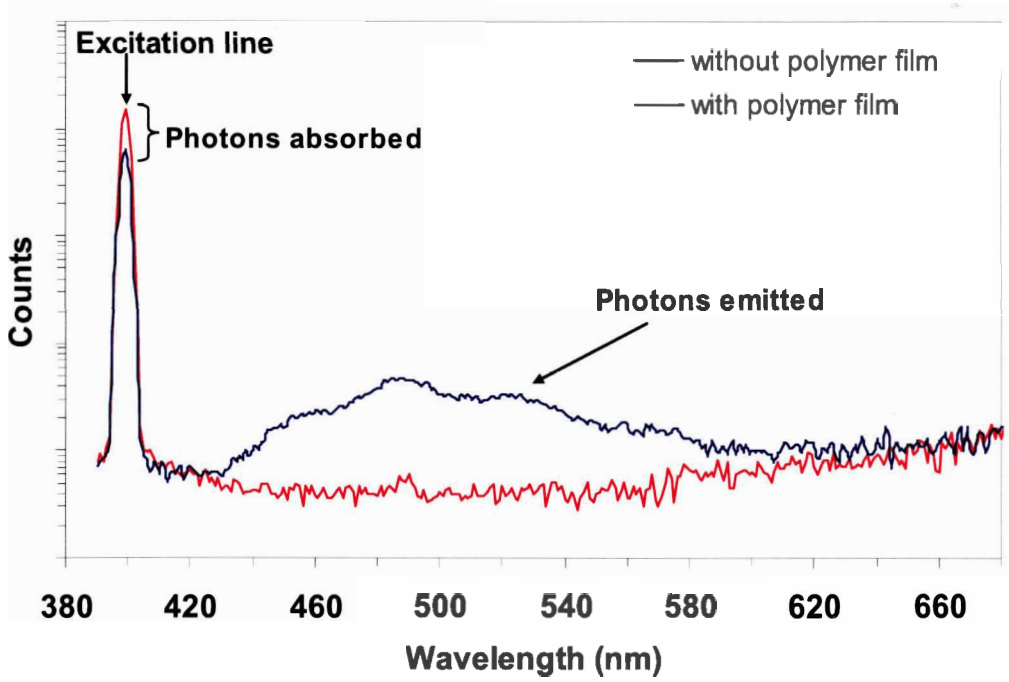

Figure 1.5: A sample experiment of quantum yield measurement.

Electronic energy transfer in molecular and polymeric systems is an area of active research.[29, 34] In general, energy transfer requires a donor (D) and an acceptor (A), in which the excited donor transfers the excited state to the acceptor, as illustrated in Equation 1.4. The efficiency of the energy transfer is related to the rate of the energy transfer from the donor to the acceptor which must be greater than the rates of radiative and non-radiative decay of the donor. Efficient electronic energy transfer will not be realized if these requirements are not met.

$$D^* + A \rightarrow D + A^*$$

Equation 1.4: Electronic energy transfer from donor (D) to acceptor (A).

Electronic energy transfer can occur either through a trivial radiative mechanism - *via* the absorption of the emitted radiation - or through a

nonradiative mechanism. Nonradiative energy transfer can occur *via* the coulomb mechanism (Förster) or by an electron exchange mechanism (Dexter).

Radiative energy transfer (or trivial energy transfer) is a two step process, which does not involve the interaction of the donor and the acceptor. In the first step, D* radiatively decays to form D and a photon, and in the second step, the photon is absorbed by the acceptor (A) to form its excited state (A*). In the ideal case, the donor has a high quantum yield of emission and its emission overlaps well with the absorption of the acceptor. The donor-acceptor separation is weakly dependent on the energy transfer interaction.

The Förster energy transfer is a nonradiative energy transfer mechanism, which deals with the electrostatic dipole-dipole interactions of the molecules. This process relates the rate of energy transfer with the distance between the donor and acceptor (represented as R in Equation 1.5), the Förster radius (R_0), which is related to the spectral overlap integral between the emission of the host and absorption of the guest, and the average donor exciton lifetime for recombination (K_D) in absence of energy transfer. As the distance between the donor and acceptor increases, the probability of energy transfer decreases. Typical "R" values lie in the range of 3-10 nm. Also, the spin is conserved in Förster energy transfer.[30]

$$K_{ET}(Coulomb) = K_D\left(\frac{R_0}{R}\right)^6$$

Equation 1.5: Rate of Förster energy transfer

Dexter energy transfer, or electron exchange, is a short range nonradiative

energy transfer process between molecules separated by <1 nm. As the separation of the donor and acceptor (R) increases, its probability decreases exponentially as described in Equation 1.6. Furthermore, this type of energy transfer allows spin forbidden transitions, as long as the overall spin multiplicity is conserved. The probability of energy transfer is also related to the product of the electron and hole transfer rates from the donor to the acceptor.[30]

$$K_{ET}(Exchange) \sim e^{-2R/L} J$$

Equation 1.6: Rate of energy transfer in terms of electron exchange. R is the donor-acceptor separation, L is a constant related to average orbital radius' of the donor and acceptor, and J is the spectral overlap.

In a host-guest system, the donor is the host and the acceptor is the guest. To obtain efficient electroluminescence, the guest materials must have a high photoluminescence quantum yield, the host must have good charge transport properties, and there must be a small separation between the host and guest.

Electroluminescence (EL) is emission observed upon the application of an electric field on a polymer and is observed from Light Emitting Diodes (LED). A schematic diagram of a simple LED is depicted in Figure 1.6a. This LED consists of a transparent conducting anode (typically Indium Tin Oxide (ITO)), an emitting molecule (or polymer), and a low work function metal cathode such as calcium. The EL spectra corresponds well with its solid state photoluminescence spectra, indicating that the excited state structure is similar regardless the excitation method.

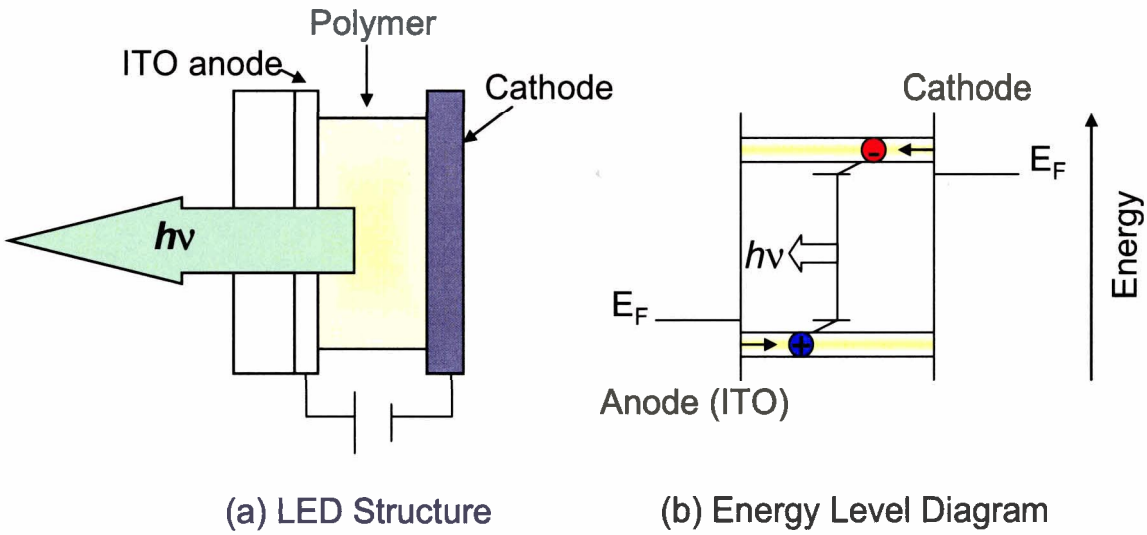

Figure 1.6: LED device structure and its corresponding energy level diagram. E_F = Fermi energy level.

Light emitting diodes are bipolar devices, where holes (h^+) and electrons (e^-) are transported in the polymer. Upon application of an electric field, a hole and electron are simultaneously injected into the polymer, whereby the hole-electron pair forms an exciton. Recombination of the exciton results in the emission of light. This process is illustrated in Figure 1.6b. Multi-layer device structures are commonly fabricated to facilitate and/or balance the hole and electron transport.

Device efficiency is a measure of the number of photons emitted through the transparent electrode per injected electron and is commonly referred to as external quantum efficiency (Φ_{EL}). The Φ_{EL} of an LED is related to several factors including the solid state photoluminescence efficiency, the fraction of the photons which are emitted from the front surface of the device, and the fraction of electrons and holes which recombine with each other.

1.4.1.2 Properties of Conjugated Polymers and Oligomers

The mean conjugation length of the conjugated polymer is often related to the maximum wavelength of both absorption and emission spectra. This has been confirmed experimentally in acetylene,[35] thiophene,[36] phenylene[37] and phenylenevinylene[38] oligomers with various numbers of repeating units. As an example, Figure 1.7 depicts the absorption (a) and emission (b) spectra of oligo-thiophenes from 2 to 6 units long.[36] It is clear that as the number of thiophenes increase, both the absorption and emission wavelengths increase due to larger conjugation lengths. Also, the molar extinction coefficients increase incrementally from 1.6×10^4 to ~6×10^4 liters/(mole·cm) due to an increase in the transition dipole moment. In addition, the solution quantum yield of luminescence increases from 0.07 to 0.40 with increasing conjugation length, indicating that the rate of non-radiative decay decreases with conjugation length. This result is somewhat counterintuitive, considering that the more red shifted the emission is, the more efficient the internal conversion becomes because energy is transferred to the vibrational modes more readily. This increase in Φ_{pl} with higher conjugation lengths can be explained by: (a) an increased structural stability of an unspecified origin[36] or (b) the lack of singlet fission (process where two triplet excitons are produced from the fission of one singlet excited state).[39]

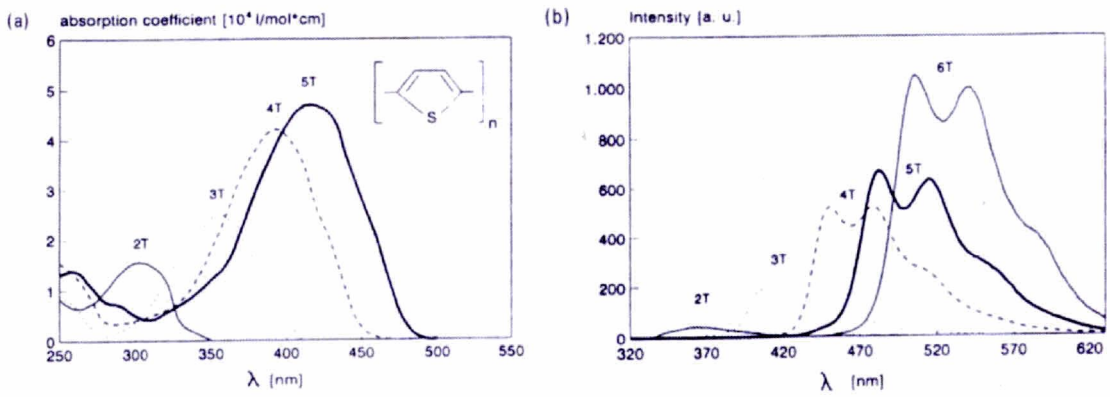

Figure 1.7: Absorption (a) and emission (b) spectra of oligothiophenes (T) with n repeat units. Reproduced with permission from Elsevier © 1993.[36]

In the solid state, the absorption and emission wavelength maxima increases (red shift), with respect to their corresponding solution values, while the Φ_{pl} decreases pronouncedly. For instance, the absorption maxima of regio-regular poly(3-alkylthiophene)s in solution is at ~440 nm, while in the solid state it was at ~550 nm; the emission maximum in solution is at ~560 nm with a quantum yield of 40%, while in the solid state the emission maximum is at ~740 nm with a quantum yield of 2%.[40] This red shift in the solid state is attributed to strong π-π intermolecular interactions due to aggregate formation,[41] and/or excimer formation.[42]

Aggregate states are identified as interchain species that occur in the ground state. Upon aggregation, both the ground and excited state wave-functions are delocalized over many polymers, resulting in a shift in both the absorption and emission maxima with respect to the isolated species in solution. Evidence of this phenomenon has been observed in both molecular (anthracene)[42] and polymeric systems (ladder poly(phenylene)s).[43]

An excimer is a photoexcited emissive intermolecular singlet excited state complex which is delocalized over two molecular units.[42] This excimer cannot be directly excited since the ground state of the dimer is dissociative. A classic excimer forming molecule is pyrene whose absorption spectrum is not related to the concentration. However, in the emission spectrum, the emergence of a broad, featureless, red-shifted peak occurs with increasing concentration which is attributed to excimers.[42] This phenomenon has been observed in rigid-rod conjugated polymers such as poly(*p*-phenylene-2,6-benzobisoxazole) by Jenekhe and co-workers.[44]

These aggregate and excimer states are induced by strong intermolecular interactions between two or more molecules (or polymer units). The interaction between the wavefunctions of the molecules results in the formation of two or more new states, as depicted in Figure 1.8. As a consequence, the absorption spectrum of an aggregate may blue-shift and/or red-shift, depending on the orientation of the molecular packing: parallel, head-to-tail or oblique.[45a] An optical transition is allowed only for a non-zero transition moment. Therefore, a blue-shift in the absorption spectrum is observed for a parallel orientation, while a red-shift is observed for a head-to-tail orientation. For an oblique orientation, both orientations have non-zero transition moments, which results in band splitting. The emission spectra of these aggregate or excimer states is red shifted compared to their isolated molecules, due to fast internal conversion. For parallel aggregates, the emission is optically forbidden and therefore leads to a strong decrease in the quantum yield of luminescence.

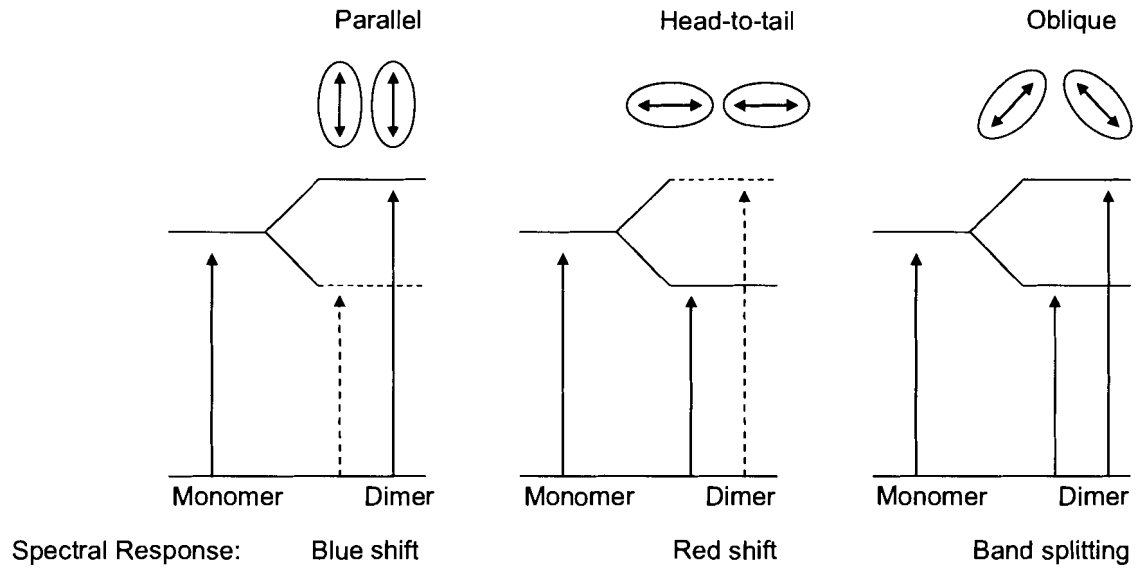

Figure 1.8: A simplified excitonic band structure of isolated (monomer) and aggregated (dimer) phases with their corresponding spectral shifts.

In conjugated polymers, the absorption maximum in the film state red-shifts (indicating a head-to-tail orientation) and a decrease in the quantum yield of luminescence are observed with respect to their solution state properties. Furthermore, the X-ray diffraction of P3ATs, for instance, shows strong evidence for a parallel aggregation.[17, 19] These differences may be explained with a model which is a combination of the planarization of the polymer backbone (that leads to additional π-conjugation)[14, 17, 19] and the aggregation phenomenon.[45] Therefore, the red-shift in the absorption is explained by the planarization of the polymer backbone, which outweighs the aggregation, while the decrease in the quantum yield of luminescence is observed due to the aggregation phenomenon.

1.4.1.2.1 Quantum Yield of Photoluminescence

The efficiency of LED devices is proportional to the solid state photo-luminescence efficiency of the emitting polymer. Photophysical investigations have been performed on model polymers to understand the origin of the intermolecular interactions. For example, the effects of steric interaction on the intermolecular interactions were investigated by Xu and Holdcroft by analyzing the degree of regioregularity on the photophysical properties of poly(3-hexylthiophene).[46] The authors found that the solid state absorption and emission wavelengths increased with regio-regularity, however their photo-luminescent efficiency decreased. The difference between solution and solid state maxima also increased with regio-regularity. Therefore, as the head-to-tail couplings increased, intermolecular π-stacking distance decreased (Figure 1.9), and the quantum yield of photo-luminescence also decreased. Furthermore, modifying the alkyl side chain with sterically encumbered cyclohexyl[47] or aryl[48] groups enhanced the solid state emission efficiency by decreasing intermolecular interactions. From these fundamental studies, it is clear that the solid state luminescence efficiency - hence intermolecular interactions - can be controlled by varying the substitution patterns and the steric interactions of the side chain substituents on the polymer backbone.

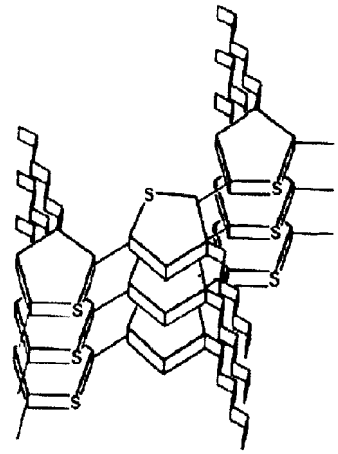

Figure 1.9: Solid state ordering of regio-regular poly(3-alkylthiophene)s. Reproduced with permission from the American Chemical Society © 1993.[46]

Another variable that significantly affects the solid state luminescence of conjugated polymers is the pendant alkyl chain length. The luminescent properties of poly(2,5-dialkoxy-1,4-phenylene vinylene)s (PAPVs)[49a] and poly(9,9-dialkylfluorenes)s (PAFs)[49b-c] are two examples where the influence of alkyl chain length have been investigated. The optimal chain length for luminescence is decyl and octyl for PAPVs[49a] and PAF[49b], respectively; shorter alkyl chains do not sufficiently overcome π-π intermolecular interactions whereas crystallization of longer alkyl chains induces local order.[49]

Host-guest systems have been studied in both molecular based LEDs (OLEDs) and polymeric based LEDs. The work on molecular LEDs by the Kodak research group showed that only a small concentration of the guest was required to enhance the solid state emission efficiency.[50] An example of a molecular host-guest type system that Kodak studied is the tris(8-hydroxyquinoline) aluminum (Alq_3) *host*- coumarine *guest* combination. In the experiment, the Alq_3 matrix was directly excited and the electronic excitation energy was completely transferred to

the isolated coumarine dye. As a result, the solid state photo- and electro-luminescence efficiency increased three fold and the device operational lifetime was enhanced.[50] Similarly, host-guest systems formed using polymer/dye,[51] polymer blend,[52] and copolymer[53] combinations have proved useful in enhancing the emission intensity in the solid state by isolating the emitting species.

An example of a polymer/dye combination is given by Bradley *et. al*, where red emitting tetraphenylporphorine (TPP) was dispersed in a blue emitting poly(fluorene) (PF) matrix.[51] It was found that red emission (PL), originating from the TPP, was dominant at only 1% (weight). In addition, the solid state quantum yield of EL increased five-fold with addition of the TPP moiety. At concentrations greater than 11%, non-radiative decay, caused possibly by excimers, decreased the quantum yield of luminescence.

Polymer blends offer an alternative approach to increase the efficiency of host-guest type systems. For instance, Yang and co-workers investigated poly(fluorene) (host) and poly(phenylenevinylene) (guest) polymer blends and found that the film photoluminescence properties mimicked a solid solution – such that the solid state emission spectrum of the blend resembled the solution emission spectrum of the PPV. Furthermore, LED device performance was enhanced by 70%.[52c-d]

In both of these polymer host-guest examples, phase separation due to the eventual incompatibility of the two segments seemed to affect LED performance.[52a, 54] To maintain uniformity and to reduce phase separation in the polymer film, copolymers have been investigated as alternatives.

An example of a host-guest copolymer system has been reported by

Theander and co-workers.[53e] They found that a small concentration of phenylenevinylene (guest) on a poly(fluorene) (host) backbone resulted in a dramatic increase in the Φ_{pl}. Furthermore, copolymerization of silole units with fluorene reported by Jen and co-workers[52d] resulted in the enhancement of the LED performance.

1.4.1.2.2 Band Gap Tuning

Although the emission efficiency is an important factor in PLEDs, the emission colour is also crucial. For a full colour display, three types of luminescent polymers are required in the PLED device fabrication: red, green, and blue emitters. It is preferable that only one class of polymer be synthesized, which can be tuned by some technique (e.g. synthetic or physical). In all colour tuning methods, only the effective conjugation length of the emitting species - *via* molecular control - is altered. The three common methods to tune the emission colour are by (a) varying the type of guest in a host-guest system, (b) varying the conjugation length by varying the steric constraints on the polymer backbone (side chains and alternating copolymers), and (c) breaking the conjugation length.

Varying the guest in molecular and polymeric systems is a simple approach to tune the emission wavelength. One way that this can be obtained is by introducing defects (or guests) of various conjugation lengths. In molecular systems, co-evaporation of a small concentration of different guests will modulate the emission colour.[50] For instance, by doping a green emitting AlQ_3 system with an orange emitting 4-(dicyanomethylene)-2-tert-butyl-6-(1,1,7,7-tetramethy-

ljulolidyl-9-enyl)-4H-pyran (DCJTB), one observes emission of an orange colour because the emission is dominated by the presence of DCJTB.[50e] Additionally, researchers at Sanyo have shown that the use of several co-dopants is an effective approach to vary the emission wavelength by means of sequential energy transfer, as illustrated in Figure 1.10.[55]

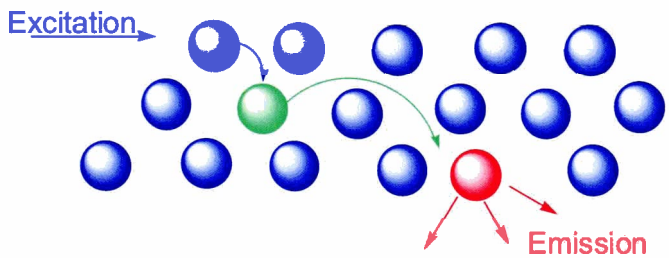

Figure 1.10: Energy transfer in a co-dopant system

In polymeric systems, the emission colour can be tuned by either blending or copolymerization with different guests. For efficient energy transfer, the wide- and narrow- bandgap polymers in the blend must form a homogeneous mixture (i.e. weakly phase separated). If this requirement is not met, the blend will behave as two independent emitters and the emission colour will strongly depend on the applied current in the LED.[54] A successful example of emission colour tuning *via* polymer blends is by K. Müllen and co-workers.[54b] Their system consisted of a blue emitting ladder-type poly(*p*-phenylene) (LPPP) and a red-light-emitting poly(perylene-co-diethynylbenzene) (PPDB) guest, shown in Figure 1.11. The emission observed from these blends was dominated by the PPDB, despite direct excitation of the LPPP matrix.

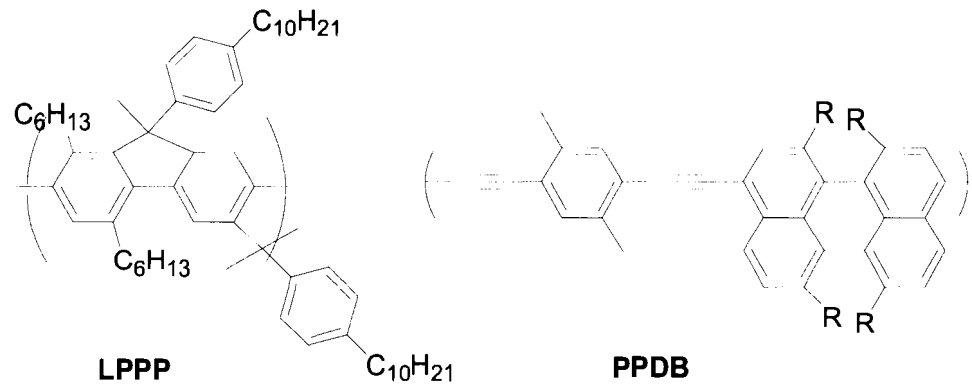

LPPP **PPDB**

Figure 1.11: Molecular structures of polymers for blends

Copolymerization is a more desirable route to produce PLED- based full colour displays since phase segregation is not as prominent in copolymer systems as polymer blends. An example of such a copolymer system was recently studied by R. H. Friend and co-workers.[53a] In this investigation, the effect of attaching perylene dyes on the main chain, end groups, and side chains of poly(9,9-dialkylfluorene)s dramatically influenced the polymers optical properties. Similar to blends and molecular systems, the energy absorbed by the polyfluorene host was transferred to the perylene guest. The colour emitted depended on the guest structure and where it was attached. Similarly, Swager and coworkers attached anthracene terminal groups to poly(*p*-phenyleneethynylene)s and observed that energy transferred from the main-chain to the end groups with >95% efficiency.[53f] However, deep blue emitters are difficult to obtain using this method because energy transfer requires a lower energy guest.

Alternatively, the effective conjugation length maybe altered with the steric interaction of the side chains to obtain various emission colours. In general, the

greater the steric interaction of the side chains on the backbone of the polymer, the more twisted the backbone and the more blue shifted the emission colour becomes. For instance, Inganäs *et. al.* tuned the emission colour of poly(alkyl-thiophene)s by varying the bulkiness of the side chains, as shown in Figure 1.12.[48] The emission maxima varied from 442 nm (Polymer 1, Figure 1.12) to 677 nm (Polymer 2, Figure 1.12), covering the range of the entire visible spectrum. Although these polymers emission colour could be tuned, the high energy emitters had a low Φ_{pl} (~1%) in both solution and solid state, which is undesirable. Additionally, this method was quite cumbersome due to the large number of steps involved in the synthesis.

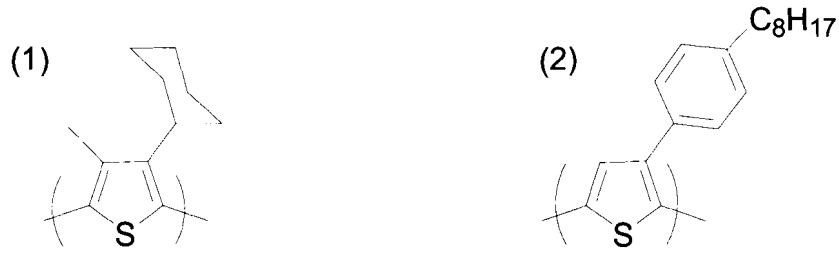

Blue emitter, 442 nm Red emitter, 677 nm

Figure 1.12: Molecular structures of various regio-regular poly(3-alkylthiophene)s

Alternating copolymers can also control the steric and electronic interactions on the polymer backbone. For instance, the blue emitting polyfluorenes are a nice starting point, because more planar units may be introduced to the polymer backbone to increase the extent of conjugation. For instance, the Dow research group has investigated a wide variety of fluorene alternating copolymers, as depicted in Figure 1.13.[56] These polymers vary the emission colour and have a good quantum yield of luminescence. Fluorene

based polymers have been shown to be promising materials for PLED applications due to their high brightness and high operational stability.[56b]

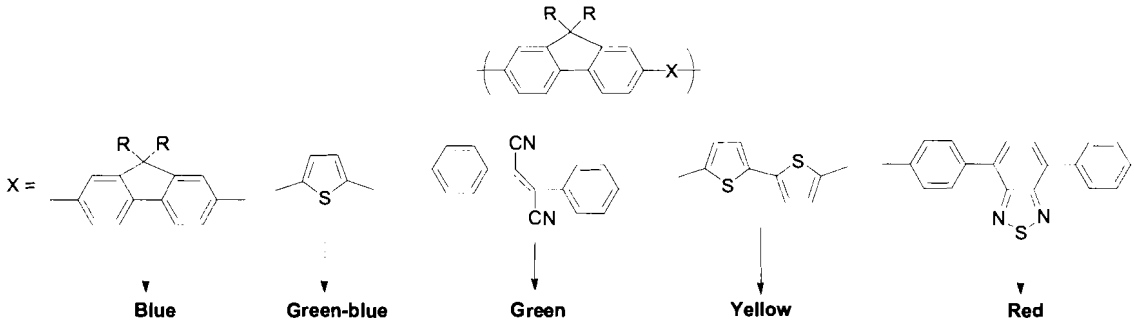

Figure 1.13: Molecular structures of various fluorene alternating copolymers.

For poly(phenylenevinylene)s, partial elimination, shown in Scheme 1.11, is a common method to control the conjugation lengths. Zhang and co-workers initially attempted this by adjusting the temperature and time of elimination for converting the precursor polymer to its final conjugated form.[29d] As a result, incomplete elimination of the leaving group generated polymers with different conjugation lengths which emitted light at higher energies. The primary drawback of this method is its irreproducibility.

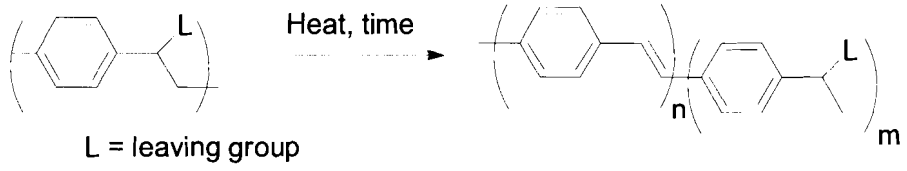

Scheme 1.11: Partial elimination approach to tune the colour of emission

1.4.1.2.3 Spectral Purity and Stability

Spectral purity is the definition of a colour and is determined by the National Television Standards according to their Commission Internationale de l'Eclairage (CIE) coordinates. Colour stability is the lack of change in the

emission colour, regardless on the magnitude of the current applied and the operation time.[57] It is essential that the display has both good spectral purity and good spectral stability for a clean and reproducible image.

A common phenomenon which affects spectral purity and stability in organic molecules is red tailing. Red tailing is low energy emission from aggregate states in the polymer. This is not a problem in red emitting materials since infrared emission is not observed. Yellow emission may be observed in green emitters and green emission may be observed in blue emitters. The former is not as detrimental since the sensitivity of the eye to yellow is lower than that of green; however, this effect poses a problem in the blue region because the sensitivity of the eye for green light is 10 times greater than that of blue. For this reason, investigations to understand and to minimize red-tailing in blue emitters have been a recent topic of intense research.[58-66]

Poly(fluorene)s are one of the most studied classes of blue emitters due to their good operational stability and relatively simple synthesis. Solutions of poly(fluorene)s display blue-violet emission. A light blue emission is observed in the solid-state; however, an irreversible light blue to green colour shift is observed upon continual operation of the LED device. This effect has been observed in both PL and EL and is illustrated in Figure 1.14.[58b] This spectral impurity and instability is attributed to molecular aggregation and/or excimer formation[58] and/or fluorenone formation.[59]

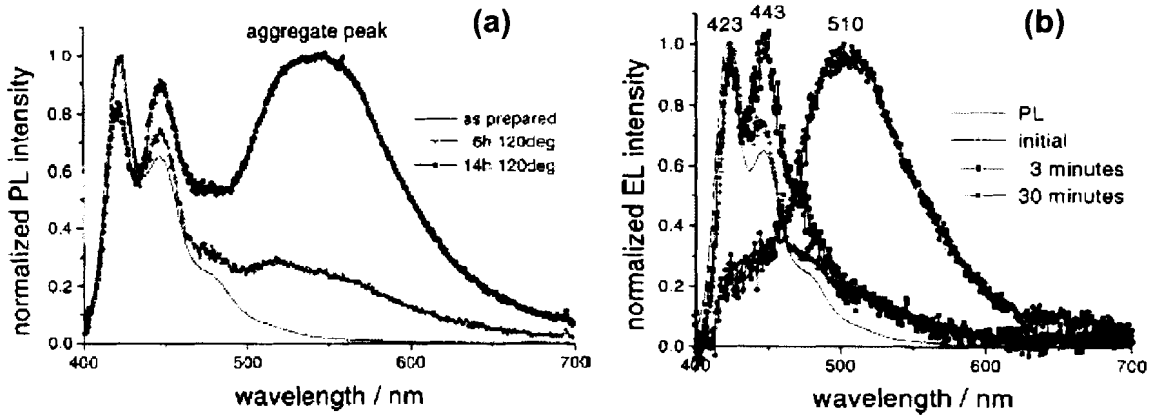

Figure 1.14: (a) Photoluminescence spectra of a PF film as prepared and after annealing at various temperatures (b) Electroluminescence spectra of a PF as a function of time. Reproduced with permission from American Institute of Physics © 2000.[58b]

Bradley and co-workers studied the photo-physics of PF films cast from various solvents.[58a] They found that polymer films formed from solvents which dissolved the polymer well exhibited less red tailing than films formed from poorly solvated polymers. This result suggested that aggregation played a significant role in determining the spectral properties of poly(fluorene)s. This aggregation theory was supported by the Toyota and Samsung research groups; they found that the colour stability was related to the molecular weight of the conjugated polymer.[58b] Specifically, lower molecular weight segments had a greater tendency to crystallize and form green emitting aggregates while higher molecular weight segments formed random coils without aggregating.

There have been several modifications to the fluorene monomer and polymer to exclude the aggregation and/or excimer phenomenon. These include: the attachment of aromatic groups[60] or dendritic groups[61] at the 9- and 9'-positions of fluorene, hyperbranching,[62] blending,[63] end-capping polymers with

aromatic groups including post-polymerizable styrene end groups,[64] and the introduction of anthracene[65] or carbazole[66] on the backbone. All of these methods have helped suppress the aggregation phenomenon.

List and co-workers suggested that fluorenone formation (or keto defects) in monoalkylfluorenes and/or photo- (or electro-) oxidation of dialkylated fluorene units was the primary reason for the increased green emission in poly(fluorene)s.[59] Evidence that the low energy peak (see Figure 1.14) was due to fluorenone formation (and not an excimer nor aggregation formation) were: (a) ketone band in the IR spectrum,[59a] (b) direct excitation of the low energy trap, (c) concentration independence on the low energy emission, and (d) vibronic structure of the low energy emission at low temperature.[59b]

1.5 Patterning of conjugated polymers

The spatially controlled deposition of conjugated polymers is of interest in microelectronic and high resolution display applications for the controlled formation of micron-sized domains.[67] In conjugated polymers, several methods have been developed for patterning, such as photo-lithography,[68-69] inkjet printing[70] and screen printing.[71]

Photo-lithography is the most common form of spatially controlled deposition in the microelectronics and display industries and its concept is illustrated in Scheme 1.12. A polymer photo-resist is coated onto a substrate. A photo-mask, consisting of transparent and opaque regions, is placed (and possibly aligned) over the polymer and the sample is irradiated. During photolysis, cross-linking[68] or supra-molecular hydrogen bonding[69] occurs at the

exposed areas, which renders the film insoluble. Upon development, a positive image is formed where the irradiated areas are insoluble.

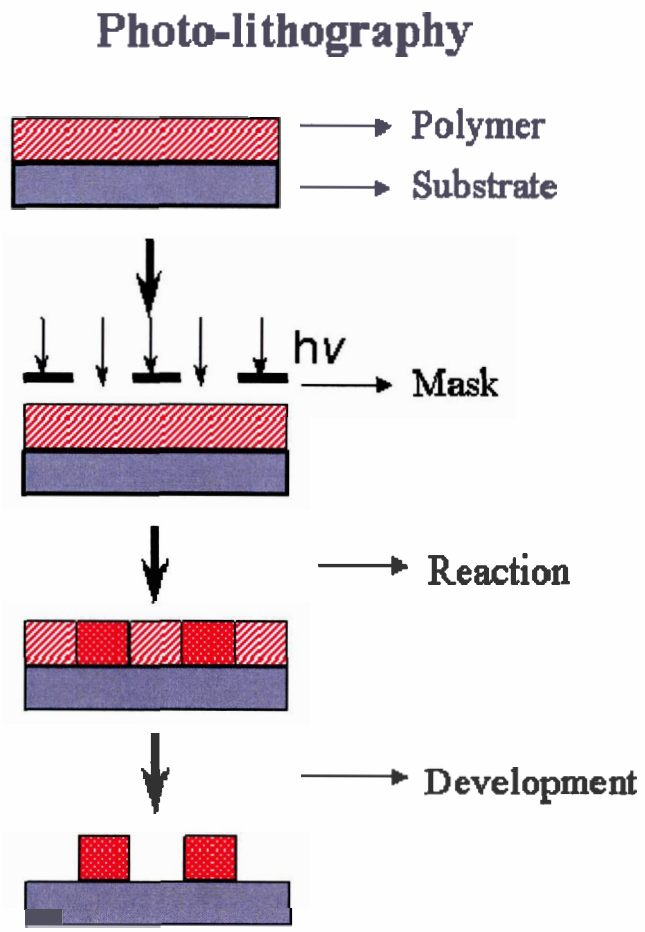

Scheme 1.12: Photo-lithographic process

Photolithography has been demonstrated with conjugated polymers.[68-69] For instance, photo-crosslinking of poly(3-alkylthiophene)s have been patterned *via* laser direct-write photo-lithography. An optical micrograph of such an image is illustrated in Figure 1.15.[68a]

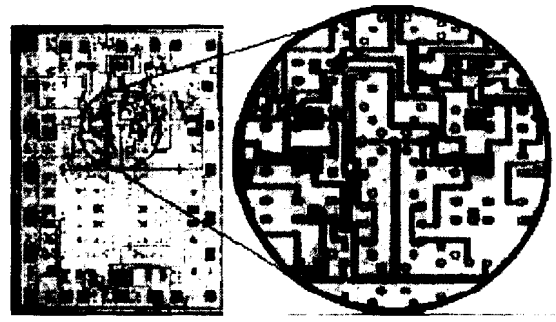

Figure 1.15: Optical micrograph of P3AT circuitry by laser direct-write photo-lithography. Reproduced with permission from Elsevier © 1992.[68a]

In this case, high intensity incident light is used, to form crosslinked regions, in addition to structural defects and PL quenchers. These structural defects also affected the electrical conductivity.

Yu and Holdcroft have developed a method in which acid sensitive units were placed on the polymer backbone and brief low power irradiation times resulted in intermolecular hydrogen bonding.[69] In this method, tetrahydropyran (THP) groups are attached to the alkyl chain of P3ATs. Deprotection of the THP units in the presence of a catalytic amount of acid, as shown by TGA analysis, occurs approximately 100°C lower than in the absence of acid. The presence of a catalytic amount of acid (*via* a photo-acid generator), followed by thermal cleavage of the THP formed a hydroxyl functionalized P3AT, dihydropyran, and acid, as illustrated in Scheme 1.13. The resulting polymer was insoluble.

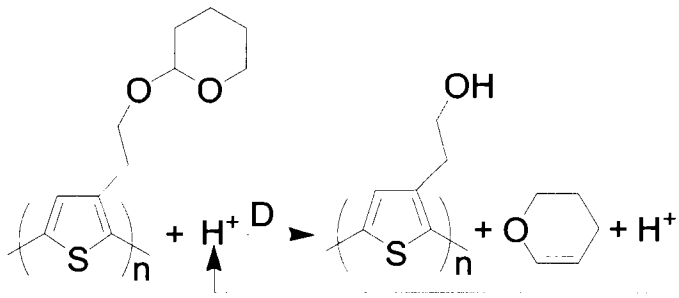

Scheme 1.13: Acid-catalyzed deprotection of THP functionalized P3ATs

A recent photo-lithographic method is the use of cross-linkable oxetane functionalized polymers to form full colour (RGB) PLEDs, as shown in Figure 1.16.[72] In this case, covalent cross linkages *via* an acid catalyzed ring opening reaction rendered these luminescent polymers insoluble. These polymers displayed similar spectral properties, before and after imaging.

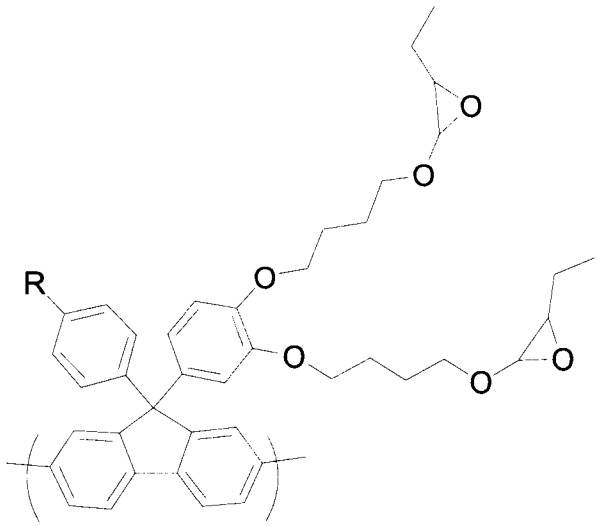

Figure 1.16: Poly(fluorene) derivative with oxetane functional groups

1.6 Project overview

Conjugated polymers are of considerable interest due to their inherent electrical and optical properties and are incorporated as active components in transistors, LEDs, solar cells and electrochromic displays. Research described in this manuscript focuses on PLEDs.

The three major classes of conjugated polymers used in PLEDs are derivatives of poly(thiophene)s (PTs), poly(phenylenevinylene)s (PPVs) and poly(fluorene)s (PFs). For these polymers to be useful in display technologies, their solid state intermolecular aggregation needs to be reduced in order to improve their emission efficiency. In addition, their emission colour needs to be tuned to emit the three primary colours - red, green, and blue.

Two synthetic methods have been developed to control the intermolecular interactions and to tune the emission colour. They are post-functionalization, which is described in Chapter 2, and self-forming host-guest systems, which is described in Chapter 3. Both of these methods simultaneously increased the quantum yield of luminescence and tuned the emission colour of the aforementioned polymers. In Chapter 4, the synthesis and emission properties of image-forming tetrahydropyran (THP) containing conjugated polymers are investigated, since these polymers are important for the development of high-resolution PLED displays.

1.7 References

1. H. Shirakawa, E. J. Louis, A. G. MacDiramid, C. K. Chiang, A. J. Heeger, *J. Chem. Soc., Chem. Commun.* **1977**, 578.

2. G. Tourillon; in Handbook of Conducting Polymers; T. A. Stotheim, Ed. Marcel Dekker: New York, 1986; Pg 294.

3. A. F. Diaz, K. K. Kanazawa, G. P. Gardini, *J. Chem. Soc., Chem. Commun*, **1979**, 635.

4. (a) K. Y. Jen, R. Oboodi, R. L. Elsenbaumer, *Polym. Mater. Sci. Eng.* **1985**, *53*, 79. (b) R. L. Elsenbaumer, K. -Y. Jen, R. Oboodi, *Synth. Met.* **1986**, *15*, 169.

5. G. G. Miller, R. L. Elsenbaumer, *J. Chem. Soc., Chem. Commun.* **1986**, 1346.

6. (a) C. D. Dimitrakopoulos, D. J. Mascaro, *Adv. Mater.* **2002**, *14*, 99. (b) F. Garnier, R. Hajlaoui, A. Yassar, P. Srivastava, *Science* **1994**, *265*, 1684. (c) Z. Bao, *Adv. Mater.* **2000**, *12*, 227. (d) G. H. Gelinck, T. C. T. Geuns, D. M. de Leeuw, *Appl. Phys. Lett.* **2000**, *77*, 1487. (e) H. E. A. Huitena, G. H. Gelinck, J. B. P. H. van der Putter, K. E. Kuijk, C. M. Hart, E. Cantatore, P. T. Herwig, A. J. J. M. van Breemen, D. M. de Leeuw, *Nature* **2001**, *414*, 599. (f) B. S. Ong, Y. Wu, P. Liu, S. Gardner *J. Am. Chem. Soc.* **2004**, *126*, 3378.

7. L. Akcelrud, *Prog. Polym. Sci.* **2003**, *28*, 875. (b) R. H. Friend, R. W. Gymer, A. B. Holmes, J. H. Burroughes, R. N. Marks, C. Taliani, D. D. C. Bradley, D. A. dos Santos, J. L. Brédas, M. Löglund, W. R. Salaneck, *Nature* **1999**, *397*, 121. (c) A. Kraft, A. Grimsdale, A. B. Holmes, *Angew. Chem. Int.* **1998**, *37*, 402. (d) J. R. Sheats, Y. L. Chang, D. B. Roitman, A. Socking, *Acc. Chem. Res.* **1999**, *32*, 193. (d) S. Miyata H. S. Nalwa, in Organic electroluminescent materials and devices. Amsterdam: Gordon & Breach; 1997. (e) X. Gong, J. C. Ostrowski, M. R. Robinson, D. Moses, G. C. Bazan, A. J. Heeger, *Adv. Mater.* **2002**, *14*, 581. (f) R. H. Partridge, *Polymer* **1983**, *24*, 733. (g) J. H. Burroughes, D. D. C. Bradley, A. R. Brown, R. N. Marks, K. MacKay, R. H. Friend, P. L. Burns, A. B. Holmes, *Nature* **1990**, *347*, 539.

8. (a) E. Smela, *Adv. Mater.* **2003**, *15*, 481. (b) E. Smela, in Electroactive Polymer Actuators as Artificial Muscles: Reality, Potential and Challenges (Ed: Y. Bar-Cohen), SPIE Press, Bellingham 2001. (c) T. F. Otero, in Conductive Polymers: Transport, Photophysics and Applications (Ed: H. S. Nalwa) Vol. 4, John Wiley & Sons. New York. 1997.

9. (a) J. Christoph, J. Brabec, N. S. Sariciftci, J. C. Hummelen, *Adv. Funct. Mater.* **2001**, *11*, 15. (b) J. Xue, S. Uchida, B. P. Rand, S. R. Forrest, *Appl. Phys. Lett.* **2004**, *84*, 3013. (c) N. S. Sariciftci, L. Smilowitz, A. J. Heeger, F. Wudl, *Science* **1992**, *258*, 1474. (d) S. Morita, A. A. Zakhidov, K. Yoshino, *Solid State Commun.* **1992**, *82*, 249.

10. R. D. McCullough, R. D. Lowe, M. Jayaraman, D. L. Anderson, *J. Org. Chem.* **1993**, *58*, 904.

11. A. Köhler, J. S. Wilson, R. H. Friend, *Adv. Mater.* **2002**, *14*,701.

12. J. Roncali, *Chem. Rev.* **1992**, *92*, 711-738.

13. (a) Y. Ohmori, M. Uchida, K. Muro, K. Yoshino, *Jpn. J. Appl. Phys.* **1991**, *30*, L1941. (b) R. Sugimoto, S. Takeda, H. B. Gu, K. Yoshino, *Chem. Express* **1986**, *1*, 635.

14. (a) H. Mao, B. Xu, S. Holdcroft, *Macromolecules* **1993**, *26*, 1163. (b) S. Amou, O. Haba, K. Shirato, T. Hayakawa, M. Ueda, K. Takeuchi, M. Asai, *J. Polym. Sci. Part A: Polym. Chem.* **1999**, *37*, 1943. (c) O. Haba, T. Hayakawa, M. Ueda, H. Kawaguchi, T. Kawazoe, *Reactive & Functional Polymers* **1998**, *37*, 163.

15. (a) M. S. A. Abdou, X. Lu, Z. W. Xie, F. Orfino, M. J. Deen, S. Holdcroft, *Chem. Mater.* **1995**, *7*, 631. (b) F. Chen, P. G. Mehta, L. Takiff, R. D. McCullough, *J. Mater. Chem.* **1996**, *6*, 1763.

16. T. Yamamoto, A. Morita, Y. Miyazaki, T. Maruyama, H. Wakayama, Z. -H. Zhou, Y. Nakamura, T. Kanbara, S. Sasaki, K. Kubota, *Macromolecules* **1992**, *25*, 1214.

17. (a) R. D. McCullough, R. D. Lowe, *J. Chem. Soc., Chem. Commun.* **1992**, 70. (b) R. D. McCullough, R. D. Lowe, M. Jayaraman, D. L. Anderson, *J. Org. Chem.* **1993**, *58*, 904. (c) R. S. Loewe, S. M. Khersonsky, R. D. McCullough, *Adv. Mater.* **1999**, *11*, 250. (d) R. S. Loewe, P. C. Ewbank, J. Liu, L. Zhai, R. D. McCullough, *Macromolecules* **2001**, *34*, 4324.

18. R. Taylor "Electrophilic Substitution of Thiophene and its Derivatives" in Thiophene and its Derivatives; Ed: S. Gronowitz, Wiley 1985.

19. (a) T. -A. Chen, R. D. Reike, *J. Am. Chem. Soc.* **1992**, *114*, 10087. (b) T. -A. Chen, R. A. O'Brian, R. D. Reike, *Macromolecules* **1993**, *26*, 3462. (c) T. -A. Chen, R. D. Reike, *Synth. Met.* **1993**, *60*, 175. (d) T.-A. Chen, X. Wu, R. D. Reike, *J. Am. Chem. Soc.* **1995**, *117*, 233.

20. "Metal Catalyzed Cross-Coupling Reactions" Eds. F. Diederich and P. J. Stang, Weinheim; New York: Wiley-VCH, 1998.

21. (a) M. Rehahn, A. D. Schluter, G. Wegner, W. J. Feast, *Polymer* **1989**, *30*, 1054. (b) M. Ranger, M. Leclerc, *Chem. Commun.* **1997**, 1597. (c) G. Zotti, G. Schiavon, S. Zecchin, J. -F. Morin, M. Leclerc, *Macromolecules* **2002**, *35*, 2122. (d) B. Tsuie, J. L. Reddinger, G. A. Sotzing, J. Soloducho, A. R. Katritzky, J. R. Reynolds, *J. Mater. Chem.* **1999**, *9*, 2189. (e) J. Ding, M. Day, G. Robertson, J. Roovers, *Macromolecules* **2002**, *35*, 3474.

22. Z. Bao, W. Chan, L. Lu, *Chem. Mater.* **1993**, *5*, 2.

23. Metal-Catalyzed Cross Coupling Reactions; Eds: F. Diederich and P.J. Stang, Wiley-VCH, 1998.

24. H. G. Gilch, W. L. J. Wheelwright, *Polym. Sci. Part A. Polym. Chem.* **1966**, *4*, 1337.

25. (a) W. J. Swatos, B. Gordon, *Polym. Prepr.* **1990**, *30*, 505. (b) F. Wudl, P. M. Allemand, G. Srdanov, Z. Ni, D. McBranch, *ACS Symp. Ser.* **1991**, *455*, 683. (c) P. L. Burn, A. Kraft, D. R. Baigent, D. D. C. Bradley, A. R. Brown, R. H. Friend, R. W. Gymer, A. B. Holmes, R. W. Jackson, *J. Am. Chem. Soc.* **1993**, *115*, 10117.

26. (a) B. Hsieh, Y. Yu, A. C. VanLaeken, H. Lee, *Macromolecules* **1997**, *30*, 8094. (b) E. M. Sanford, A. L. Perkins, B. Tang, A. M. Kubasiak, J. T. Reeves, K. W. Paulisse, *Chem. Commun.* **1999**, 2347.

27. (a) W. J. Swatos, B. Gordon, *Polym. Prepr.* **1990**, *30*, 505. (b) P. L. Burn, A. W. Grice, A. Tajbhaksh, D. D. C. Bradley, A. C. Thomas, *Adv. Mater.* **1997**, *9*, 1171.

28. (a) R. A. Wessling, R. G. Zimmerman, US Patent 3,401,152, 1968. (b) R. A., Wessling, R. G. Zimmerman, US Patent 3,532,643, 1970. (c) R. Wessling, *J. Polym. Sci., Polym. Symp.* **1985**, *72*, 55. (d) C. Zhang, D. Braun, A. J. Heeger, *J. Appl. Phys.* **1993**, *73*, 5177.

29. J. Guillet, in "Photophysics and Photochemistry", 1985, Cambridge University Press, London.

30. (a) J. R. Lakowitz, in "Principles of Fluorescence Spectroscopy", 2nd edition, 1999, Kluwer Academic, New York. (b) M. Klessinger, J. Michl, in "Excited States and Photochemistry of Organic Molecules" New York: VCH, 1995.

31. D. F. Eaton, *Pure Appl. Chem.* **1988**, *60*, 1107.

32. (a) S. Hamai, F. Hirayama, *J. Phys. Chem.* **1983**, *87*, 83. (b) S. R. Meech, D. Phillips, *J. Photochem.* **1983**, *23*, 83. (c) W. H. Melhuish, *J. Phys. Chem.* **1961**, *65*, 229. (d) T. Karstens, K. Kobs, *J. Phys. Chem.*

1980, *84*, 1871.

33. (a) J. C. de Mello, H. F. Wittmann, R. H. Friend, *Adv. Mater.* **1997**, *9*, 230. (b) L. -O. Pålsson, A. P. Monkman, *Adv. Mater.* **2002**, *14*, 757.

34. M. Klessinger, J. Michl, in Excited States and Photochemistry of Organic Molecules; New York: VCH 1995.

35. G. M. Carter, J. V. Hryniewicz, M. K. Thakur, Y. J. Chen, M. E. Meyer, *Appl. Phys. Lett.* **1986**, *49*, 16.

36. H. Chosrovian, S. Rentsch, D. Grebner, D. U. Dahm, E. Birckner, H. Naarmann, *Synth. Met.* **1993**, *60*, 23.

37. (a) B. E. Kohler, B. West, *J. Chem. Phys.* **1983**, *79*, 583. (b) K. Migashita, M. Kaneto, *Macromol. Chem. Rapid Commun.* **1994**, *15*, 511.

38. S. Schmidt, M. L. Anderson, D. Dunphy, T. Wehrmeister, K. Müllen, N. R. Armstrong, *Adv. Mater.* **1995**, *7*, 722.

39. D. Beljonne, J. Cornil, R. H. Friend, R. A. J. Janssen, J. L. Brédas, *J. Am. Chem. Soc.* **1996**, *118*, 6453.

40. P. J. Brown, D. S. Thomas, A. Köhler, J. S. Wilson, J. -S. Kim, C. M. Ramsdale, H. Sirringhaus, R. H. Friend, *Phys. Rev. B* **2003**, *67*, 64203.

41. M. Pope, C. E. Swenberg, in Electronic processes in Organic Crystals, Oxford University Press, New York, 2nd edition, 1999.

42. J. B. Birks, in Photophysics of Aromatic Molecules, Wiley Interscience, London, 1970.

43. U. Lemmer, S. Heun, R. F. Mahrt, U. Scherf, M. Hopmeier, U. Siegner, E. O. Gobel, K. Mullen, H. Bassler, *Chem. Phys. Lett.* **1995**, *240*, 373.

44. (a) S. A. Jenekhe, J. A. Osaheni, *Science* **1994**, *265*, 739. (b) J. A. Osaheni, S. A. Jenekhe, *Macromolecules* **1994**, *27*, 739.

45. (a) M. Pope, C. E. Swenberg in Electronic Processes in Organic Crystals and Polymers, Oxford University Press, New York, 2nd Edition, 1999. (b) J. Cornil, D. A. dos Santos, X. Crispin, R. Silbey, J. L. Brédas, *J. Am. Chem. Soc.* **1998**, *120*, 1280. (c) G. Gigli, F. Della Sala, M. Lomascolo, M. Anni, G. Barbarella, A. Di Carlo, P. Lugli, R. Cingolani, *Phys. Rev. Lett.* **2001**, *86*, 167.

46. B. Xu, S. Holdcroft, *Macromolecules* **1993**, *26*, 4457.

47. W. A. Goedel, N. S. Somanathan, V. Enkelmann, G. Wegner, *Makromol. Chem.* **1992**, *193*, 1195.

48. M. Theandher, O. Inganäs, W. Mammo, T. Olinga, M. Svensson, M. R. Andersson, *J. Phys. Chem. B* **1999**, *103*, 7771.

49. (a) S. Vaidyanathan, H. Dong, M. E. Galvin. *Synth. Met.* **2004**, *142*, 1. (b) J. Teetsov, M. A. Fox, *J. Mater. Chem.* **1999**, *9*, 2117. (c) H. Cheun, B. Tanto, W. Chunwaschirasiri, B. Larson, M. J. Winokur, *Appl. Phys. Lett.* **2004**, *84*, 22.

50. (a) K. M. Vaeth, C. W. Tang, *J. Appl. Phys.* **2002**, *92*, 3447. (b) C. H. Chen, C. W. Tang, *Appl. Phys. Lett.* **2001**, *79*, 3711. (c) C. H. Chen, C. W. Tang, J. Shi, K. P. Klubek, *Thin Solid Films* **2000**, *363*, 327. (d) C. H. Chen, K. P. Klubek, S. A. Van Slyke, C. W. Tang, *Proceedings of SPIE-The International Society for Optical Engineering* **1998**, *3421*, 78. (e) C. H. Chen, C. W. Tang, J. Shi, P. Klubek, *Macromolecular Symposia* **1998**, *125*, 49.

51. T. Virgili, D. G. Lidzey, D. D. C. Bradley, *Adv. Mater.* **2000**, *12*, 58.

52. (a) J. -S. Kim, P. K. H. Ho, C. E. Murphy, R. H. Friend, *Macromolecules* **2004**, *37*, 2861-2871. (b) L. C. Palilis, D. G. Lidzey, M. Redecker, D. D. C. Bradley, M. Inbasekaran, E. P. Woo, W. W. Wub, *Synth. Met.* **2000**, *111*, 159. (c) G. He, J. Liu, Y. Li, Y. Yang, *Appl. Phys. Lett.* **2002**, *80*, 1891. (d) J. Liu, Y. Shi, Y. Yang, *Appl. Phys. Lett.* **2001**, 578.

53. (a) C. Ego, D. Marsitzky, S. Becker, J. Zhang, A. C. Grimsdale, K. Müllen, D. J. MacKenzie, C. Silva, R. H. Friend, *J. Am. Chem. Soc.* **2003**, *125*, 437 (c) Q. Hou, Y. Xu, W. Yang, M. Yuan, J. Peng, Y. Cao, *J. Mater. Chem.* **2002**, *12*, 2887-2892. (d) M. S. Liu, J. Luo, A. K.-Y. Jen, *Chem. Mater.* **2003**, *15*, 3496-3500. (e) M. Theander, T. Granlund, D. M. Johanson, A. Ruseckas, V. Sundström, M. R. Andersson, O. Inganäs, *Adv. Mater.* **2001**, *13*, 323. (f) T. M. Swager, C. J. Gil, M. S. Wrighton, *J. Phys. Chem.* **1995**, *99*, 4886.

54. (a) M. Berggren, O. Inganäs, G. Gustafsson, J. Rasmusson, M. R. Andersson, T. Hjertberg, O.Wennerström, *Nature* **1994**, *372*, 444. (b) S. Tasch, C. Hochfilzer, E. J. W. List, G. Leising, H. Quante, P. Schlichting, U. Rohr, Y. Geerts, U. Scherf, K. Müllen, *Phys. Rev. B.* **1997**, *56*, 4479.

55. (a) Y. Hamada, H. Kanno, T. Tsujioka, H. Takahashi, T. Usuki, *Applied Physics Letters* **1999**, *75*, 1682. (b) H. Kanno, Y. Hamada, H. Takahashi, *ieee Journal of Selected Topics in Quantum Electronics* **2004**, *10*, 30.

56. (a) M. Bernius, M. Inbasekaran, E. Woo, W. Wu, L. Wujkowski, *Journal of Materials Science: Materials in Electronics* **2000**, *11*, 111. (b) M. T. Bernius, M. Inbasekaran, J. O'Brien, W. Wu, *Adv. Mater.* **2000**, *12*, 1737 and references therein.

57. Organic Light-Emitting Devices: A Survey; Ed: Joseph Shinar, New York: Springer, 2004.

58. (a) M. Grell, D. D. C. Bradley, X. Long, T. Chamberlain, M. Inbasekaran, E. P. Woo, M. Soliman, *Acta. Polym.* **1998**, *49*, 439. (b) K.-H. Weinfurtner, H. Fujikawa, S. Tokito, Y. Taga, *Appl. Phys. Lett.* **2000**, *76*, 2502.

59. (a) E. J. W. List, U. Scherf, *Adv. Mater.* **2002**, *14*, 477. (b) L. Romaner, A. Pogantsch, P. Scandiucci de Freitas, U. Scherf, M. Gaal, E. Zojer, E. J. W. List, *Adv. Funct. Mater.* **2003**, *13*, 597.

60. J. H. Lee, D. H. Hwang, *Chem. Commun.* **2003**, 2836.

61. C. -H. Chou, C.-F. Shu, *Macromolecules* **2002**, *35*, 9673.

62. J. Li, Z. Bo, *Macromolecules* **2004**, *37*, 2013.

63. A. P. Kulkarni, S. A. Jenekhe, *Macromolecules* **2003**, *36*, 5285.

64. G. Klärner, J. -I. Lee, V. Y. Lee, E. Chan, J.-P. Chen, A. Nelson, D. Markiewicz, R. Siemens, J. C. Scott, R. D. Miller, *Chem. Mater.* **1999**, *11*, 1800.

65. G. Klärner, M. H. Davey, W. -D. Chen, J. C. Scott, R. D. Miller, *Adv. Mater.* **1998**, *10*, 993.

66. (a) S.Tirapattur, M. Belletête, N. Drolet, M. Leclerc, G. Durocher, *Chemical Physics Letters* **2003**, *370*, 799. (b) Y. Li, J. Ding, M. Day, Y. Tao, J. Lu, M. D'iorio, *Chem. Mater.* **2003**, *15*, 4936.

67. S. Holdcroft, *Adv Mater* **2001**,*13*,1753 and references therein.

68. (a) M. S. A. Abdou, Z. W. Xie, A. Leung, S. Holdcroft, *Synth. Met.* **1992**, *52*, 159. (b) M. S. A. Abdou, S. Holdcroft, *Macromolecules* **1993**, *26*, 2954. (c) M. S. A. Abdou, M. I. Arroyo, G. Diaz-Quijada, S. Holdcroft, *Chem. Mater.* **1991**, *3*, 1003.

69. (a) J. Yu, S. Holdcroft, *Macromolecules* **2000**, *33*, 5073. (b) J. Yu, M. Abley, C. Yang, S. Holdcroft, *Chem. Commun.* **1998**, 1503. (c) J. Yu, S. Holdcroft, *Chem. Mater.* **2002**, *14*, 3705. (d) J. Yu, S. Holdcroft, *Chem. Mater.* **2001**, *13*, 526.

70. T. R. Hebner, C. C. Wu, D. Marcy, M. H. Lu, J. C. Sturm, *Appl. Phys. Lett.* **1998**, *72*, 519

71. D. A. Pardo, G. E. Jabbour, N. Peyghambarian, *Adv. Mater.* **2000**,*12*,1249.

72. C. D. Müller, A. Falcou, N. Reckefuss M. Rojahn, V. Wiederhirn, P. Rudati, H. Frohne, O. Nuyken, H. Becker, K. Meerholz, *Nature* **2003**, *421*, 829.

Chapter 2.

Tuning Optical Properties of Poly(thiophene)s and Poly(*p*-phenylenevinylene)s via Post-functionalization

Sections of this Chapter have been reproduced in part with permission from:

- *Macromolecules* **2001**, *34*, 141
- *Macromolecules* **2001**, *34*, 3130
- *Macromolecules* **2002**, *35*, 6900
- *Chem. Mater.* **2002**, *14*, 1424
- In Chromogenic Phenomena in Polymers: Tunable Optical Properties. An American Chemical Society Publication. 2004, Eds. S.A. Jenekhe and D.J. Kiserow. Oxford University Press. Chapter 17.

Note: Synthetic portions were primarily performed by Dr. Yuning Li.

2.1 Introduction

Conjugated polymers with tunable structures and properties are desirable for large area polymer LED applications. One possible facile approach towards tailored structures and tunable properties is by post-functionalization of conjugated polymers, where reactions are performed on the polymers themselves, rather than the cumbersome monomer synthesis approach. This post-functional approach has been applied extensively to conventional non conjugated polymers. Such a methodology applied to conjugated polymers would considerably simplify the procedures for acquiring complex structures and greatly diversify the functional groups available – since many monomers cannot survive the harsh polymerization techniques.

In recent years, the use of post-functionalization of conjugated polymers (polyacetylene,[1] polyaniline,[2] polypyrrole,[3,4b] and poly(thiophene)s[5]) as a method to modify the polymers' properties has drawn attention. However, the post-functional method employed was electrochemical, which limits its applicability.

In this chapter, post-functionalization of poly(thiophene)s (Part 1, Section 2.2.1) and poly(p-phenylenevinylene)s (Part 2, Section 2.2.2) are investigated as a facile alternative approach to tune the optical properties and to increase the luminescence efficiency.

2.2 Results and Discussion

2.2.1 Part 1: Poly(thiophene)s

The *nucleophilic* substitution of over-oxidized poly(thiophene)s with Cl, Br, or methoxy groups in the 4-position using an electrochemical method has been investigated.[4] On the basis of electronic effects alone, however, the 4-position of the thiophene ring in poly(3-alkylthiophene)s (P3ATs) should be more susceptible to *electrophilic* substitution due to the high electron density on the backbone that originates from the extended π-system and the electron donating effect of the 3-alkyl side chain. The replacement of the hydrogen on the 4-position of P3ATs by functional groups *via* electrophilic substitution, and further derivatization employing Pd-catalyzed cross coupling methods, should provide a useful strategy to tailor the structure and the band gap of the polymers and therefore control their electro-optical properties.

Previous studies on poly(thiophene)s indicated that they are generally poor emitters for PLEDs.[6] Interchain interactions are considered largely responsible for the drastic decrease of quantum yield of the polymer films compared with polymer solution as described in Section 1.4.1.2. In the first part of this chapter, post-fuctionalization is applied to obtain poly(thiophene)s with favored structures for improved luminescence properties. To that end, the steric and electronic effects of incorporated functional groups on the optical properties of the polymers are discussed.

2.2.1.1 Synthesis

2.2.1.1.1 Electrophilic Aromatic Substitution

As illustrated in Scheme 2.1, when regioregular P3HT was treated with *N*-bromosuccinimide (NBS), a yellow solid was obtained in 99% yield after work-up.

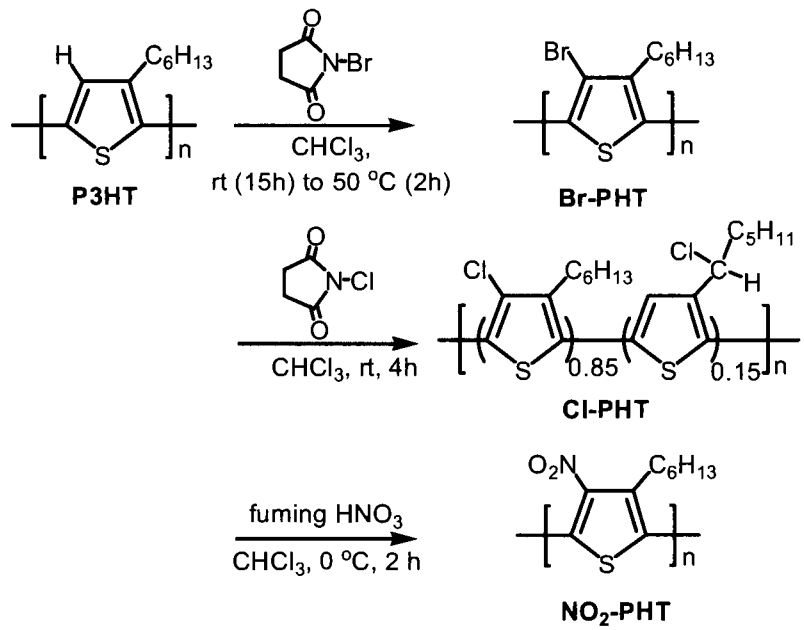

Scheme 2.1: Electrophilic aromatic substitution of poly(3-hexylthiophene).

The ^{1}H NMR spectrum of this product showed the disappearance of the aromatic hydrogens of P3HT (at 6.99 ppm) and a slight shift of the α-methylene hydrogen peak of the hexyl group from 2.80 to 2.71 ppm (Figure 2.1). A minor peak at 2.85 ppm was ascribed to the α-methylene group in terminal units. The disappearance of signals for the aromatic carbons of P3HT, the appearance of four new peaks in the aromatic region (at 142.66, 130.38, 129.41, and 115.81 ppm) in the ^{13}C NMR spectrum, IR spectroscopy, and elemental analysis (see the Experimental Section) indicated the product to be poly(3-bromo-4-

hexylthiophene) (Br-PHT). Similarly, using N-chlorosuccinimide (NCS) produced the chlorinated product poly(3-chloro-4-hexylthiophene) (Cl-PHT) in 98% yield based on 100% substitution. No aromatic hydrogens corresponding to P3HT remained in the product, but a small peak at 7.31 ppm was observed in the ^{1}H NMR spectrum (Figure 2.1). Two minor peaks at 5.02 and 2.10 ppm (and two minor peaks at 56.83 and 39.95 ppm in ^{13}C NMR spectrum) were assigned to α-methylene and, β-methylene hydrogens of the side chain, respectively, using DEPT and ^{1}H-^{13}C COSY. It is thus concluded that ~85% of the aromatic hydrogens of P3HT are substituted with chlorine, while 15% of α-methylene hydrogens of the hexyl group are chlorinated, presumably through a free radical mechanism.[7] The chlorination of the methylene hydrogen is believed to sterically prevent further substitution of the aromatic hydrogen on the same thiophene ring as shown in Scheme 2.1.

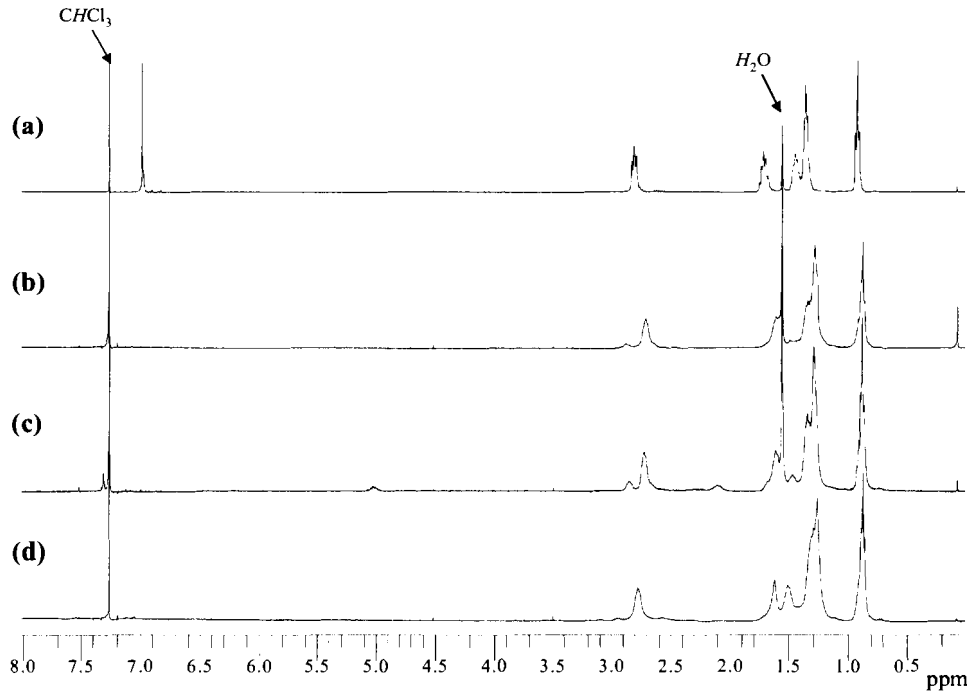

Figure 2.1: 400 MHz ^{1}H NMR spectra of (a) P3HT, (b) Br-PHT, (c) Cl-PHT, and (d) NO_2-PHT.

2.2.1.1.2 Pd-catalyzed Cross Coupling

Since the brominated polymer is reactive towards Pd-catalyzed cross coupling methods, these polymers were further post-functionalized *via* Suzuki coupling.

Suzuki coupling of phenylboronic acid with Br-PHT was conducted in THF at 80 °C in the presence of Na_2CO_3 and 2% equiv of $Pd(PPh_3)_4$ for 48 h (Scheme 2.2). The phenyl substituted P3HT (Ph-PHT) showed the emergence of aromatic protons at 7.27 and 7.15 ppm in the ^{1}H NMR spectrum (Figure 2.2). All protons of the hexyl group shifted upfield compared to those of Br-PHT, for example, α-methylene protons shifted from 2.72 to 2.26 ppm. From the integrals of the

aromatic and -CH_3 protons, the substitution of Br by phenyl was estimated to be >99%, a value consistent with elemental analysis (Br < 0.3%). Other *para*- or *meta*-substituted phenylboronic acids, 1-naphthylboronic acid, and 2-thiopheneboronic acid also reacted quantitatively with Br-PHT, indicating that these reactions are tolerant to other functional groups. It is noteworthy that more bulky *ortho*-substituted reagents, 2-methylphenylboronic acid and 2-methoxyphenylboronic acid, also reacted quantitatively with Br-PHT to give products o-Tolyl-PHT and 2-MeOPh-PHT, even though these reactions are subject to steric congestion. With this approach, a variety of 3,4-disubstituted polymers containing various functional groups (

Figure 2.3) were obtained. The complete substitution of bromo groups was confirmed by NMR spectroscopy and elemental analysis.

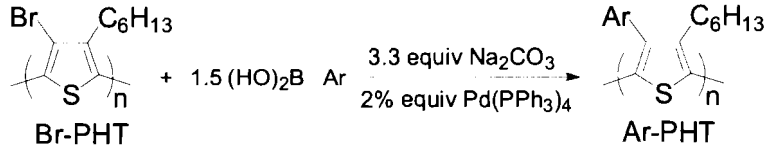

Scheme 2.2: Pd-catalyzed cross coupling of Br-PHT.

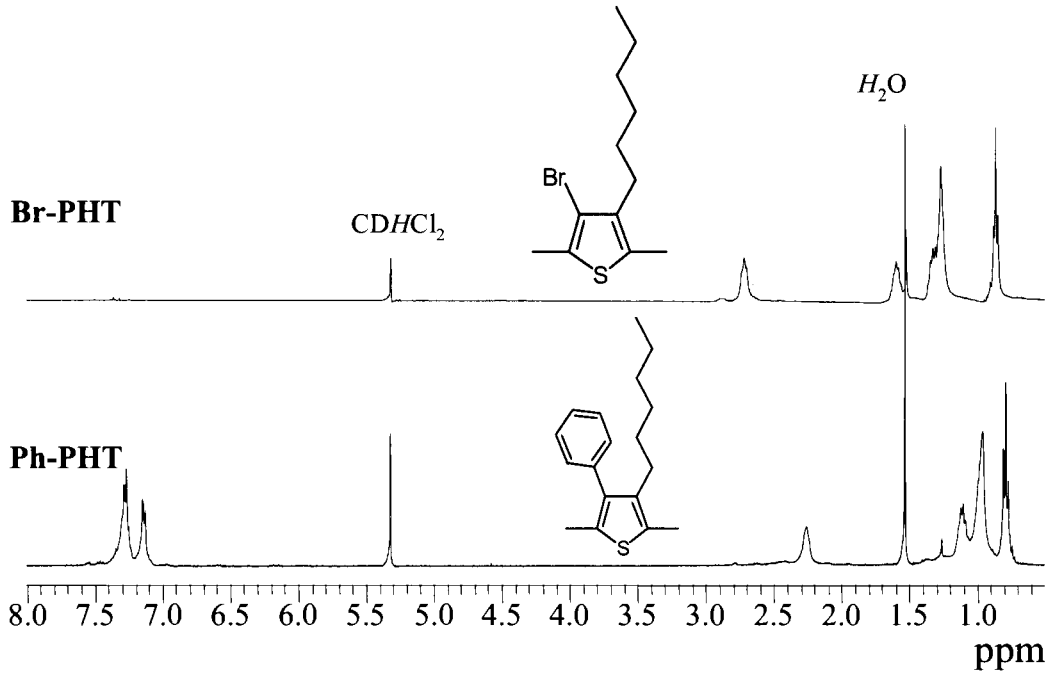

Figure 2.2: The 400 MHz ^{1}H NMR spectra of P3HT (in $CDCl_3$) Br-PHT and Ph-PHT (in CD_2Cl_2).

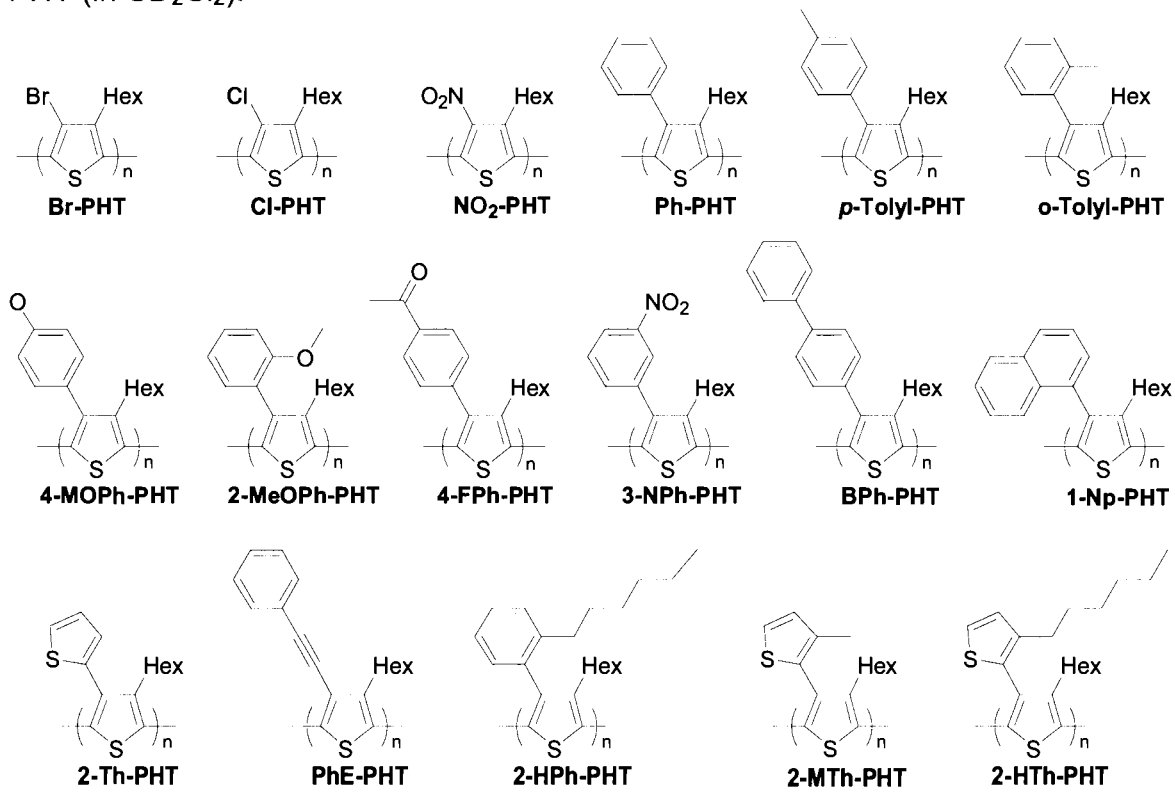

Figure 2.3: 3,4-Disubstituted poly(thiophene)s.

2.2.1.2 Photophysical Properties

As shown in Table 2.1, the absorption spectrum of Br-PHT is blue-shifted (λ_{max}, 339 nm) with respect to that of P3HT, indicating an increased degree of twisting in the polymer backbone. A decrease in Φ_{pl} to 4% in solution (40.1% for P3HT) is observed because of the shortened conjugation length, a reduction in the rigidity of the polymer, and possibly the heavy-atom effect[10] of bromine. The solid-state Φ_{pl} of Br-PHT is not appreciably improved (Φ_{pl}, 1.8%) compared to that of P3HT (Φ_{pl},1.6%), despite its twisted structure, an observation explained in terms of the heavy-atom effect. On the other hand, the chlorinated product Cl-PHT shows a smaller blue shift in absorption λ_{max}, compared to Br-PHT, and a much higher Φ_{pl} (solution, 12%; solid state, 5.1%). The weaker heavy-atom effect of chlorine, a relief in steric congestion due to the smaller size of chloro group, and/or the different degree of substitution might contribute to the above result. More dramatic still, the introduction of a nitro group at the 4 position of the thiophene ring results in the virtual absence of fluorescence emission, indicating that the nitro group is a strong quencher of emission.[9]

Replacing the bromo group in Br-PHT with phenyl to produce Ph-PHT causes the λ_{max} of absorption to red shift from 344 to 369 nm for polymers in the solid state. The Φ_{pl} increases from 4 to 7.9% in solution and from 1.8 to 3.2% in the solid state (Table 2.1). The attachment of electron donating 4-methyl and 4-methoxy groups to the phenyl ring, forming p-Tolyl-PHT and 4-MOPh-PHT, respectively, has little influence either on λ_{max} (≤4nm, solid state) for absorption and emission (≤3nm, solid state) or on Φ_{pl} (within error) when compared to the

corresponding values for Ph-PHT. This similarity indicates that the phenyl group is electronically isolated from the π-conjugated polythiophene backbone. BPh-PHT, which contains biphenyl substituents, exhibits two absorption peaks: one at 275 nm and the other at 360 nm. The former coincides precisely with that of the biphenyl group, whereas the latter is due to the backbone π system. Furthermore, the absorption and emission profiles originating from excitation of the polymer backbone are similar to those of Ph-PHT. Like the phenyl, p-tolyl, and 4-methoxyphenyl substituents, the biphenyl groups in BPh-PHT appear to act as isolated chromophores. This can only be possible if the chromophores lie perpendicular to the thiophene ring. Introduction of the electron withdrawing 4-formyl group on the phenyl ring (4-FPh-PHT) causes a slight blue shift in absorption λ_{max} and a decrease in solution Φ_{pl} (3.4%). Substitution of Br with 3-nitrophenyl (3-NPh-PHT) causes a slight blue shift in absorption λ_{max} relative to that of Ph-PHT, but it also results in the absence of fluorescence, even though the nitro group at the meta position is virtually electronically isolated from the polymer backbone. The 2-thienyl substituted polymer (2-Th-PHT) exhibits absorption and emission maxima in a range similar to those of the phenyl derivatives. Another derivative, the phenylethynyl- substituted polymer (PhE-PHT), however, displays large red shifts in absorption λ_{max} (403 nm, solution; 410 nm, solid state) as a result of the linear ethynyl group alleviating steric repulsion. This facilitates planarity of the polymer backbone, which, together with the electron-donating effect of the phenylethynyl groups, narrows the band gap. The observed electronic effect of the ethynyl group, more pronounced than the effects

of other substituents, is due to efficient overlapping of linear sp orbitals with the main-chain π system. The Φ_{pl} of this polymer (7%, solution; 4%, solid state) is not appreciably different from that of Ph-PHT. Some representative spectra in the solid state are illustrated in Figure 2.4.

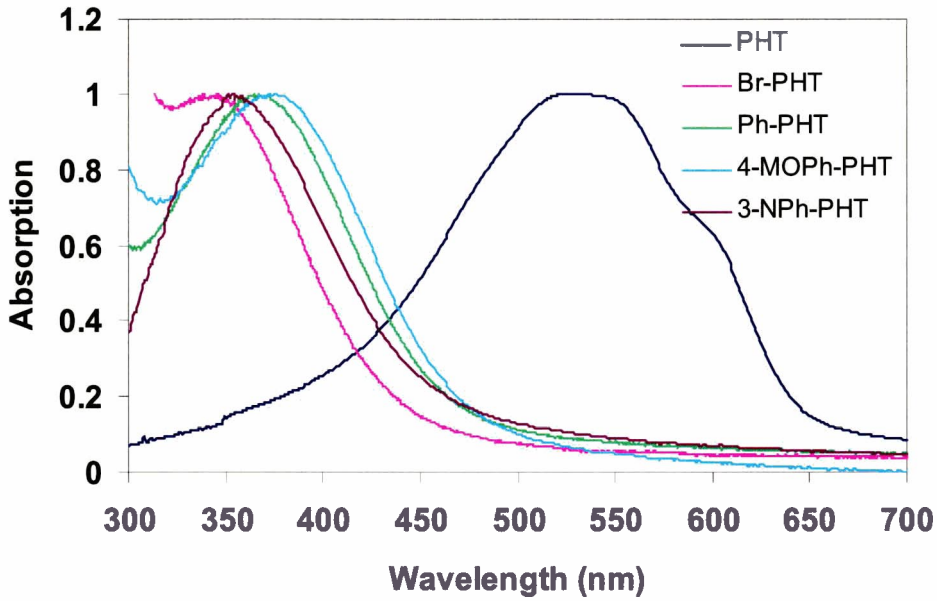

Figure 2.4: Solid state absorption spectra of substituted PHTs: electronic effects

A significant deviation from the above trends is observed for the o-tolyl-substituted polymer (o-Tolyl-PHT). This polymer exhibits a large red shift in λ_{max} and unusually high solution and solid-state values of Φ_{pl} (20.8 and 19.4%, respectively) compared to Ph-PHT. The solid-state Φ_{pl} is an order of magnitude higher than those of P3HT (1.6%) and Br-PHT (1.8%). The optical properties of these polymers are illustrated in Figure 2.5.

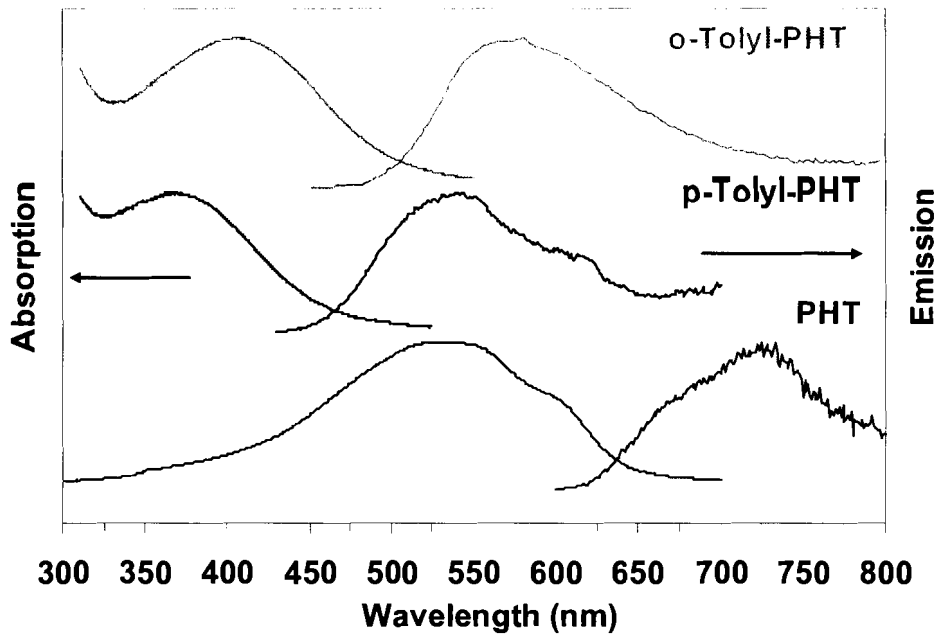

Figure 2.5: Optical properties of substituted PHTs: steric effects

The difference in the optical properties of these polymers is interpreted with the aid of space filling models - as illustrated in Figure 2.6 - and is attributed to the steric effect of the o-tolyl substituent. The steric interaction of the o-tolyl group with the hexyl substituent on the juxtaposed thienyl ring and with the neighboring sulfur atom, reinforces the orthogonality of the phenyl ring with respect to the thienyl ring. The methyl group of o-Tolyl-PHT can come into such close proximity to the sulfur atom that it restricts rotation or twisting of the interannular bond between the two thienyl rings. This conformation forces the polymer backbone to become planar and promotes a red shift in λ_{max}. In addition, the methyl group, together with a near-perpendicular phenyl ring, functions as a molecular spacer that enlarges the distance between stacks of polymer chains and, hence, increases the solid state value of Φ_{pl}. Figure 2.6 also illustrates that

a similar interaction between the phenyl group (in Ph-PHT) and the adjacent thienyl sulfur is absent. Thus, twisting of the main chain is impeded to a lesser extent in Ph- PHT than it is in o-Tolyl-PHT. Thus, a shorter wavelength of absorption and a lower solid-state Φ_{pl} value is observed for Ph-PHT. This explanation is supported by the fact that p-Tolyl-PHT, which contains a methyl group in the para position, i.e., far removed from the possibility of a methyl-thienyl sulfur interaction, exhibits properties akin to those of Ph-PHT and not those of o-Tolyl-PHT.

polymer	solution, THF			film		
	$\lambda_{max, abs.}$ (nm)	$\lambda_{max, em.}$ (nm)	Φ_{pl} (%)	$\lambda_{max, abs.}$ (nm)	$\lambda_{max, em.}$ (nm)	Φ_{pl} (%)
P3HT	442	571	40.1	550	660, 730	1.6
Br-PHT	339	504	4.0	344	520	1.8
Cl-PHT	357	516	12.0	365	527	5.1
NO_2-PHT	338	556	0.3			
Ph-PHT	363	528	7.9	369	553	3.2
p-Tolyl-PHT	364	529	8.0	368	550	3.3
o-Tolyl-PHT	400	545	20.8	410	556	19.4
4-MOPh-PHT	367	531	8.2	375	538	3.0
2-MOPh-PHT	367	535	9.7	376	545	4.4
4-FPh-PHT	350	540	3.4	360	540	2.5
3-NPh-PHT	354		~0	356		~0
BPh-PHT	275	360	1.1			
	360	531	5.8	367	538	3.3
1-Np-PHT	370	540	8.8	378	542	2.6
2-Th-PHT	370	540	8.8	378	542	5.0
PhE-PHT	403	567	7.0	415	602	4.0
2-HPh-PHT	413	555	25.1	422	583	19.6
2-MTh-PHT	401	544	12.8	405	558	9.0
2-HTh-PHT	404	544	14.2	410	555	13.9

Table 2.1: Photophysical Properties of 3,4-Disubstituted Poly(thiophene)s

Polymers 2-MOPh-PHT, 4-MOPh-PHT, and 1-Np-PHT, which contain o-methoxyphenyl, p-methoxyphenyl, and 1-naphthyl, respectively, also display optical and luminescence properties that are very similar to those of Ph-PHT even though these substituents are considerably bulkier than a simple phenyl. Although the o-methoxy group is not too dissimilar to o-tolyl, Figure 2.6 illustrates that the oxygen atom is too small, and the methyl group too far removed from the polymer backbone, to limit rotation of the backbone *via* interaction with the main-chain sulfur atom. In the case of 1-Np-PHT, Figure 2.6 illustrates that the 1-naphthyl group is too planar to interact with the adjacent sulfur atom. The above observations indicate that a subtle variation in the size or shape of the substituents greatly impacts the backbone conformation and ultimately its optical and photophysical properties. In the case of o-Tolyl-PHT, the methyl hydrogens on the o-tolyl group are in such a position that rotation of the polymer backbone is limited.

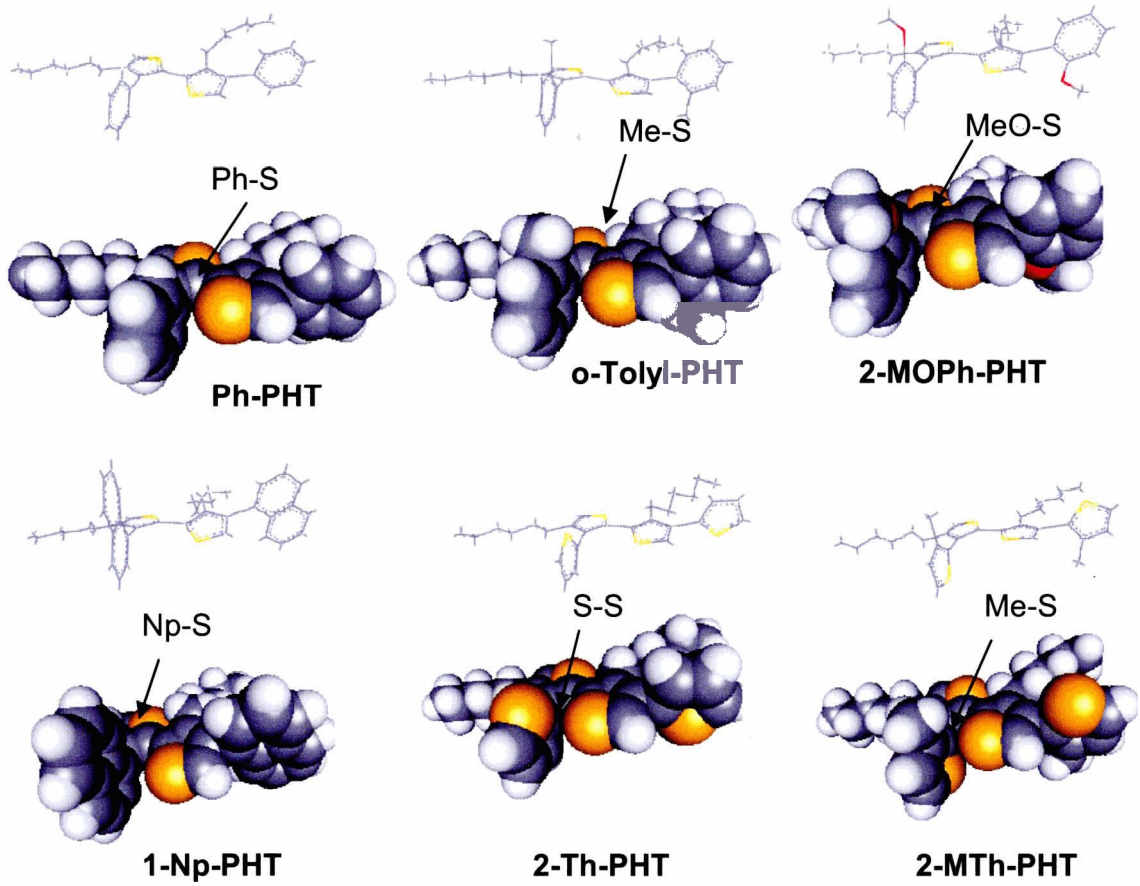

Figure 2.6: Illustrative molecular models of diad units for various polymers. The arrows highlight the presence or absence of steric interactions of substituents with the neighboring sulfur atom.

To test this hypothesis, several structural analogues of o-Tolyl-PHT, namely, 2-HPh-PHT, 2-MTh-PHT, and 2-HTh-PHT, were designed and synthesized using Br-PHT as the base polymer (see Scheme 2.2). A common structural feature of 2-HPh-PHT, 2-MTh-PHT, and 2-HTh-PHT is the alkyl substituent on the phenyl or thienyl side group having a point of attachment that is juxtaposed to the polymer chain. Solution and film spectra of 2-HPh-PHT are slightly red-shifted by 12-13 nm (λ_{max}, 413 and 422 nm, respectively) with respect to those of o-Tolyl-PHT, and Φ_{pl} increases to 25.1% in solution, indicating that the

longer alkyl side chain on the phenyl group further increases the planarity and rigidity of the backbone. The solid-state Φ_{pl} (19.6%) is similar to o-Tolyl-PHT. A similar red shift in optical absorption is observed for 2-(3-methyl)thienyl and 2-(3-hexyl)thienyl groups. For example, λ_{max} values in solution are 401 nm for 2-MTh-PHT and 404 nm for 2-HTh-PHT compared to 370 nm for the 2-thienyl-substituted polymer 2-Th-PHT. Quantum yields of luminescence values for 2-MTh-PHT and 2-HTh-PHT are 12.8 and 14.2% in solution and 9.0 and 13.9% in the solid state, respectively. These values are much higher than those for 2-Th-PHT (8.8%, solution; 5.0%, solid state). Similarly to the case of o-Tolyl-PHT vs Ph-PHT, the methyl hydrogens on the 2-methylthienyl group of 2-MTh-PHT can sterically interfere with the sulfur on the adjacent main-chain thienyl group thus limiting rotation about the main-chain interannular bond (see Figure 2.6). A similar argument can be made for 2-HTh-PHT and 2-HPh-PHT, where the hexyl α-methylene hydrogens of the 2-hexylthienyl and 2-hexylphenyl substituents might interact with the neighboring main-chain sulfur atom.

Although o-alkylphenyl- and 2-(3-alkyl)thienyl-substituted polymers exhibit red-shifted absorption spectra relative to Ph-PHT or 2-Th-PHT, their effective conjugation lengths, as judged by the absorption and emission spectra, are nevertheless lower than that of the parent polymer P3HT. Because fluorescence quantum efficiency is perceived to increase with conjugation length in poly(thiophene)s,[10] it was considered that partial substitution of P3HT would allow for a more conjugated structure, providing a means to increase Φ_{pl} and, at the same time, tune emission wavelengths. Partial substitution of P3HT was

achieved by partial bromination of P3HT followed by the appropriate Suzuki coupling. As shown in Table 2.2, a series of partially brominated P3HT polymers (0-100% bromination) was synthesized. The solution absorption λ_{max} values of these partially brominated poly(thiophene)s decrease linearly (R^2 = 0.9924) with increased Br content, as illustrated in Figure 2.8 (□ series). Furthermore, the absorption λ_{max} values of the polymer films varied between 550 nm (0% bromination, P3HT) and 344 nm (100% bromination, Br-PHT). The solution Φ_{pl} values decreased from 40.1 to 4% as the degree of substitution increased from 0 to 100%. In contrast, the solid-state Φ_{pl} showed no clear trends except that substituted polymers generally exhibit higher values.

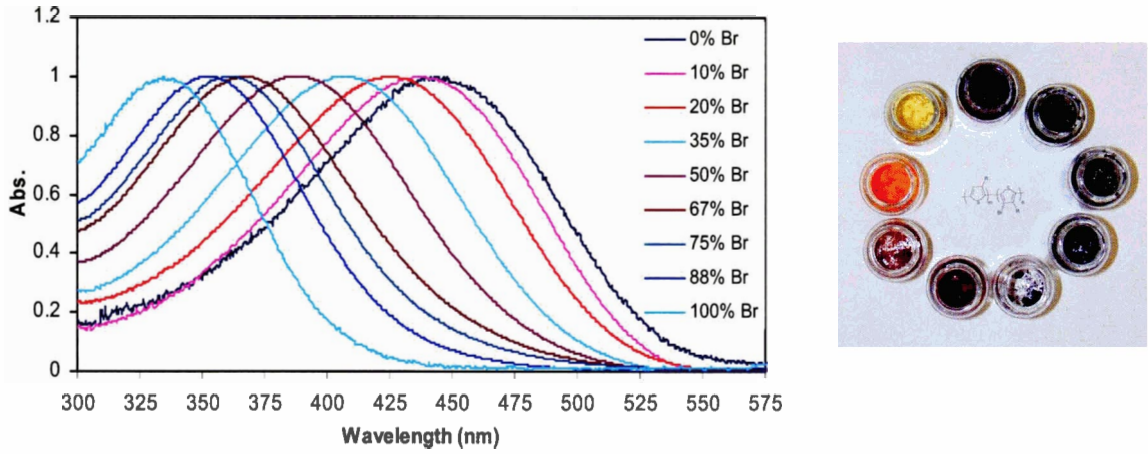

Figure 2.7: Solution absorption spectra of bromo-substituted P3HTs (left), picture of these polymers.

polymer	solution, THF			film		
	$\lambda_{max, abs.}$ (nm)	$\lambda_{max, em.}$ (nm)	Φ_{pl} (%)	$\lambda_{max, abs.}$ (nm)	$\lambda_{max, em.}$ (nm)	Φ_{pl} (%)
Br-PHT0[a]	442	571	40.1	550	660, 730	1.6
10	439	570	36.7	535	710	1.8
20	425	570	32.3	515	718	3.2
38	408	561	27.6	433	656	1.8
50	388	556	20.9	405	620	5.0
67	367	548	11.9	378	590	3.6
75	359	535	9.4	370	571	4.0
89	352	520	6.3	359	559	4.4
100[b]	339	504	4.0	344	520	1.8
o-Tolyl-PHT0[a]	442	571	40.1	550	660, 730	1.6
10	444	570	35.7	537	710	2.5
20	442	570	34.2	528	708	3.1
38	437	569	28.2	492	700	4.4
50	432	566	24.2	460	640	12.8
67	430	566	31.0	462	638	13.2
75	420	563	30.2	437	610	20.5
89	418	561	27.8	432	593	22.3
100[c]	400	545	20.8	410	556	19.4

[a] P3HT in Table 2.1.[b] Br-PHT in Table 2.1.[c] *o*-Tolyl-PHT in Table 2.1.

Table 2.2: Photophysical Properties of Partially Substituted P3HT

Substitution of the bromo groups in the brominated polymers by o-tolyl groups yields the corresponding partially substituted o-Tolyl-PHT polymers. The λ_{max} of absorption decreases with increasing degree of substitution from 442 to 400 nm in solution and from 550 to 410 nm in the solid state, but the decrease is less pronounced than that for the corresponding brominated derivatives. The Φ_{pl} of the corresponding polymer solutions generally decreases with increasing degree of substitution, but the solid-state Φ_{pl} increases, reaching a maximum value of 22.3% for o-Tolyl-PHT89, as depicted in Figure 2.8 (● series). In addition, the emission wavelengths of polymers are generally red shifted

compared to those of the corresponding Br substituted polymers. Emission spectra of polymer films having a degree of substitution between 50 and 100% are shown in Figure 2.9. The emission wavelengths range from 556 to 640 nm.

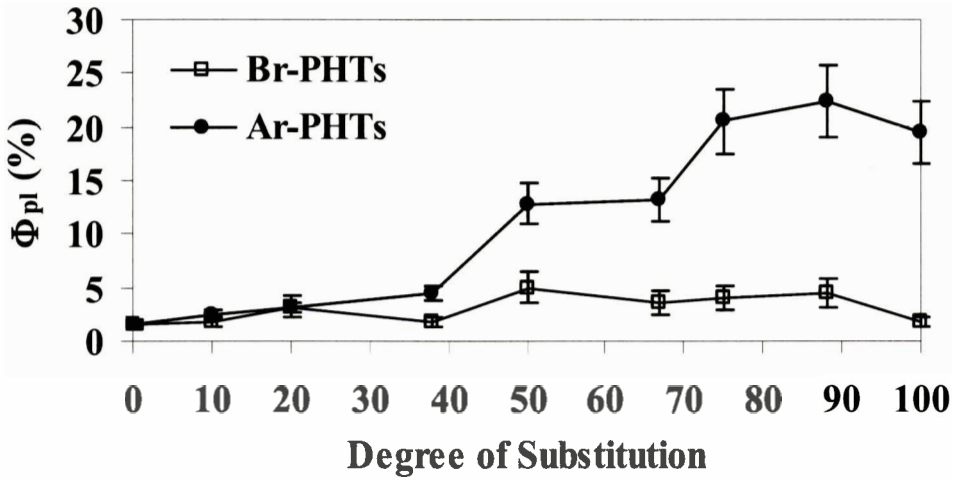

Figure 2.8: Solid state Φ_{pl} (%) trends, as a function of degree of substitution

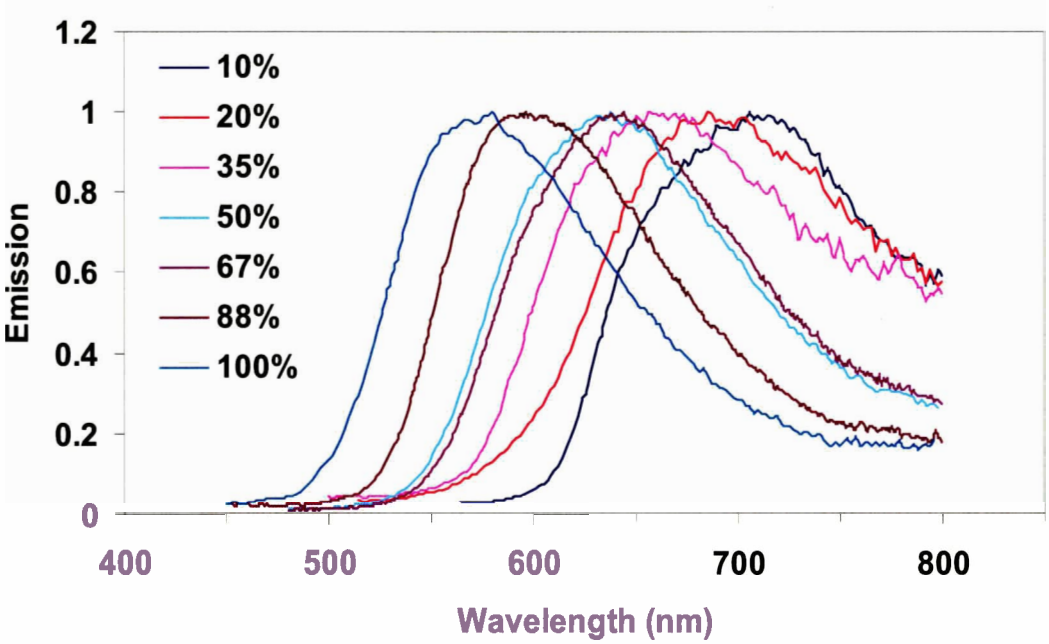

Figure 2.9: Solid state photoluminescence spectra of Ar-PHT series, percentages represent the degree of substitution.

XRD patterns of various solution cast o-Tolyl-PHT films are shown in Figure 2.10. The XRD pattern of P3HT (Figure 2.10a) exhibits typical diffraction peaks corresponding to lamellae formation (a axis, d spacing of 16.1 Å).[11,12] The anisotropic nature of the pattern (see inset) and the absence of a peak originating from π stacking (b axis) indicates that the chains are orientated with their a axis perpendicular to the plane of the substrate. This is also observed for o-Tolyl-PHT polymers containing 10 and 20% substitution, as evidenced by strong first-order reflections at 2θ = 5.35° and 5.19°, indicative of 16.5- and 17.0-Å lamellar spacings, respectively. These a-axis values are larger than the original d spacing corresponding to P3HT, as illustrated in Figure 2.11, indicating that the o-tolyl group interferes with interdigitation of the hexyl side chains.[11c,13] The XRD pattern of o-Tolyl-PHT38 also provides evidence that the o-tolyl groups disrupts semi-crystallinity. Two broad amorphous peaks are observed: the first superimposed on the first-order reflection at 5.19°; and second, at 20.8°. The isotropic nature of the XRD pattern, as can be inferred from the inset of Figure 2.10d, illustrates that a transition occurs from an ordered polymer with its a axis perpendicular to the substrate to one that exhibits no preferential surface ordering. For o-Tolyl-PHT50, the peak at 2θ = 5.25°, which represents a d-spacing of 16.8 Å, is much weaker, and two broad peaks at 2θ = 6.0° and 20.4°, which correspond to the calculated d-spacings of 14.7 and 4.3 Å, respectively, become pronounced. As the degree of substitution is further increased from 50 to 100%, the XRD patterns become weaker, and the position of the second amorphous diffraction/scattering halo at

~20° remains unchanged in its position, whereas the first broad peak shifts incrementally from 6.0° (d spacing, 14.7 Å) to 7.6° (d spacing, 11.7 Å) to reflect changes in short-range packing of polymer chains. The increasing amorphous nature of polymers with increasing degree of substitution implies that π-π interactions are progressively suppressed.

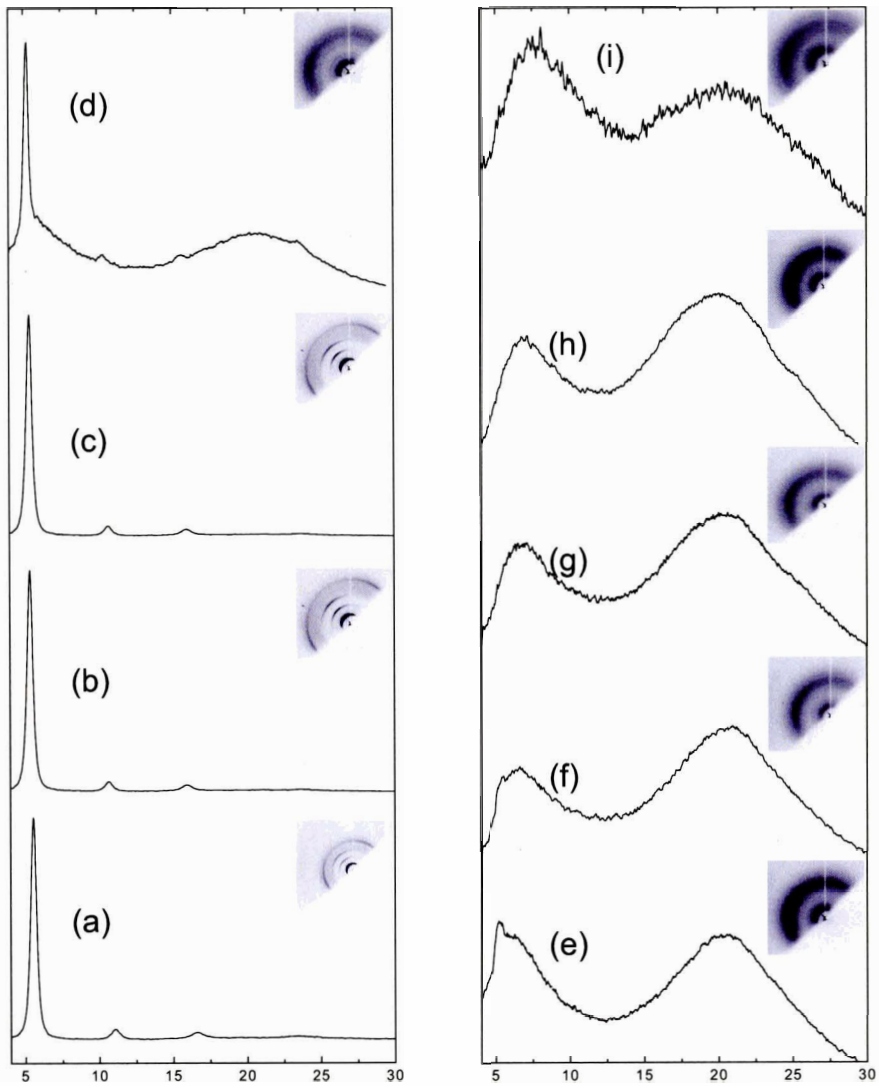

Figure 2.10: X-ray diffraction patterns of o-tolyl-substituted P3HTs: (a) 0, (b) 10, (c) 20, (d) 38, (e) 50, (f) 67, (g) 75, (h) 89, (i) 100% substitution.

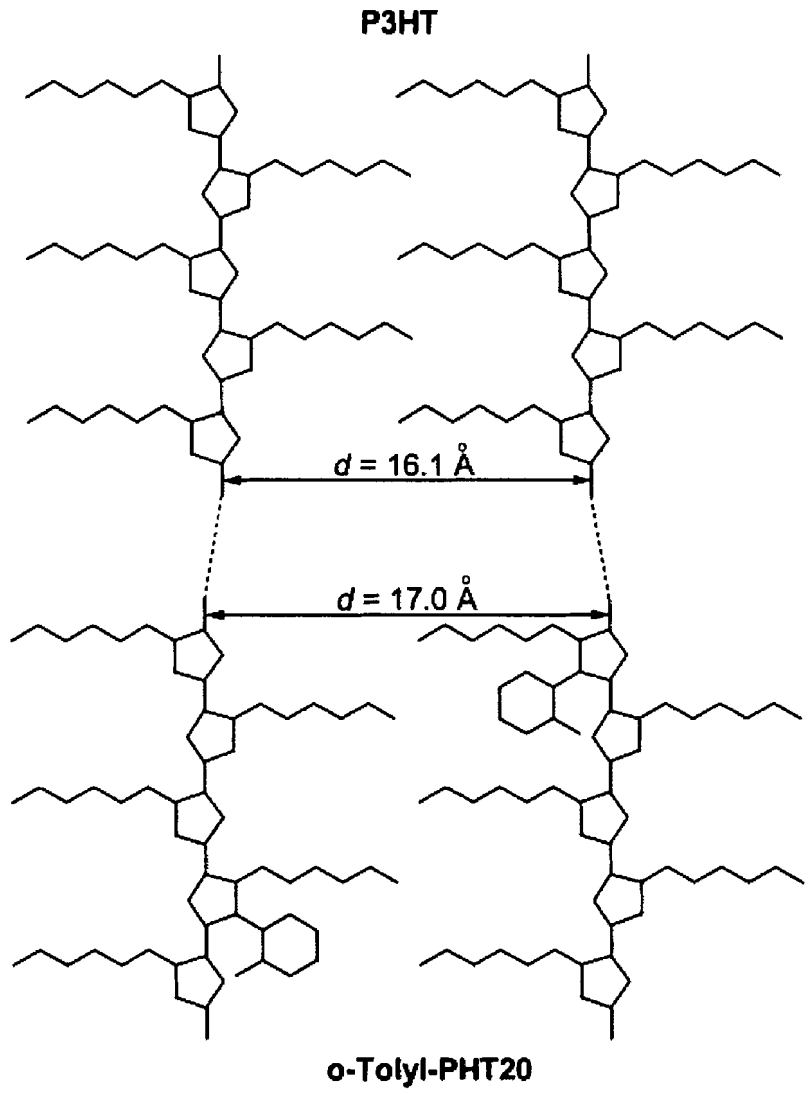

Figure 2.11: Influence of the a-axis d spacing of 20% *o*-tolyl-substituted P3HTs

2.2.1.3 Polymer LEDs

Polymer LEDs using polymers P3HT, *o*-Tolyl-PHT50, *o*-Tolyl-PHT75, *o*-Tolyl-PHT88, and *o*-Tolyl-PHT100 as emitting layers were fabricated. The devices were configured with indium-tin-oxide (ITO) anode/ polymer emitting layer/ triphenyltriazine (TPT)[14] electron transport layer (300Å)/ magnesium-silver alloy (9:1) cathode (1200 Å). Figure 2.12 shows the EL spectra measured from

the devices. It was found that the electroluminescence maxima of these polymers (EL λ_{max}: 660 and 730 nm for P3HT, 642 nm for *o*-Tolyl-PHT50, 594 nm for *o*-Tolyl-PHT88, and 558 nm for *o*-Tolyl-PHT100) agree well to their solid state photoluminescence maxima (PL λ_{max}) (refer to Table 2.2), except for *o*-Tolyl-PHT75 whose EL λ_{max} (626 nm) was longer than its PL λ_{max} (610 nm). The device made with P3HT showed very poor electroluminescence (internal Φ_{EL}: 0.01%). On the other hand, devices made with *o*-tolyl-substituted poly(thiophene)s exhibited much enhanced electroluminescence efficiency (internal Φ_{EL}: 1.8% for *o*-Tolyl-PHT50, 0.7% for *o*-Tolyl-PHT75, 1.7% for *o*-Tolyl-PHT88, and 1.3% for *o*-Tolyl-PHT100).

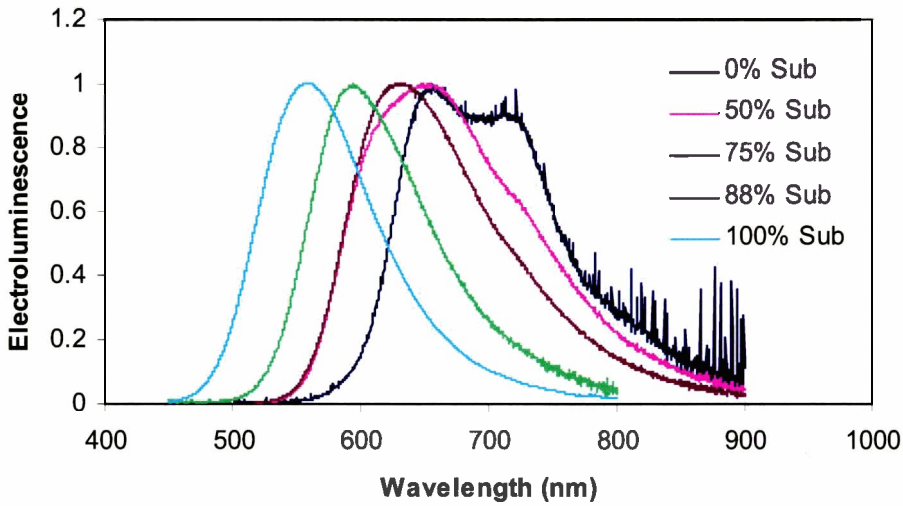

Figure 2.12: Electroluminescence spectra of Ar-PHT series.

2.2.2 Part 2: Poly(p-phenelyenevinylene)s

Poly(p-phenylenevinylene)s (PPVs) are one of the most extensively investigated polymers employed as emitting layers in polymer light-emitting diodes (LEDs).[15] They are processable, offer structural diversity, and are highly luminescent. However, their fluorescence yield is also substantially lower in the solid state due to interchain interactions. Strategies to enhance the emission efficiency in PPVs include the use of copolymers containing wide band gap or insulating segments,[16-19] incorporation of bulky side-chain groups,[20] and the use of polymer blends to isolate the emitting material in a polymer matrix.[21]

Another challenge in the development of light-emitting conjugated polymers is the tuning of emission wavelength, which is important with respect to full-color displays.[15d,e] The use of segmented conjugated PPVs containing varying conjugation lengths has drawn much attention as a strategy to control the color of emission and to enhance the emission efficiency.[16-19] The enhancement of fluorescence efficiency is considered to be due to trapping and confinement of excitons.[18b,d] One method to obtain segmented conjugated PPVs involves partial elimination of nonconjugated precursor polymers through the control of elimination time (or temperature),[18] as described in Section 1.4.1.2.2.[19] However, elimination reactions of precursor polymers are usually difficult to precisely control the conjugation lengths.

In this part, the introduction of wide band-gap units into the main chain, and to obtain segmented PPVs is approached in a typical PPV derivative, poly(p-2,5-dihexyloxy-phenyelenevinylene) (DHO-PPV). Because DHO-PPV possesses

an extensively π-conjugated electron-rich backbone, the hydrogen atoms at the 3- and 6-positions of the phenylenes are susceptible to electrophilic substitution. There also exists the possibility of addition to the vinylene group in the main chain to create nonconjugated segments.[22] By controlling the fraction of nonconjugated units *via* post-functionalization, it may be possible to obtain PPVs with desired conjugated lengths to tune the emission color and to enhance the emission efficiency. The optical properties of post-halogenated DHO-PPV (with Br and Cl) are investigated, for the potential of increased emission efficiency and colour tunabilty.

2.2.2.1 Synthesis

All polymers investigated in this part were synthesized by Dr. Yuning Li, therefore the synthetic portion is only described briefly. Poly(*p*-2,5-dihexyloxy-phenylenevinylene) (DHO-PPV) was reacted with an equivalent of NBS (or NCS) (based on the repeating unit) in chloroform or chloroform-acetic acid mixture at room temperature for 24 h (Scheme 2.3). ^{1}H NMR and IR spectroscopies were used to analyze these polymers. ^{1}H NMR and FT-IR revealed that both phenylene and vinylene were partially substituted. Furthermore, evidence from IR (carbonyl peak) and ^{1}H NMR also show confirmation for addition of the NBS or NCS across the vinylene groups and is estimated that ~22% of NCS reacts across the vinylene groups and 78% predominantly chlorinates the phenylene rings.

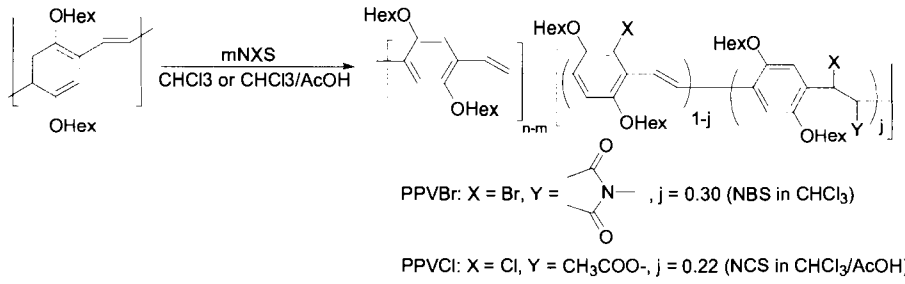

Scheme 2.3: Synthesis of halogenated PPVs

PPVBr and PPVCl prepared with NXS/PPV ≥0.5 (molar ratio of NXS per repeating unit) showed remarkably improved solubility in common organic solvents, as the result of their more flexible polymer backbone and/or the steric effect of the incorporated halogen and succinimide (or acetate) groups that prevents chain aggregation. However, when the NXS/PPV reaction ratio was <0.35, the resulting polymers were less soluble than the original DHO-PPV. GPC analysis indicated an abrupt increase in apparent molecular weight with lower NXS/PPV reaction ratios. (Samples were dissolved in hot THF and used for measurement immediately.) The poor solubility and the increase in molecular weight were considered to be due to enhanced intermolecular interactions between polymer chains. It is unclear whether this is caused by the increased polarity of the polymer or a reduction in the polymer's rigidity that facilitates a rapid formation of aggregates. The decrease in apparent molecular weights of polymers for NXS/PPV = 0.35 is ascribed to a further decrease of rigidity of the polymer chain caused by the addition reaction across the vinylene and further losses in π-conjugation along the chain.

2.2.2.2 Photophysical Properties

The UV-vis absorption and photoluminescence properties of PPVBrs and PPVCIs in solution (Table 2.3) and in the solid state (Table 2.4) were investigated. DHO-PPV in THF solution displays an absorption maximum at 472 nm. After halogenation, the resulting polymers were expected to possess shorter conjugation lengths and a blue shift of λ_{max}. However, PPVBr and PPVCl prepared with NXS/PPV = 0.10 exhibited a λ_{max} at 474 and 476 nm, respectively. The slight red shift with respect to DHO-PPV is due to a slight decrease in the optical band gap, caused by the intermolecular aggregation, or the electronic effect of halogen atoms on the phenyl rings. Furthermore, when the NXS/PPV reaction ratio was <0.35, the resulting polymers were less soluble than the original DHO-PPV. When the NXS/PPV reaction ratio was ≥0.2, the absorption maximum of the halogenated polymers decreased as the NXS/PPV ratio increased, which indicates that conjugation lengths was consequently reduced. The emission maximum ($\lambda_{em,\ max}$) of polymers blue shifts gradually from 546 to 465 nm for PPVBr and to 475 nm for PPVCl (Figure 2.13), respectively, as the NXS/PPV reaction ratio is increased from 0 to 1. The fluorescence efficiency (Φ_{pl}) of DHO-PPV was determined to be 50%. The effect of Φ_{pl} on the NXS/PPV reaction ratios are shown in Figure 2.14. An enhancement of Φ_{pl} (up to 66% for PPVBr and 62% for PPVCl) was observed when the NXS/PPV reaction ratio increased from 0.10 to 0.5. This increase can be explained by exciton confinement[18b,d] in the "quantum well" of the segmented conjugated polymers

(Figure 2.15). A further increase in the NBS/PPV reaction ratio (≥0.75) yields polymers with decreasing Φ_{pl}. At these levels of post-functionalization the polymers possess substantially reduced degrees of π-conjugation.

NXS/PPV molar ratio	PPV-Br solution, THF			PPV-Cl solution, THF		
	$\lambda_{max, abs.}$ (nm)	$\lambda_{max, em.}$ (nm)	Φ_{pl} (%)	$\lambda_{max, abs.}$ (nm)	$\lambda_{max, em.}$ (nm)	Φ_{pl} (%)
0.00	472	546	0.50	472	546	0.50
0.10	474	546	0.51	476	545	0.52
0.20	451	541	0.56	457	543	0.49
0.35	414	529	0.63	422	528	0.62
0.50	395	525	0.66	393	519	0.52
0.75	377	516	0.36	359	493	0.20
1.00	312	465	0.07	309	475	0.03

Table 2.3: Solution Optical Properties of Halogenated PPVs

NXS/PPV molar ratio	PPV-Br film			PPV-Cl film		
	$\lambda_{max, abs.}$ (nm)	$\lambda_{max, em.}$ (nm)	Φ_{pl} (%)	$\lambda_{max, abs.}$ (nm)	$\lambda_{max, em.}$ (nm)	Φ_{pl} (%)
0.00	487	580	0.13	487	580	0.13
0.10	492	581	0.07	493	583	0.07
0.20	464	577	0.10	470	577	0.10
0.35	423	557	0.11	428	580	0.12
0.50	398	545	0.32	396	540	0.20
0.75	380	535	0.27	358	504	0.19
1.00	345	516	0.03	350	479	0.04

Table 2.4: Solid State Optical Properties of Halogenated PPVs

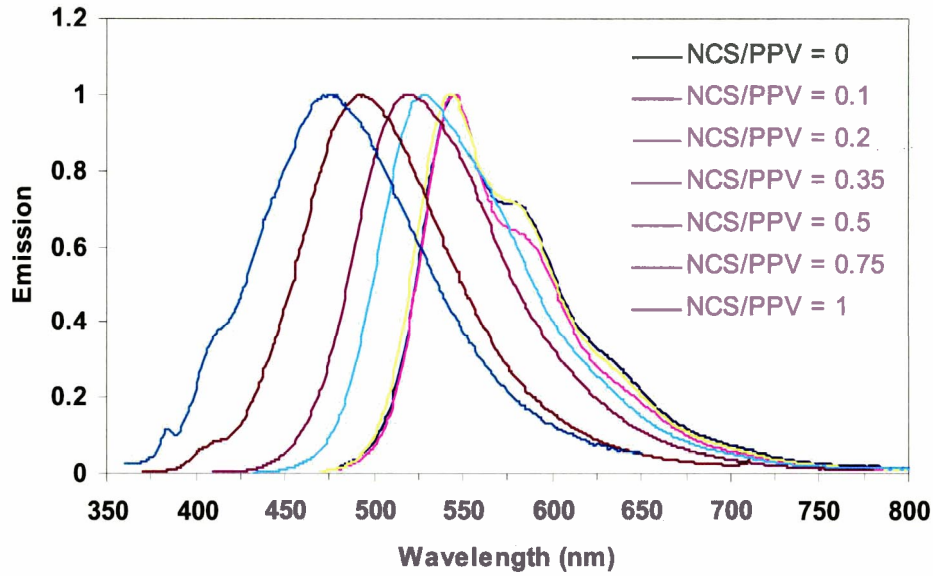

Figure 2.13: Emission spectra of PPV-Cl polymers in THF

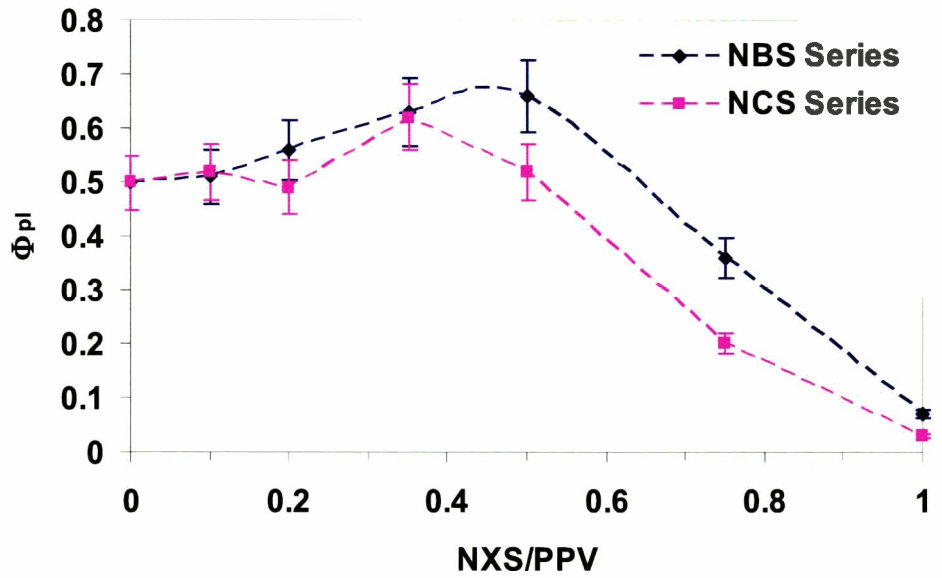

Figure 2.14: Φ_{pl} of halogenated PPV polymers in THF

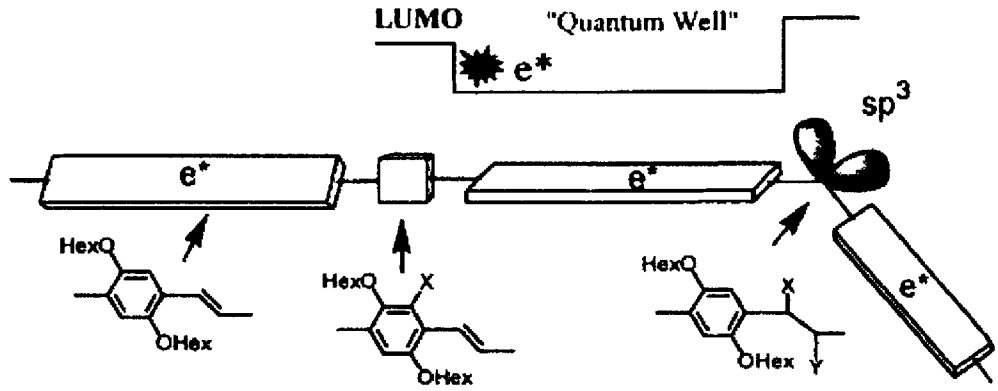

Figure 2.15: The exciton confinement effect in halogenated PPVs.

Solid-state UV-vis absorption spectra of polymers prepared from NXS/PPV = 0.1 showed a red shift of λ_{max} (Table 2.4). Polymers prepared from NXS/PPV ≥0.2 gave absorption maxima that blue shift with increasing reaction ratios, resulting from dissociation of polymer chains and/or the shortening of conjugation lengths. A picture of these polymers is depicted in Figure 2.16. Fluorescence data showed that emission maxima ($\lambda_{em,max}$) were similar for polymers prepared from NXS/PPV = 0-0.35. As the NXS/PPV reaction ratio increased from 0.35 to 1, the emission maximum blue-shifted from 557 to 516 nm for PPVBr and from 580 to 479 nm for PPVCl (Figure 2.17). π-Stacking and/or aggregation of conjugated polymers in the solid state usually causes a red shift in the emission spectrum relative to solution spectra.[24] The $\lambda_{em,max}$ of the DHO-PPV film red-shifted 34 nm compared to its dilute THF solution and Φ_{pl} decreased dramatically from 50% in solution to 13% in the solid state. When lower NXS/PPV reaction ratios (0.10-0.35) were used, the polymer films exhibited larger red shifts in $\lambda_{em,max}$ relative to the solution phase, and the Φ_{pl} of these polymers decreased to an even lower value than that of DHO-PPV (Table 2.4). These results support the

assumption of enhanced interchain interactions. When the NXS/PPV reaction ratio was increased to 0.50-0.75, the interchain interactions are suppressed, which is manifested by a smaller red shift of $\lambda_{em,max}$, compared with the solution phase. The Φ_{pl} of polymer films increases up to 32% for PPVBr and 20% for PPVCl (Figure 2.18). This change is believed to be the result of the above-mentioned exciton confinement effect associated with segmentation and the steric effect associated with both the halogenated phenylene and the vinylene groups that inhibit interchain face-to-face quenching. More heavily halogenated polymers (NXS/PPV ≥1) gave only weak emission, as destruction of the π-conjugated system approaches completion.

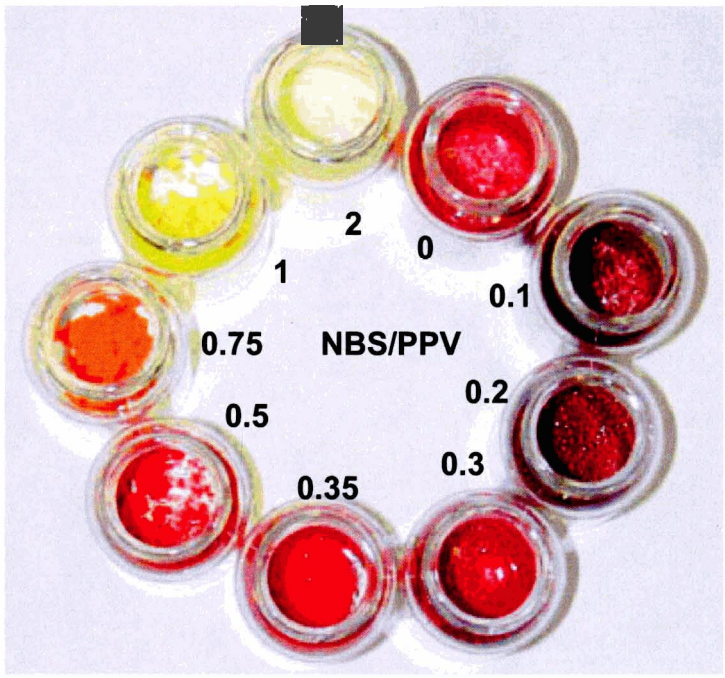

Figure 2.16: Picture of brominated PPVs to various extents, numbers are the NBS/PPV ratios.

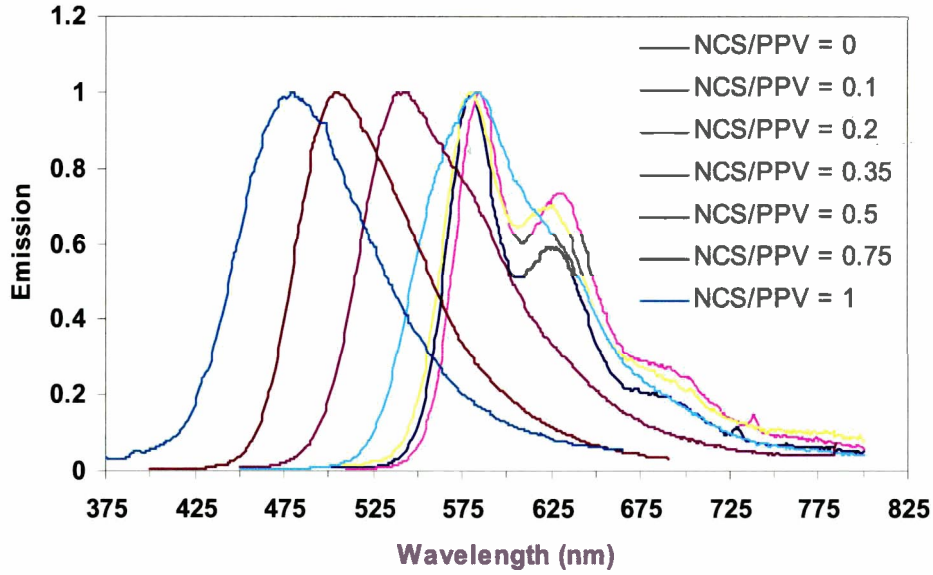

Figure 2.17: Emission spectra of PPV-Cl polymers of films

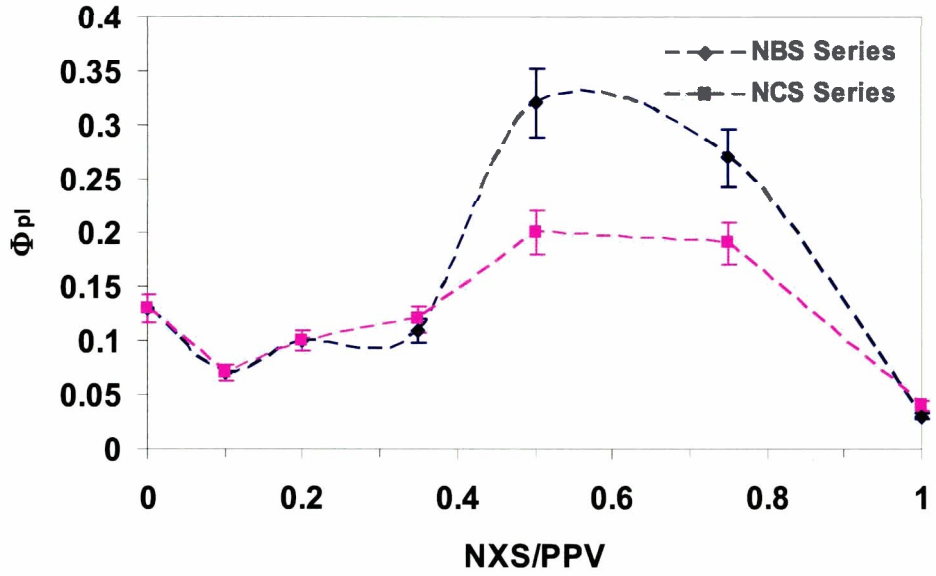

Figure 2.18: Solid state Φ_{pl} of halogenated PPV polymers.

2.3 Conclusion

2.3.1 Postfunctionalization of Poly(3-hexythiophene)

Postfunctionalization of poly(3-hexylthiophene) provides an opportunity to systematically study the influence of substituents on the photophysical properties of 3,4-disubstituted poly(thiophene)s, while maintaining the same degree of polymerization. Substitution with phenyl, *p*-tolyl, 2- and 4-methoxyphenyl, biphenyl, 1-naphthyl, 2-thienyl, and phenylethylenyl groups causes a red shift in the absorption and emission λ_{max} values, and imposes a slight increase in the solid-state Φ_{pl}. Polymers containing o-tolyl, o-hexylphenyl, 2-(3-methyl)thienyl, and 2-(3-hexyl)thienyl groups exhibit a significantly higher Φ_{pl} in the solid state (9-22%) compared to P3HT (1.6%) and Br-PHT (1.8%). The methyl hydrogens on the o-tolyl groups and the hexyl α-methylene hydrogens on the 2-hexylthienyl and 2-hexylphenyl substituents serve to limit rotation of the backbone and force the phenyl or thienyl group perpendicular to the main-chain π system.

Such a conformation not only increases the planarity and rigidity of the polymer backbone but also enlarges the interplanar distance to the point that highly substituted films are amorphous. The suppression of π stacking, together with rigidification of the main chain, leads to a significant enhancement of luminescence yield.

Molecular order/disorder and optical/photophysical properties of polymers were controlled by partial post-functionalization of P3HT with o-tolyl groups. For degrees of substitution ranging from 50 to 100%, the solid-state Φ_{pl} is enhanced

to 13-22%, and the emission wavelength can be readily tuned from 556 to 640 nm. The post-functionalization approach allows for a series of highly luminescent poly(thiophene)s to be prepared from a weakly luminescent parent poly(3-hexylthiophene).

2.3.2 Posthalogenation of Poly(p-2,5-dihexyloxy-phenyelenevinylene)

Post-halogenation of DHO-PPV with NBS and NCS under mild conditions modifies the structure and properties of this polymer. Halogenation occurs at both phenylene and vinylene groups; the former produces more sterically encumbered phenylene groups with wide band gaps, while the latter affords saturated units. The solubility of the resulting polymers is decreased when the extent of post-functionalization is limited, but increases with increasing degrees of reaction. These polymers, both in solution and in the solid state, show a red shift in the λ_{max} with low degrees of post-fuctionalization but a blue shift upon further reaction. Fluorescence efficiency of these polymers in solution increases when the NXS/PPV reaction ratio lies between 0.1 and 0.5 and falls as the NXS/PPV reaction ratio is further increased. Polymers from NXS/PPV = 0.50-0.75 displayed a 150% and 50% enhancement in Φ_{pl} in the solid state for bromo and chloro derivatives, respectively.

The above results indicated that interchain interactions exist in polymers prepared with lower degrees of post-reaction, but with further reaction, aggregation of polymer chains can be suppressed, leading to the enhancement of Φ_{pl} in the solid state. This study provides a new method to control the emission

color and enhance the fluorescence efficiency of PPVs and illustrates the role of aggregation on their photophysical properties.

2.4 Experimental

2.4.1 Measurements

400-MHz ^{1}H and 100-MHz ^{13}C NMR spectra were obtained in $CDCl_3$ or CD_2Cl_2 on a 400-MHz Bruker AMX400 spectrometer; the chemical shifts are reported in ppm, referenced to $CHCl_3$ (δ 7.26) or $CDHCl_2$ (δ 5.32) in ^{1}H NMR and to $CDCl_3$ (δ 77.0) in ^{13}C NMR, respectively. IR spectra were recorded on a Bomen Michelson MB series spectrophotometer. Gel permeation chromatography (GPC) analysis of polymers was conducted on a Waters Model 510 HPLC equipped with μ-Styragel columns using THF as an eluant with polystyrene as standards. Elemental analysis was performed by Canadian Microanalytical Service Ltd.

UV-vis absorption spectra were obtained on a Cary 3E (Varian) spectrophotometer. fluorescence measurements were carried out on a PTI QuantumMaster model QM-1 spectrometer. Polymer solutions in THF with o.d. = 0.05-0.1 were deoxygenated prior fluorescence measurement and the quantum yield of polymers was determined against quinine bisulfate standard (Φ_{pl} = 0.546 in 1.0 N H_2SO_4). Spin-coated polymer films with o.d. = 0.1-0.2 were protected under an argon flow during fluorescence measurement and the quantum yield was reported against 9,10-diphenylanthracene in PMMA ($<10^{-3}$ M) (Φ_{pl} = 0.83). The fabrication of PLED devices was conducted as follows. Polymer (3 mg) was

dissolved in chloroform (0.5 ml) and filtered through a 0.2 μm Teflon filter and spin coated at 2000 RPM on a UV ozone pre-cleaned patterned ITO substrate. Triphenyltriazine (TPT) and cathode were deposited subsequently using vacuum evaporation at 6×10^{-6} Torr.

X-ray diffractometry was performed on a Rigaku D/MAX-RAPID X-ray microdiffraction system using Cu Kα radiation (λ = 1.5418 Å). Polymer films were prepared on silicon wafer or quartz glass substrate by solution casting of polymers in chloroform and were annealed for 15 min at 150 °C prior to measurement. The X-ray diffraction pattern was produced by integrating a 45° wide slice normal to the film. Molecular models of polymer dyad units were prepared using WebLab Viewer Pro (Molecular Simulations, Inc.). In these illustrative examples, the polymer backbone was forced to be coplanar and the aromatic substituents were set perpendicular to the backbone.

2.4.2 Materials

N-Bromosuccinimide (NBS) and *N*-chlorosuccinimide (NCS) were purchased from Aldrich and used as received. Chloroform and carbon tetrachloride were dried over CaH_2 and distilled prior to use. Boronic acids, tributyltin compounds, methyl acrylate, styrene, vinyl biphenyl, and tetrakis(triphenylphosphine)palladium (0) ($Pd(PPh_3)_4$) were purchased from Sigma-Aldrich Canada Ltd. and used as received. Regioregular poly(3-hexylthiophene) (P3HT) was prepared according to the method reported by McCullough et al.[25] (M_n = 11 000, M_w/M_n = 1.51; head-to-tail diad content >95%).

1,4-Dihexyloxybenzene and 2,5-bis(chloromethyl)-1,4-dihexyloxybenzene were prepared according to reported methods.[23,26]

2.4.3 Synthesis

These are only examples, not all inclusive. Please refer to references on title page for additional details.

Bromination of P3HT (P3HT-Br). To a flask containing P3HT (0.30 g, 1.8 mmol) in chloroform (20 mL) was added NBS (0.387 g, 2.17 mmol). The solution was stirred at room temperature for 15 h and heated at 50 °C for 2 h. The reaction mixture was then poured into a saturated $NaHCO_3$ solution (50 mL). The organic layer was washed with water five times and dried over $MgSO_4$. Precipitation into methanol gave a yellow solid (0.440 g, yield: 99% based on 100% substitution). GPC: M_n = 12 900, M_w/M_n = 1.53. ^{1}H NMR: δ 2.71 (br, α-methylene), 1.60 (br), 1.33 (br), 1.28 (br), 0.87 (br, CH_3). ^{13}C NMR: 142.66, 130.38, 129.41, 115.81, 31.37, 30.40, 29.69, 29.44, 29.05, 22.56, 14.11. IR (KBr): 2954-2856, 1729, 1458, 1377, 1172, 1100, 817, 759 cm^{-1}. Elemental analysis: Calcd for $C_{10}H_{13}BrS$: C, 48.99; H, 5.34; Br, 32.59; S, 13.08. Found: C, 50.07; H, 5.26; Br, 30.76; S, 12.92.

Example procedure for Suzuki coupling (o-Tolyl-PHT). To a 20 mL Schlenk flask under nitrogen were placed P3HT-Br (50 mg, 0.30 mmol), a boronic acid (0.45 mmol), and THF (5 mL). After the polymer dissolved completely, 2M Na_2CO_3 solution (0.5 mL, 1.0 mmol) was added and the flask was sealed with a glass stopper. The mixture was then heated to 80 °C for 48 h. The reaction mixture was diluted with chloroform and washed with water 3-5 times to remove

the excess boronic acid. The organic layer was dried with $MgSO_4$ and the polymer was precipitated from methanol. The polymer was purified with methanol (water in the case of 2h) using a Soxhlet extractor. The polymer was dissolved in chloroform and passed through a silica gel column using chloroform as an eluent to remove trace catalyst. The polymer was again precipitated from methanol and dried under vacuum. Yield: 50 mg; GPC: Mn = 13 400, Mw/Mn = 1.87; ^{1}H NMR (CD_2Cl_2): δ 7.27 (m), 7.15 (m), 2.26 (α-methylene), 1.42 (m), 0.96 (br), 0.79 (t, CH_3, J = 7.3 Hz); ^{13}C NMR: 141.94, 141.00, 136.80, 131.49, 130.17, 130.07, 127.79, 126.93, 31.24, 29.27, 28.97, 27.83, 22.40, 14.03; IR (KBr): 3059-2856, 1727, 1602, 1463, 1444, 1378, 1072, 914, 761, 700 cm^{-1}, Anal. Calcd for $C_{16}H_{18}S$: C, 79.29; H, 7.49; S, 13.23. Found: C, 78.25; H, 7.54; S, 12.97; Br < 0.3.

Partially *o*-tolyl-substituted P3HTs were prepared by (i) partial bromination with NBS and (ii) Suzuki coupling of the brominated polymers with *o*-tolylboronic acid.

Bromination of DHO-PPV (PPVBr). A typical procedure is as follows. To a 20-mL Schlenk flask containing DHO-PPV (50.0 mg, 0.165 mmol) in chloroform (5 mL) was added NBS (29.4 mg, 0.165 mmol). The solution was stirred at room temperature in the absence of light for 24 h. The reaction mixture was then poured into a saturated $NaHCO_3$ solution (20 mL). The organic layer was washed with water 5 times and dried over $MgSO_4$. After the solvents were evaporated, the polymer was dissolved in chloroform and passed through a silica gel column. With the solvent evaporated, a yellow solid was obtained (57.6 mg). ^{1}H NMR: δ7.5 (br), 7.0 (br), 6.7 (br), 6.0 (br), 3.88 (br, PhOCH_2-), 2.70 (br), 1.75 (br), 1.52

(br), 1.34 (br), 0.90 (br, CH_3). IR (neat): 2954, 2931, 2859, 1712, 1503, 1469, 1417, 1386, 1208, 1029, 872, 727 cm^{-1}. Elemental analysis: C, 64.98; H, 7.66; Br, 13.72.

2.5 References

1. A. Guiseppi-Elie, G. E. J. Wnek, *Polym. Sci., Part A: Polym. Chem.* **1985**, *23*, 2601.

2. (a) J. -Y. Bergeron, J. -W. Chevalier, L. H. J. Dao, *Chem. Soc., Chem. Commun.* **1990**, 180. (b) J. Yue, A. J. Epstein, *J. Am. Chem. Soc.* **1990**, *112*, 2800. (c) J. Yue, Z. H. Wang, K. R. Cromack, A. J. Epstein, A. G. MacDiarmid, *J. Am. Chem. Soc.* **1991**, *113*, 2665. (d) C. Barbero, M. C. Miras, B. Schnyder, O. Haas, R. Kotz, *J. Mater. Chem.* **1994**, *4*, 1775.

3. F. T. A. Vork, M. T. Ubbink, L. J. J. Janssen, E. Barendrecht, *Recl. Trav. Chim. Pays-Bas* **1985**, *104*, 215.

4. (a) H. Harada, T. Fuchigami, T. Nonaka, *J. Electroanal. Chem.* **1991**, *303*, 139. (b) Z. Qi, N. G. Rees, P. Pickup, *Chem. Mater.* **1996**, *8*, 701.

5. A. A. Pud, *Synth. Met.* **1994**, *66*, 1 and references therein.

6. (a) I. D. W. Samuel, G. Rumble, R. H. Friend, In *Primary Photoexcitations in Conjugated Polymers: Molecular Excitation versus Semiconductor Band Model*, N. S. Sariciftci, Ed.; World Scientific Publishing Co.: Singapore, 1997. (b) B. Xu, S. Holdcroft, *Macromolecules* **1993**, *26*, 4457. (b) N. C. Greenham, I. D. W. Samuel, G. R. Hayes, R. T. Phillips, Y. A. R. R. Kessener, S. C. Moratti, A. B. Holmes, R. H. Friend, *Chem. Phys. Lett.* **1995**, *241*, 89. (c) F. Chen, B. Mehta, L. Takiff, R. D. McCullough, *J. Mater. Chem.* **1996**, *6*, 1763.

7. M. G. Reinecke, P. Pedaja, in The Chemistry of Heterocyclic Compounds, Thiophene and Its Derivatives, Part 2; S. Gronowitz, Ed.; John Wiley and Sons: New York, 1986; Vol. 44, p 221 and references therein.

8. H. Saadeh, T. Goodson III, L. Yu, *Macromolecules* **1997**, *30*, 4608.

9. D. A. Skoog, J. L. Leary, in Principles of Instrumental Analysis, Fourth edition, 1992, pg 180.

10. (a) H. Chosrovian, S. Rentsch, D. Grebner, D. U. Dahm, E. Brickner, *Synth. Met.* **1993**, *60*, 23. (b) J. K. Herrema, P. F. van Hutten, R. E. Gill, J. Wildeman, R. H. Wieringa, G. Hadziioannou, *Macromolecules* **1995**, *28*, 8102. (c) D. Beljonne, J. Cornil, R. H. Friend, R. A. J. Janssen, J. L. Brédas, *J. Am. Chem. Soc.* **1996**, *118*, 6453.

11. (a) M. J. Winokur, D. Spiegel, Y. Kim, S. Hotta, A. J. Heeger, *Synth. Met.* **1989**, *28*, C419. (b) M. Leclerc, F. M. Diaz, G. Wegner, *Makromol.*

Chem. **1989**, *190*, 3105. (c) R. D. McCullough, S. Tristram-Nagle, S. P. Williams, R. D. Lowe, M. Jayaraman, *J. Am. Chem. Soc.* **1993**, *115*, 4910. (d) T. Chen, X. Wu, R. D. Rieke, *J. Am. Chem. Soc.* **1995**, *117*, 233.

12. T. J. Prosa, M. J. Winokur, J. Moulton, P. Smith, A. J. Heeger, *Macromolecules* **1992**, *25*, 4364.

13. T. J. Prosa, M. J. Winokur, R. D. McCullough, *Macromolecules* **1996**, *29*, 3654.

14. Z. P. Popovic, H. Aziz, N. X. Hu, A. Ioannidis, P. N. M. dos Anjos, *J. Appl. Phys.* **2001**, *89*, 4673.

15. (a) J. H. Burroughes, D. D. C. Bradley, A. R. Brown, H. N. Marks, K. Mackay, R. H. Friend, P. L. Burns, A. B. Holmes, *Nature* **1990**, *347*, 539. (b) G. Gustafsson, Y. Cao, G. M. Treacy, F. Klavetter, N. Colaneri, A. J. Heeger, *Nature* **1992**, *357*, 447. (c) A. B. Holmes, D. D. C. Bradley, A. R. Brown, P. L. Burn, J. H. Burroughes, R. H. Friend, N. C. Greenham, R. W. Gymer, D. A. Halliday, R. W. Jackson, A. Kraft, J. H. F. Martens, K. Pichler, I. D. W. Samuel, *Synth. Met.* **1993**, *55-57*, 4031. (d) I. D. W. Samuel, G. Rumble, R. H. Friend, in *Primary Photoexcitations in Conjugated Polymers: Molecular Excitation versus Semiconductor Band Model*; N. S. Sariciftci, Ed.; World Scientific Publishing Co.: Singapore, 1997; pp 140-173. (e) A. Kraft, A. C. Grimsdale, A. B. Holmes, *Angew. Chem., Int. Ed.* **1998**, *37*, 402. (f) G. Yu, J. Wang, J. McElvain, A. J. Heeger, *Adv. Mater.* **1998**, *10*, 1431.

16. (a) T. Ohnishi, S. Doi, Y. Tsuchida, T. Noguchi, *IEEE Trans. Electron Devices* **1997**, *44* (8), 1253. (b) Y. Pang, J. Li, B. Hu, F. E. Karasz, *Macromolecules* **1999**, *32*, 3946. (c) B. Xu, J. Zhang, Y. Pan, Z. Peng, *Synth. Met.* **1999**, *107*, 47.

17. (a) I. K. Spilipoulos, J. A. Mikroyannidis, *Macromolecules* **2001**, *34*, 5711. (b) A. M. Sarker, E. E. Gurel, M. Zheng, P. M. Lahti, F. E. Karasz, *Macromolecules* **2001**, *34*, 5897.

18. (a) P. L. Burn, A. B. Holmes, A. Kraft, D. D. C. Bradley, A. R. Brown, R. H. Friend, *J. Chem. Soc., Chem. Commun.* **1992**, 32. (b) P. L. Burn, A. B. Holmes, A. Kraft, D. D. C. Bradley, A. R. Brown, R. H. Friend, R. W. Gymer, *Nature* **1992**, *356*, 47. (c) A. R. Brown, N. C. Greenham, J. H. Burroughes, D. D. C. Bradley, R. H. Friend, P. L. Burn, A. Kraft, A. B. Holmes, *Chem. Phys. Lett.* **1992**, *200*, 46. (d) A. R. Brown, P. L. Burn, D. D. C. Bradley, R. H. Friend, A. Kraft, A. B. Holmes, *Mol. Cryst. Liq. Cryst.* **1992**, *216*, 111. (e) P. L. Burn, A. Kraft, D. R. Baigent, D. D. C. Bradley, A. R. Brown, R. H. Friend, R. W. Gymer, A. B. Holmes, R. W. Jackson, *J. Am. Chem. Soc.* **1993**, *115*, 10117. (f) E. G. Staring, R. C. J. E. Demandt, D. Braun, G. L. J. Rikken, Y. A. R. R. Kessener, T. H. J.

Venhuizen, H. Wynberg, W. Hoeve ten, K. J. Spoelstra, *Adv. Mater.* **1994**, *6*, 934. (g) D. Braun, E. G. J. Staring, R. C. J. E. Demandt, G. L. J. Rikken, Y. A. R. R. Kessener, A. H. J. Venhuizen, *Synth. Met.* **1994**, *66*, 75.

19. (a) M. M. de Kok, A. J. J. M. van Breemen, P. J. Adriaensens, A. van Dixhoorn, J. M. Gelan, D. J. Vanderzande, *Acta Polym.* **1998**, *49*, 510. (b) G. Padmanaban, S. Ramakrishnan, *J. Am. Chem. Soc.* **2000**, *122*, 2244.

20. R. Jakubiak, Z. Bao, L. Rothberg, *Synth. Met.* **2000**, *114*, 61.

21. (a) M. Yan, L. J. Rothberg, E. W. Kwock, T. M. Miller, *Phys. Rev. Lett.* **1995**, *75*, 1992. (b) H. Vestweber, A. Greiner, U. Lemmer, R. F. Fahrt, R. Richert, W. Heitz, H. Bassler, *Adv. Mater.* **1992**, *4*, 661. (c) H. Hong, D. Davidov, Y. Avny, H. Chayet, E. Z. Faraggi, R. Neumann, *Adv. Mater.* **1995**, *7*, 846. (d) H. von Seggern, P. Schmidt-Winkel, C. Zhang, B. Kraabel, A. J. Heeger, H. -W. Schmidt, *Polym. Prepr.* **1993**, *34*, 532. (e) C. Zhang, H. von Seggern, K. Pakbaz, B. Kraabel, H. -W. Schmidt, A. J. Heeger, *Synth. Met.* **1994**, *62*, 35.

22. (a) B. R. Hsieh, *Polym. Bull.* **1991**, *25*, 177 (b) T. Yamamoto, *Chem. Lett.* **1993**, 1959. (c) T. Yamamoto, W. Yamada, M. Takagi, K. Kizu, T. Maruyamata, N. Ooba, S. Tomaru, T. Kurihara, T. Kaino, K. Kubota, *Macromolecules* **1994**, *27*, 6620. (d) A. R. Marshall, U. H. Bunz, *Macromolecules* **2001**, *34*, 4688.

23. A. Delmotte, M. Biesemans, H. Rahier, M. Gielen, *Synth. Met.* **1993**, *58*, 325.

24. J. Cornil, D. A. dos Santos, X. Crispin, R. Silbey, J. L. Bredas, *J. Am. Chem. Soc.* **1998**, *120*, 1289.

25. R. D. McCullough, R. D. Low, M. Jayaraman, D. L. Anderson, *J. Org. Chem.* **1993**, *58*, 904.

Chapter 3.

Synthesis and Luminescence Properties of Poly(fluorene-*co*-thiophene) blends and copolymers

Sections of this Chapter have been reproduced in part with permission from:

- *Advanced Materials* **2004**, *16*, 716-719.
- *Macromolecules* **2004**, *Accepted.*

3.1 Introduction

Alternating poly(fluorene-*co*-thiophene)s (PFTs) are a promising class of conjugated polymers due to the efficient luminescent fluorene moiety, in combination with the hole injection/transport properties and the synthetic versatility of the thiophene moiety.[1-3] Fluorene-co-thiophene polymers generally exhibit Φ_{pl} values between 50 - 60% in solution, but only 5 - 10% in the solid state as a result of molecular aggregation.[2-3]

Methods to enhance the emission of PFTs in the solid state are strongly desirable for increased polymer LED performance. In Part 1 (Section 3.2.1), the design, synthesis and characterization of a polymer host-guest system *via* polymer blends and copolymers are studied. In Part 2 (Section 3.2.2), the host-guest concept will be used to enhance the blue colour purity and the efficiency of poly(fluorene)s.

3.2 Results and Discussion

3.2.1 Part 1: Effect of the dibromothiophene isomer

It is clear, from Part 1 in Chapter 2, that sterically encumbered ortho-linkages have a dramatic influence on the emission properties of polythiophenes. With this in mind, a series of poly(fluorene-*co*-thiophene)s with various dibromo-thiophene isomers (3,4; 2,4; 2,5) will be investigated. It is postulated that the solid state emission properties can be influenced by the type of linkage (Section 3.2.1.1) and by varying the feed ratios with different linkages (Section 3.2.1.2).

3.2.1.1 Synthesis

Alternating thiophene-co-fluorene polymers were prepared by Suzuki polycondensation of 9,9-dihexylfluorene-2,7-bis(trimethyleneborate) with either 2,5-dibromothiophene (PFT-2,5), 2,4-dibromothiophene (PFT-2,4), or 3,4-dibromothiophene (PFT-3,4), respectively according to Scheme 3.1. Proton NMR was used to characterize these polymers. Multiplet peaks associated with chemical shifts between 7.1 - 7.8 ppm are attributed to the proton resonances of the aromatic protons on the fluorene and thiophene moieties. The aliphatic moieties on the PFTs occur from 0.5-2.5 ppm in the ^{1}H NMR. These polymers possessed a molecular weight ranging from 8000 to 12,000 Daltons, with synthetic yields ~80%. The polymers were soluble in common organic solvents, such as toluene, chloroform, tetrahydrofuran, and dichloromethane.

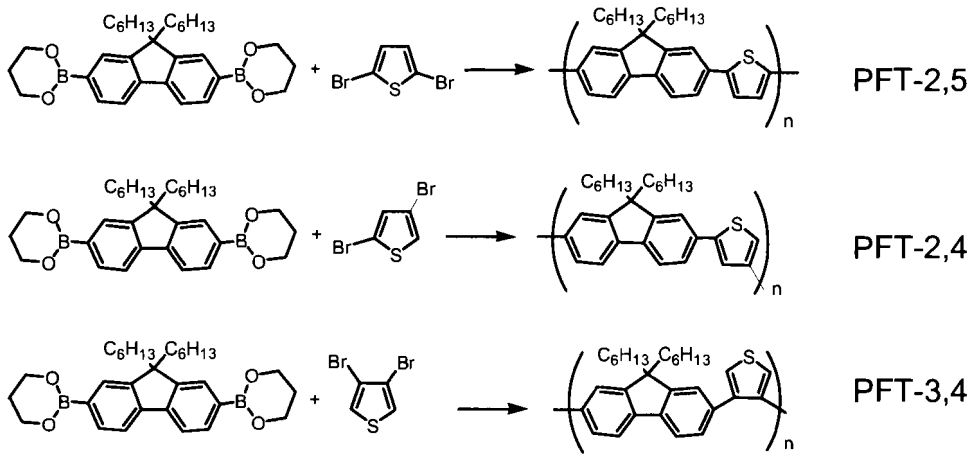

Scheme 3.1: Synthesis of alternating PFTs

Space filling models of these polymers predict the molecular shape of the

overall polymer which are linear for PFT-2,5; bent for PFT-2,4; and kinked for PFT-3,4 as depicted in Figure 3.1. From the molecular structure, these three polymers display a dramatic difference in both electronic and steric interactions, despite the similarity of the monomers.

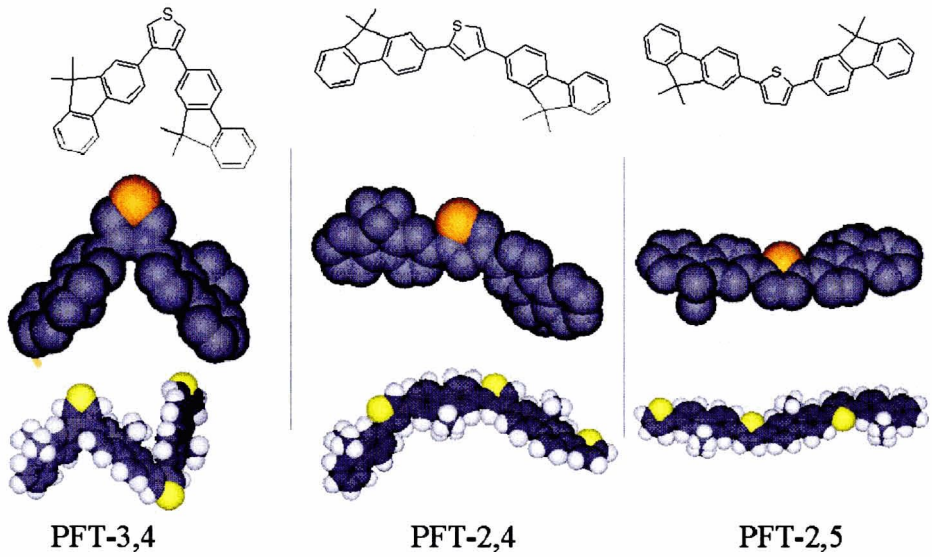

Figure 3.1: Space filling models of PFTs 3 and 6 units long

3.2.1.2 Optical Properties

The optical properties of polymer PFT-2,5, PFT-2,4 and PFT-3,4 are compared in Figure 3.2. The solution and film absorption spectra of PFT-3,4 are significantly blue shifted compared to PFT-2,4, which is blue shifted compared to PFT-2,5 due to their bent structure and lower effective conjugation length. The emission wavelengths are also blue-shifted: PFT-2,5 emission maxima are 466 nm and 482 nm for solution and film, respectively; corresponding values for PFT-2,4 are 400 nm and 457 nm, and PFT-3,4 are 383 nm and 410 nm. Quantum

yields of luminescence for PFT-2,5, PFT-2,4 and PFT-3,4 solutions are 57%, 40% and 40%, respectively. The lower yield of the latter two PFTs could be possibly due to their less rigid structure. Quantum yields of the corresponding films are much lower: 6%, 5% and 7%, respectively. Since their emission wavelengths are significantly red-shifted (16, 57 and 27 nm, respectively) compared to their solution spectra, it is evident the emitting segments exhibit enhanced coplanarity and/or aggregation in the solid state.[4]

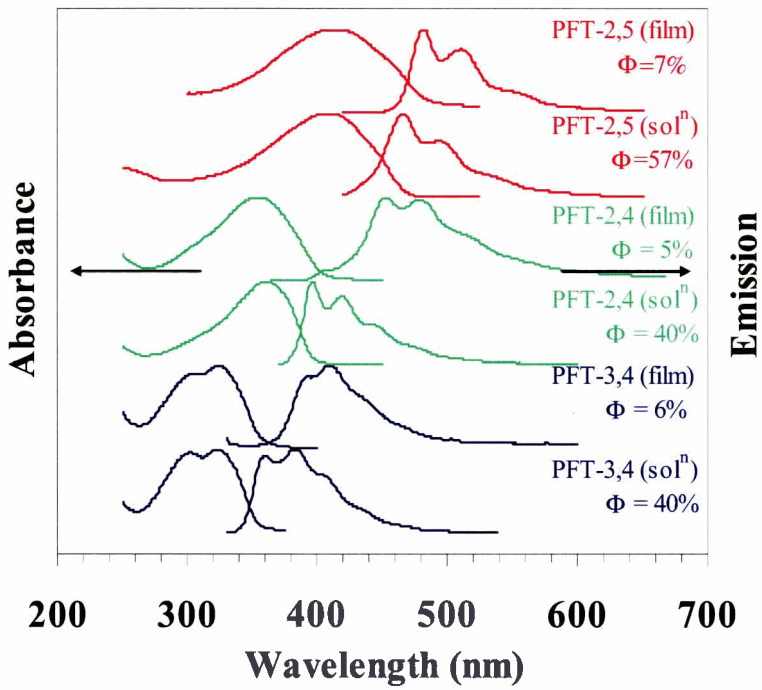

Figure 3.2: Optical properties of PFT polymers in the solution and film states

3.2.1.2 Host-guest system

A prerequisite to form a host-guest emission system is the favorable overlap of the emission spectrum of the host with the absorption spectrum of guest. Examination of Figure 3.2 illustrates that the solid-state emission of PFT-

3,4 overlaps well with both the solution and solid state absorption spectra of PFT-2,5. Thus a hybrid polymer film based on PFT-3,4 host and PFT-2,5 guest motifs, via (a) blending or (b) copolymerizing, represents a plausible host-guest system.

3.2.1.2.1 PFT Polymer Blends

Blending PFT-2,5 and PFT-3,4 was performed with various weight percentages from 0.3% to 26% of PFT-2,5 in PFT-3,4. The solid state absorption spectra of concentrations from 2.5% to 26% PFT-2,5 are depicted in Figure 3.3. As expected, the presence of two domains occur, one attributed to PFT-3,4 at ~320 nm and PFT-2,5 at ~410 nm. The weight concentration of the PFT-2,5 in PFT-3,4 corresponds well with the relative intensity.

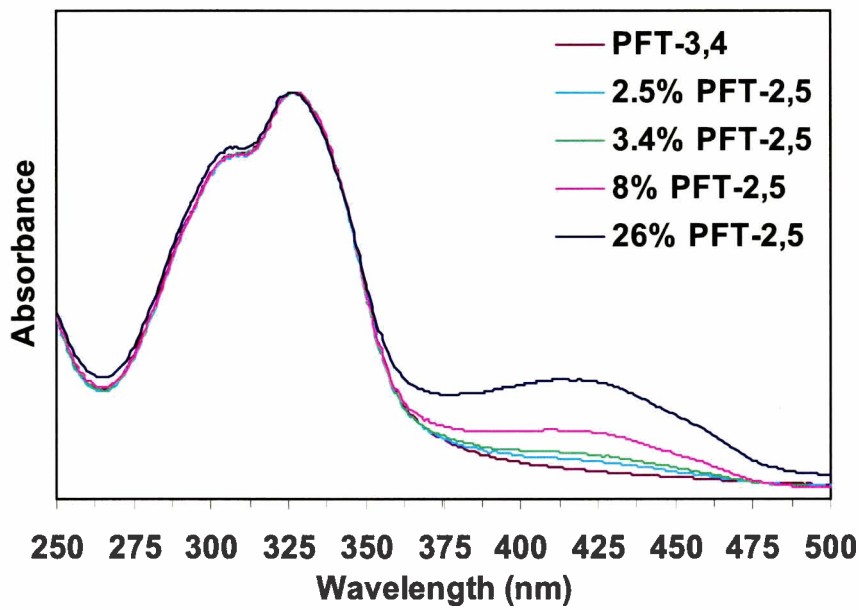

Figure 3.3: Absorption spectra of PFT-2,5/3,4 blend films.

The solid state photo-luminescence spectra (Figure 3.4) revealed emission

from PFT-2,5 domains, despite the direct excitation PFT-3,4. At concentrations lower than 2.5% PFT-2,5, emission from the PFT-3,4 emerged (not shown). Upon increasing the concentration of PFT-2,5 from 2.5% to 26%, the emission maximum wavelength increased from 472 nm to 473 nm, to 475 nm, to 476 nm; indicating an increased in aggregation and/or planarity of the polymer backbone.

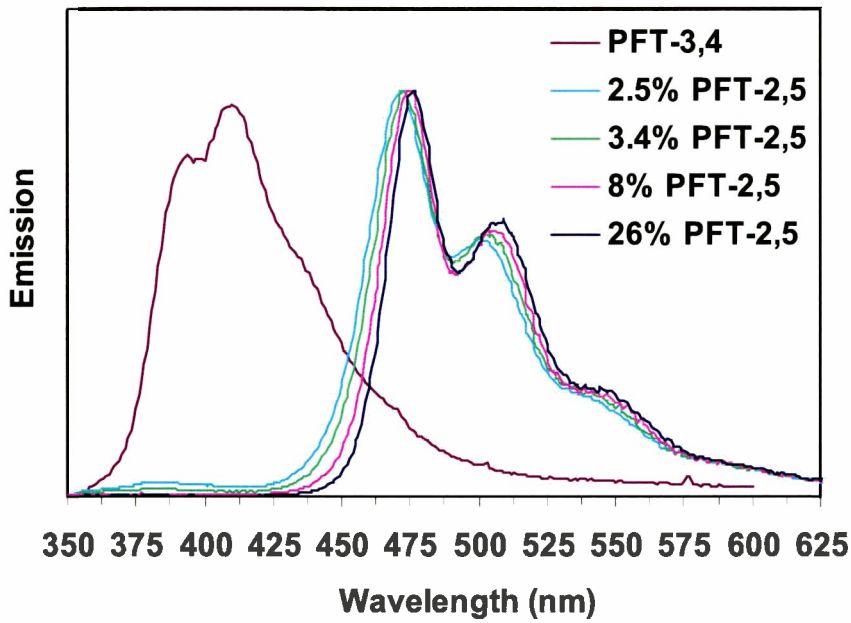

Figure 3.4: Emission spectra of PFT-2,5/3,4 blend films.

The quantum yields of luminescence varied as a function of PFT-2,5 concentration is illustrated in Figure 3.5. Quantum yields of photoluminescence values are 6% for PFT-3,4 and increase to 13.8% with the incorporation of only 0.3% of PFT-2,5, 19.4% with the incorporation of 1% of PFT-2,5, increase to 28.4% with the incorporation of 3.4% PFT-2,5; drops to 25%, with further incorporation of PFT-2,5; and finally to only 6% for neat PFT-2,5.

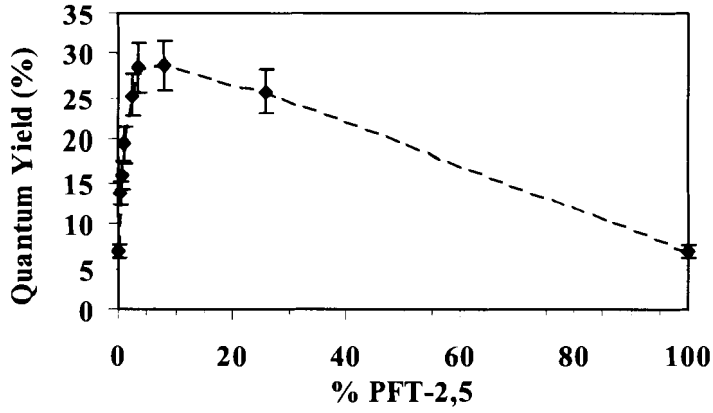

Figure 3.5: Solid state Φ_{pl} of PFT-2,5/-3,4 blends.

The polymer blends clearly show a strong enhancement in the quantum yield of luminescence. This enhancement is attributed to the isolation of the polymer emitters. Although the emission has increased four to five-fold compared to the neat PFT-2,5, this is only half the quantum yield of PFT-2,5 in solution, indicating that the emitting species are not completely isolated. The complete isolation of the emitters was not observed in this system, possibly due to close, but not complete molecular dispersion of the PFT-2,5 in PFT-3,4. Therefore, PFT copolymers will be investigated, with the intent to further isolate the emitting species.

3.2.1.2.2 PFT Copolymers

Several polymers with various feed ratios of 9,9-dihexylfluorene-2,7-bis(trimethyleneborate), 3,4-dibromothiophene, and 2,5-dibromothiophene were prepared as illustrated in Figure 3.6. Copolymers were prepared with the following ratio of 3,4-thiophene : 2,5-thiophene linkages: 0.99:0.01 (PFT-0.01A),

0.97:0.03 (PFT-0.03A), 0.96:0.04 (PFT-0.04A), 0.93:0.07 (PFT-0.07A), 0.90:0.10 (PFT-0.1A), 0.80:0.20 (PFT-0.2A) and 0.50:0.50 (PFT-0.5A).

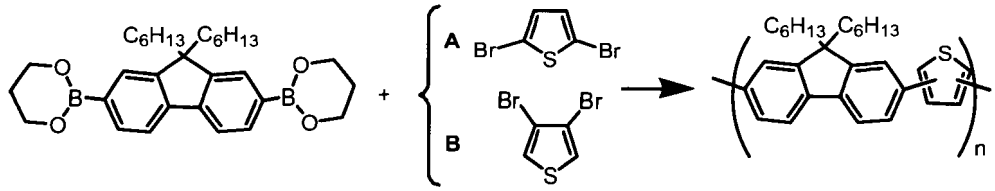

Scheme 3.2: Synthesis of randomly distribulted alternating PFT-2,5 and PFT-3,4 polymer. A polymer consisting of 10% "A" is termed PFT-0.1A.

The optical spectra of the copolymers are illustrated in Figure 3.2. Two distinct absorption peaks are observed in the solid state absorption spectrum of the seven hybrid copolymers: One exhibiting a maximum at ~322 nm due to PFT-3,4 segments; and the other at ~410 nm due to PFT-2,5 segments. The ratio of the relative intensity of the absorption bands are correlated to the ratio of PFT-2,5 to PFT-3,4 in the polymer, which indicates that the hybrid copolymers are characterized by two polymer domains: PFT-2,5 and PFT-3,4.

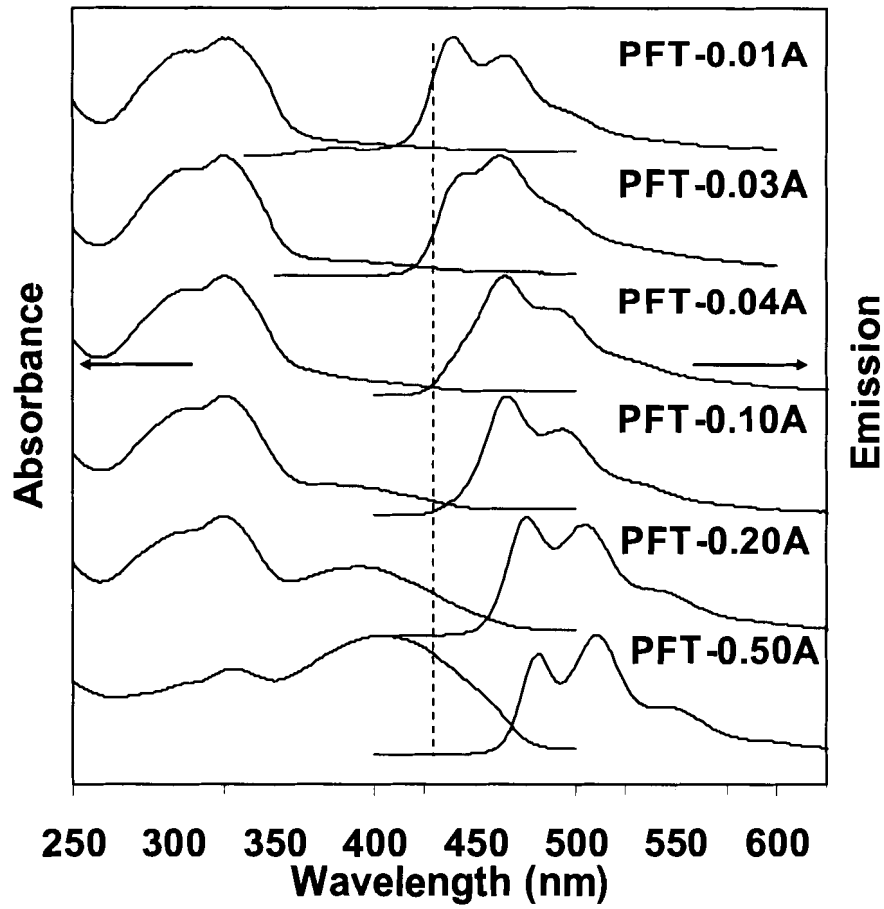

Figure 3.6: Solid state optical spectra of PFT copolymers. Refer to Scheme 3.2 for label explanation.

Photoluminescence maxima vary from 442 nm (for PFT-0.01) to 510 nm (PFT-0.5 A). PFT-0.01A (1% 2,5-linked thiophene, 99% 3,4-linked thiophene) emission is cyan-blue in colour while PFT-0.5A is green. In comparing the emission profiles with those of PFT-2,5 and PFT-3,4 (Figure 3.6), emission from the hybrids clearly emanates from PFT-2,5 motifs; negligible emission is observed from PFT-B domains, despite direct excitation of these domains with 320 nm light.

The solid state quantum yields varied significantly as shown in Figure 3.7.

The Φ_{pl} values are 6% for PFT-3,4; increase to 16% with the incorporation of 1% of the 2,5-thiophene isomer, 43% with the incorporation of 4% of the 2,5-thiophene isomer (PFT-0.04A); drop to 19%, with further incorporation of the 2,5-thiophene isomer (PFT-0.1A and PFT-0.2A); drop further to 14% when 50% of the 2,5-thiophene isomer is incorporated (PFT-0.5A); and finally only 6% for PFT-2,5.

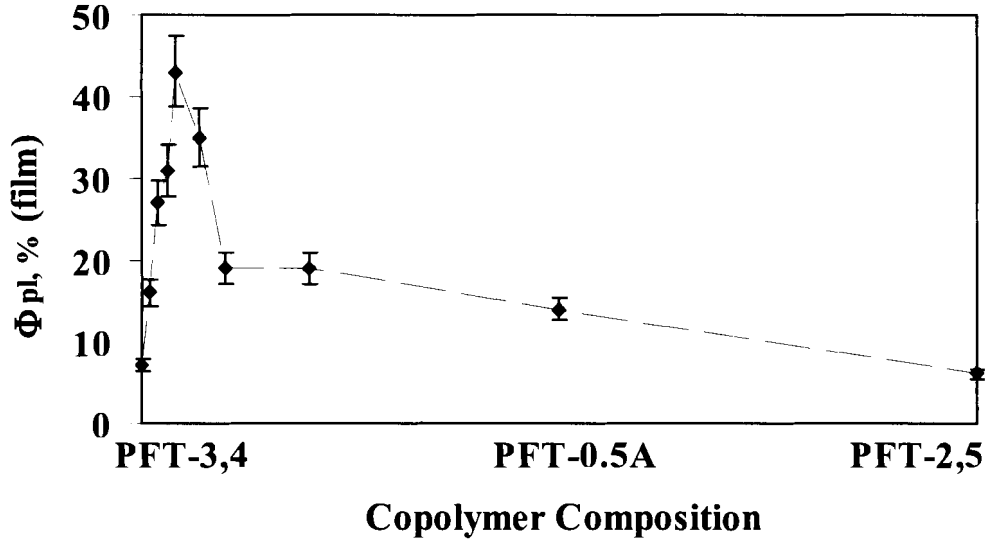

Figure 3.7: Solid state quantum yields of luminescence.

The solid state emission spectra of the seven hybrid polymers are characterized by two peaks and a shoulder, the intensity of which varied with composition. The wavelength of maximum emission red shifts from 442 nm, to 456 nm, 465 nm, to 467 nm, to 470 nm, to 476 nm, and to 510 nm upon traversing the series PFT-0.01A to PFT-0.5A; indicating the emitting 2,5-linked thiophene–fluorene copolymer becomes progressively more coplanar and aggregated. Revealingly, emission spectrum of the PFT-0.04A film was

superimposable, in wavelength and relatively absorption peaks, with that of PFT-*2,5* in solution. The two spectra are overlaid in Figure 3.8. All higher substituted polymers possessed solid state emission spectra that were red-shifted compared to the solution emission spectra of PFT-2,5, and vice versa. We conclude that films of PFT-0.04A are characterized as comprising a solid solution of a 2,5-linked thiophene–fluorene copolymer segment (PFT-2,5 segment) in a matrix of 3,4-linked thiophene–fluorene copolymer (PFT-3,4 matrix). Photoluminescence thus occurs as follows: the PFT-3,4 matrix absorbs irradiation; excitation is transferred to individual PFT-2,5 segments *via* efficient energy migration and transfer; emission occurs from isolated PFT-2,5 segments. This process is illustrated in Figure 3.8 (inset). Upon increasing the concentration of PFT-A in the hybrid copolymers the emission wavelength red shifts and the quantum yield of luminescence decreases because of the increasing propensity for aggregation.

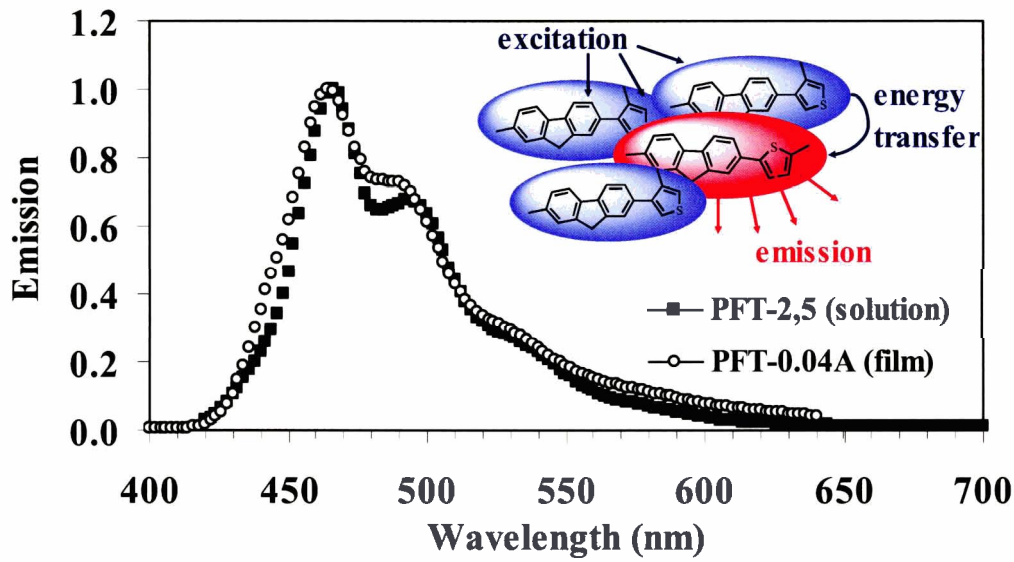

Figure 3.8: Solution emission of PFT-A (○) and solid state emission of PFT-0.04A (■). Inset: energy transfer mechanism.

3.2.2 Part 2: Spectral Purity via Host-Guest Methodology

Solutions of poly(fluorene)s[5] display a blue-violet emission with Φ_{pl} values in the range of 0.7-0.8. Red-tailing and a large decrease in the emission intensity is however observed in the solid state which is believed to be attributed to fluorenone formation,[6] molecular aggregation and/or excimer formation.[7] Red-tailing affects spectral stability, whereby an irreversible blue to green colour emission is observed, or emerges, because of the eye's sensitivity to green light. This is described in detail in Section 1.4.1.2.3.

In this section, the solution emission properties, i.e. blue colour purity and quantum yield, of polyfluorenes in the solid state are attained using a self-forming host-guest system. Alternating thiophene-co-fluorene polymers were studied with molecularly-kinked 3,4-linked thiophene and/or the molecularly-linear 2,7-linked 9,9-dihexyl-fluorene, respectively according to Scheme 3.3.

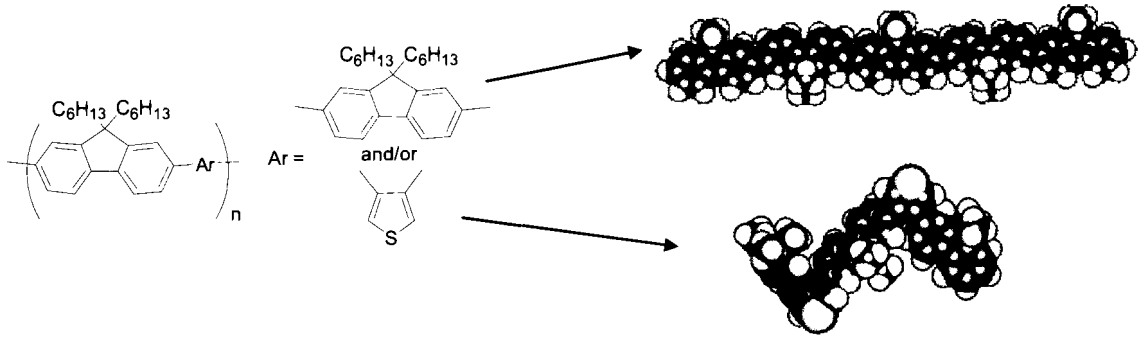

Scheme 3.3: Polymers investigated and their corresponding space filling models (5 units long).

3.2.2.1 Synthesis

Polymers were synthesized according to literature procedures *via* the Suzuki polycondensation method.[1] The copolymerization of 9,9-dihexylfluorene-2,7-bis(trimethyleneborate) with 3,4-dibromothiophene and/or 2,7-dibromo-9,9-dihexylfluorene is illustrated in Scheme 3.4. These polymers possessed a molecular weight ranging from 6000 to 35,600 Daltons, with synthetic yields ~80%. The polymers were soluble in common organic solvents, such as toluene, chloroform, tetrahydrofuran, and dichloromethane.

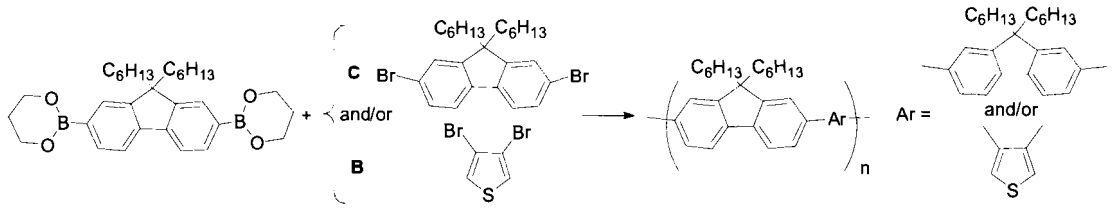

Scheme 3.4: Synthesis of PFT polymers

Polymer	C	B	Mw	PDI
PFT-3,4	0.00	1.00	8132	1.31
PFT-0.05C	0.05	0.95	5838	1.18
PFT-0.1C	0.10	0.90	9168	1.36
PFT-0.15C	0.15	0.85	15, 836	1.61
PFT-0.2C	0.20	0.80	13, 292	1.54
PFT-0.35C	0.35	0.65	18, 863	1.69
PFT-0.5C	0.50	0.50	17, 530	1.69
PDHF	1.00	0.00	35, 607	2.56

Table 3.1: Polymers Synthesized with Various Feed Ratios, and Their Corresponding Molecular Weight.

3.2.2.2 Optical Properties

The optical spectra of poly((3,4-thienylene)-2,7-(9,9-dihexylfluorene)) (PFT-3,4) and poly(9,9-dihexylfluorene) (PDHF) are compared in Figure 3.9. Solution and film absorption spectra of PFT-3,4 are blue shifted compared to PDHF due to its kinked structure and lower effective conjugation length. Emission wavelengths are also blue-shifted: PDHF emission maxima are 417 nm and 424 nm for solution and film, respectively; corresponding values for PFT-3,4 are 383 nm and 410 nm.

Quantum yields of luminescence of PFT-3,4 and PDHF solutions are 0.39 and 0.70, respectively: the lower yield of the former being possibly due to its less rigid structure and heavy atom effect induced by the sulfur in thiophene.[8] Quantum yields of the corresponding films are much lower: 0.07 and, 0.12 respectively. Since their emission wavelengths are red-shifted by 27 and 7 nm, respectively, compared to their solution spectra, it is evident the emitting segments exhibit enhanced coplanarity and/or aggregation in the solid state.[4]

Examination of Figure 3.9 illustrates that the solid-state emission of PFT-3,4 overlaps with the absorption spectra of PDHF. Thus a polymer composite, prepared by either blending or copolymerization, based on a PFT-3,4 host and a PDHF guest, should give rise to an efficient host-guest system.

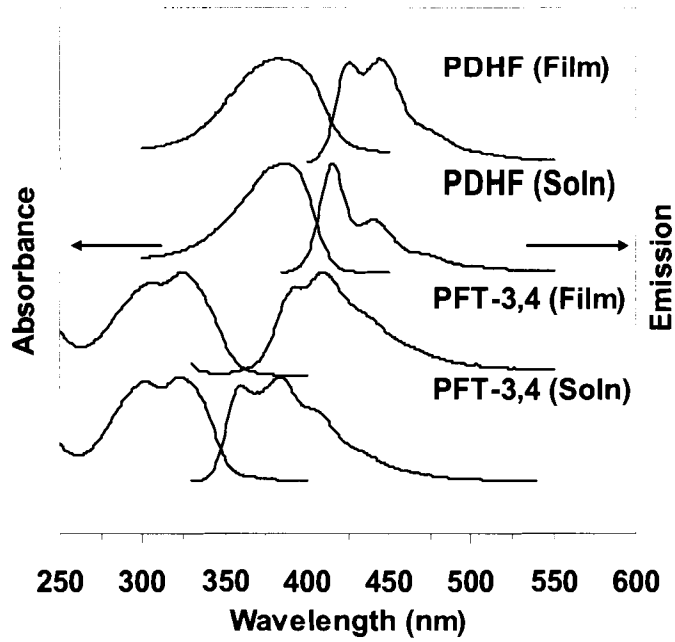

Figure 3.9: Solution and solid state optical properties of PDHF and PFT-3,4.

3.2.2.2.1 Polymer Blends

Considering the molecular similarity between the PFT-3,4 and PDHF, a polymer blend may be a feasible method for obtaining a host-guest system. Figure 3.10 illustrates the absorption and emission of blends at various concentrations. It is clear that the optical properties are dependant on the concentration of PDHF. That is, for blends with only ~4 weight percent of PDHF, the primary emitting species is PDHF, and exhibits structured emission at 416 nm and 444 nm. Furthermore, at ~16% PDHF, the emission occurs primarily at 419 nm and 448 nm, again emanating from PDHF, with negligible emission from PFT-3,4, which indicates that blends should satisfy Förster energy transfer requirements. With incorporation of 48% PDHF, the emission appears to

originate from aggregated segments, having an emission maximum at 424 nm and the shoulder at 451 nm –as judged by its spectral similarity to aggregated PDHF. Analysis of the quantum yields of luminescence in Figure 3.11, uncovers only a small dependence on the concentration of the PDHF. The values are closer to solid state values of PDHF (0.12) than to solution values (0.70) indicating that emission comes from aggregates of PDHF. From this, it can be inferred that polymer chains of PDHF are not molecularly dispersed in the PFT-3,4 matrix but rather exist as phase segregated aggregates. Therefore, the PFT-3,4/PDHF system appears to be a useful candidate to examine as host-guest copolymers in order that a molecularly dispersed system of PDHF in PFT-3,4 can be achieved.

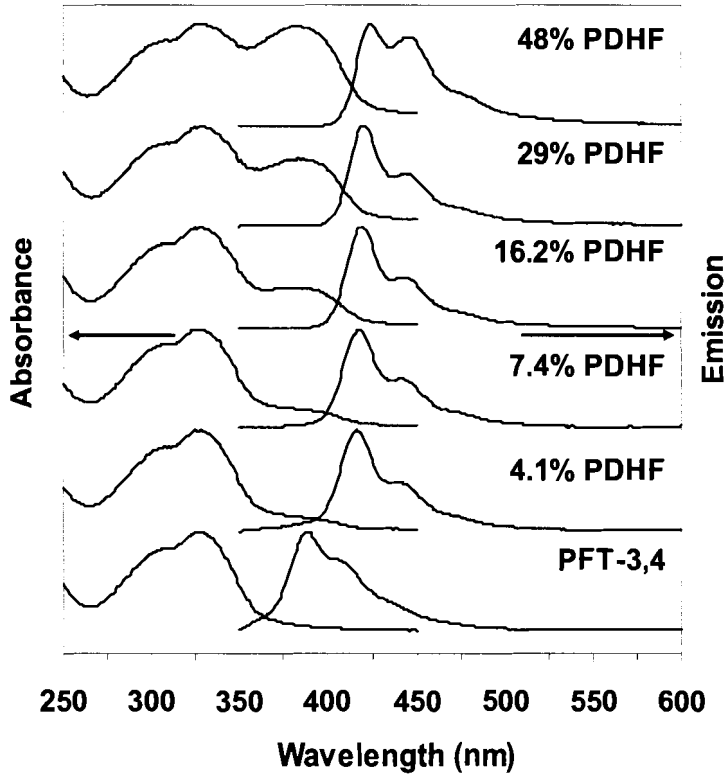

Figure 3.10: Solid state optical properties of polymer blends.

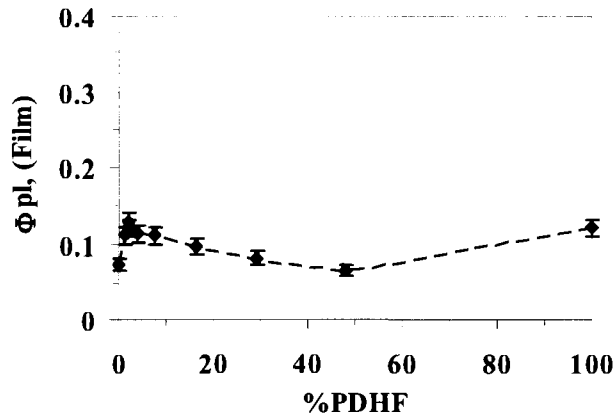

Figure 3.11: Quantum yield of luminescence of polymer blends as a function of PDHF concentration.

3.2.2.2.2 Copolymers

Several copolymers with various feed ratios of 9,9-dihexylfluorene-2,7-bis(trimethyleneborate), 3,4-dibromothiophene, and 2,7-dibromo-9,9-dihexylfluorene were prepared according to Scheme 3.4. Copolymers were prepared with the following ratios of 3,4-thiophene : 2,7-dibromo-9,9-dihexylfluorene: 0.95:0.05 (PFT-0.05C), 0.90:0.10 (PFT-0.1C), 0.85:0.15 (PFT-0.15C), 0.80:0.20 (PFT-0.20C), 0.65:0.35 (PFT-0.35C) and 0.50:0.50 (PFT-0.5C).

Two distinct absorption peaks are observed in both the solution and solid state absorption spectra of the six copolymers as shown in Figure 3.12: One occurs at a wavelength of ~322 nm, and is due to PFT-3,4 segments; while the other is a shoulder at ~368 nm due to PDHF segments. The ratio of the relative intensity of the absorption bands is correlated to the mass ratio of PDHF to PFT-3,4 in the polymer, and indicates that the hybrid copolymers are characterized by distinct polymer domains of PDHF and PFT-3,4.

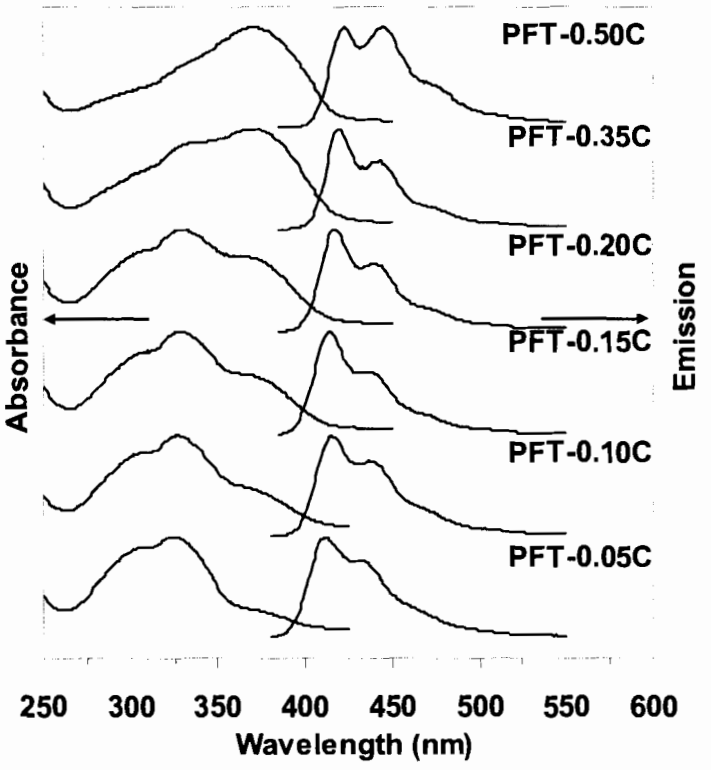

Figure 3.12: Solid state optical properties of PFT copolymers with different feed ratios.

Solution emission spectra are depicted in Figure 3.13, where direct excitation of the PFT-3,4 segment at 320 nm reveals two characteristic emission peaks for polymers containing low 2,7-dibromo-9,9-dihexylfluorene ("C") content (up to about 20%): one corresponding to PDHF and the other to PFT-3,4. The fact that emission from a PDHF domain is observed implies that energy transfer from the PFT-3,4 to the PDHF domains takes place; the fact that PFT-3,4 emission is observed means that energy transfer is incomplete. Figure 5b displays Φ_{pl} as a function of copolymer composition. It is found that as the fluorene component increases, Φ_{pl} approaches that of pure PDHF, which also indicates the emission is dominated by PDHF emission.

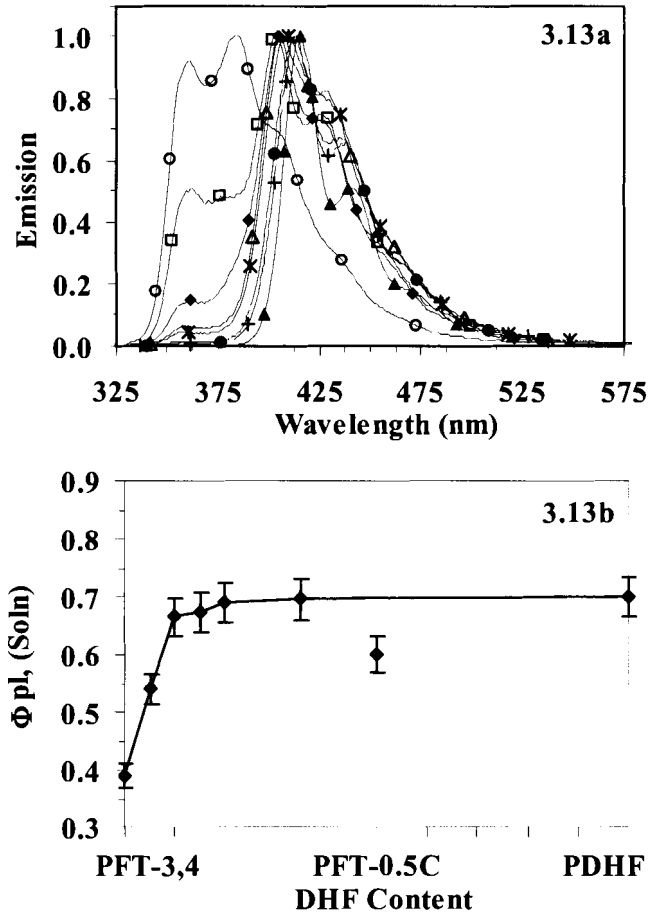

Figure 3.13: (a) Solution photo-luminescence spectra of PFT copolymers: PFT-3,4 (O), PFT-0.05C (□), PFT-0.10C (◆), PFT-0.15C (△), PFT-0.20C (∗), PFT-0.35C (●), PFT-0.5C (+), PDHF (▲). (b) Quantum yield of luminescence as a function of DHF content.

Solid state photoluminescence maxima vary from 412 nm (for PFT-0.05C) to 423 nm (PFT-0.5 C). The PFT-0.05A emission is deep blue-violet in colour; PFT-0.5C, deep blue. In comparing emission profiles with those of PDHF and PFT-3,4 (Figure 3.9), emission from the copolymers clearly emanates from PDHF units. With PDHF content ≥ 10% (PFT-0.10C), no emission is observed from the PFT-3,4 domains despite direct excitation of these domains with 320 nm light.

The solid state quantum yields vary significantly as shown in Figure 3.14.

Φ_{pl} values are 0.07 for PFT-3,4; 0.17 with the incorporation of 5% of 2,7-dibromo-9,9-dihexylfluorene (PFT-0.05C); 0.34, with additional 2,7-dibromo-9,9-dihexylfluorene. Φ_{pl} stabilizes (0.30-0.27) with incorporation of 35% 2,7-dibromo-9,9-dihexylfluorene, but drops to 0.19, with further incorporation of the 2,7-dibromo-9,9-dihexylfluorene (PFT-0.5A). Φ_{pl} is only 0.12 for PDHF.

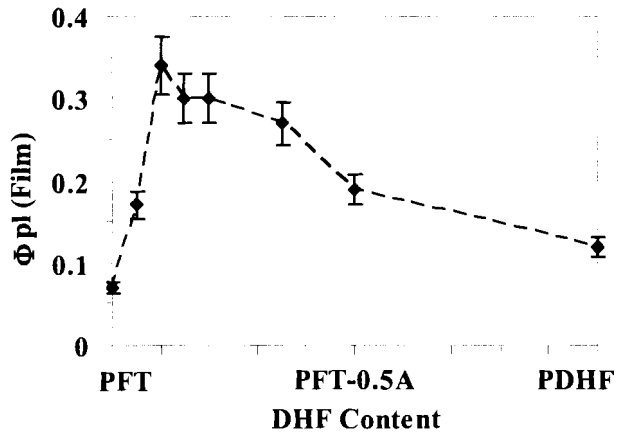

Figure 3.14: Solid state quantum yield of luminescence of PFT copolymers with various feed ratios.

The solid state emission spectra of the five hybrid polymers are characterized by two peaks and a shoulder. The wavelength of maximum emission red shifts from 410, to 412, 414, 415, 417, 420, 423, and to 424 nm upon traversing the series PFT-0.05C to PFT-0.50C which indicates that the emitting thiophene–fluorene copolymer becomes progressively more coplanar and aggregated with dihexylfluorene (DHF) content.

When the solution properties of PDHF are compared with the solid state emission of the copolymers, the PFT-0.1C film emission spectrum is observed to be similar to the solution emission properties of PDHF. The solid state PFT-

0.05C spectrum is blue shifted compared with PDHF, as depicted in Figure 3.15. Furthermore, the solid state quantum yield of luminescence of PFT-0.05C is similar to that of PFT-3,4 (in the solid state) and its yield is lower than PFT-0.1C. This result indicates that energy transfer from the PFT-3,4 domains to the PDHF, as illustrated in Figure 3.15b, in PFT-0.05C is incomplete. PFT-0.1C displays the highest quantum yield of luminescence. A sharp decline in the quantum yields of luminescence with increasing DHF content was not observed, as in the case for copolymers of fluorene with 3,4- and 2,5- linked thiophene in Part 1, most likely due to the alkyl chains on the fluorene emitter preventing molecular aggregation to some extent. Similarly, it was found in molecular based LEDs, that the bulkiness of the guest emitter deterred aggregation.[9]

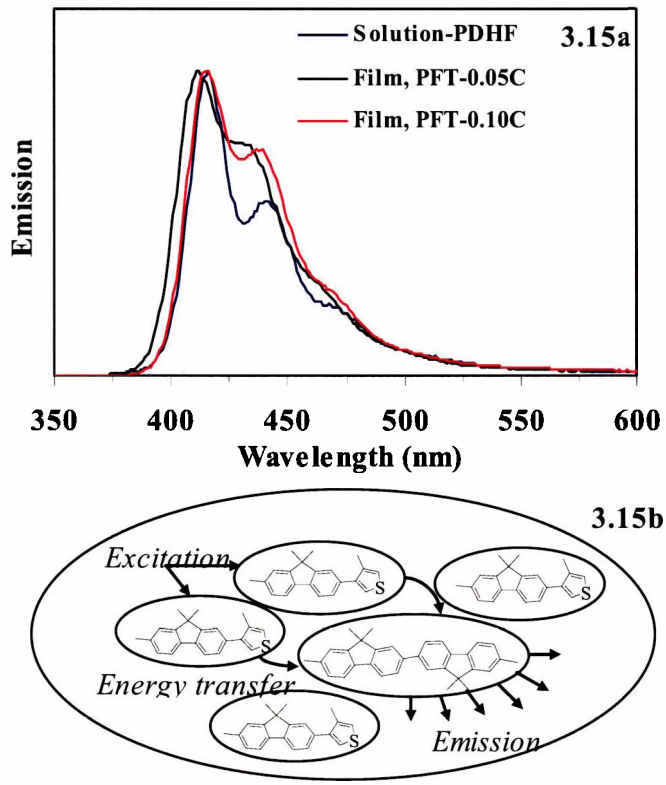

Figure 3.15: (a) Solution emission of PDHF with respect to film emission of PFT-0.05C and PFT-0.10C. (b) Energy transfer mechanism.

The dependence of quantum yield on the dihexylfluorene (DHF) content is clearly different for blends and copolymers. It is postulated that the DHF motifs in the copolymers are dispersed at the molecular level, while in the polymer blends distinct aggregated domains exist. The validity of this postulate may be examined by inspection of the energy transfer efficiency. For efficient energy transfer to occur, the absorption of the guest and the emission of the host must have significant overlap, and the distance between the donor and acceptor must be small (3-10 nm).[10] When comparing the absorption of the PDHF segment in PFT-0.05C and the 7.4% PDHF blend with the solid state emission of the PFT-3,4 (Figure 3.16), the overlap integral of the DHF segments –blends and copolymers- with the PFT-3,4 emission is similar. Since the overlap integral is the same, the efficiency of energy transfer must be dependant on the distance between the donor and acceptor. Figure 3.17 shows an expanded view analysis of the emission region of the PFT-3,4 domains in both the blend (Figure 3.17a) and copolymers (Figure 3.17b). Emission from the PFT-3,4 segment, which indicates incomplete energy transfer, is at least an order of magnitude greater for the blend than for the copolymer. This confirms that energy transfer in the blends is less efficient and indicates that DHF units in the copolymers are solid state solutions rather than phase separated aggregates.

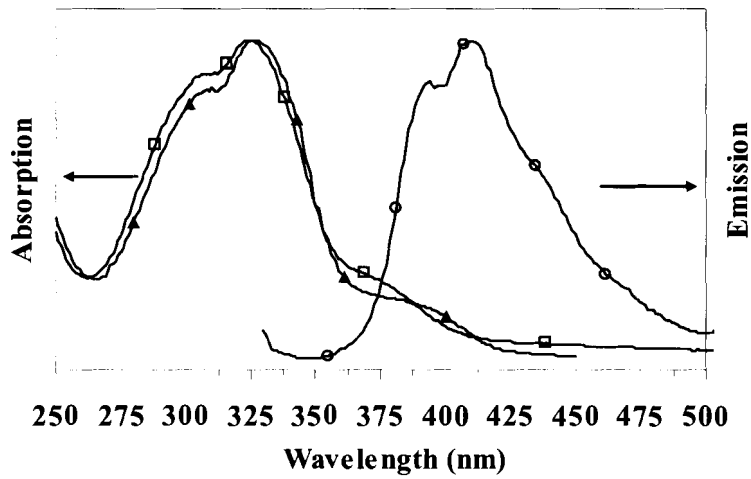

Figure 3.16: Absorption spectra of PFT-0.05C (□) and 7.1% PDHF blend (▲) and emission spectrum of PFT-3,4 solid state emission (○).

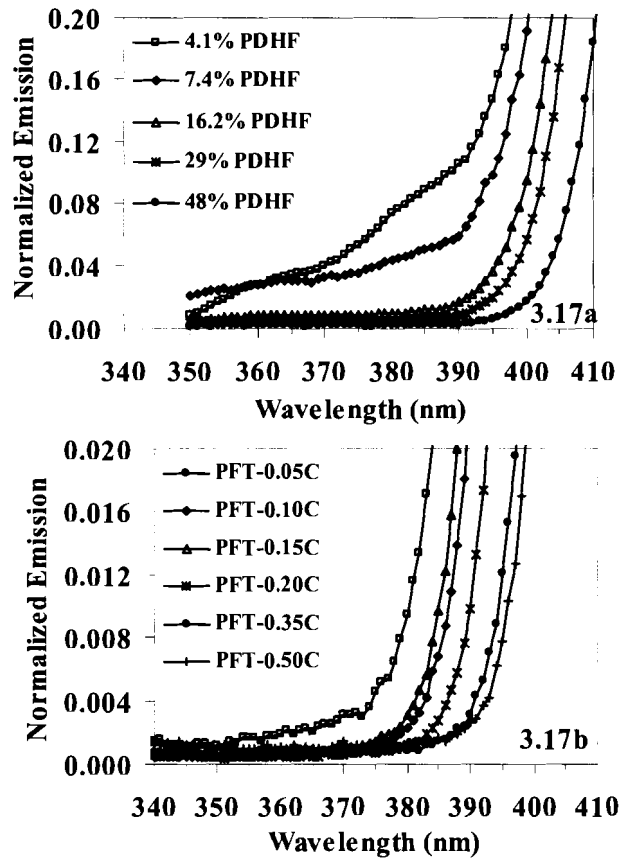

Figure 3.17: (a) Solid state emission of polymer blends in the PFT-3,4 region. (b) Solid state emission of PFT copolymers from PFT domains.

3.2.2.2.3 Device Fabrication

Light emitting diodes were fabricated from the copolymers described above. The devices had the following structure: ITO anode, poly-3,4-ethylene-dioxythiophene polystyrenesulfonate (PEDOT) hole injection layer (140 nm), PFT polymer, Mg:Ag cathode (9:1; 100nm), Ag encapsulation layer (300nm). Structured electroluminescence is observed for all polymers, with emission maxima in the range of 415nm to 426 nm, which are shown in Figure 3.18. Emission from PFT-0.05C occurs at 415 nm with a shoulder at 428 nm; emission from PFT-0.20C occurs at 417 nm with a shoulder at 444 nm; from PFT-0.35C, it occurs at 419 nm with a shoulder at 445 nm; from PFT-0.50C, 422 nm with two shoulders at 445 nm and 484 nm; and from PDHF it occurs at 426 nm, with shoulders at 446 nm, 481 nm and 521 nm. Red-tailing was significantly reduced for the PFT copolymers compared to PDHF, thus providing an alternative method to obtain colour purity in blue emitting polymers.

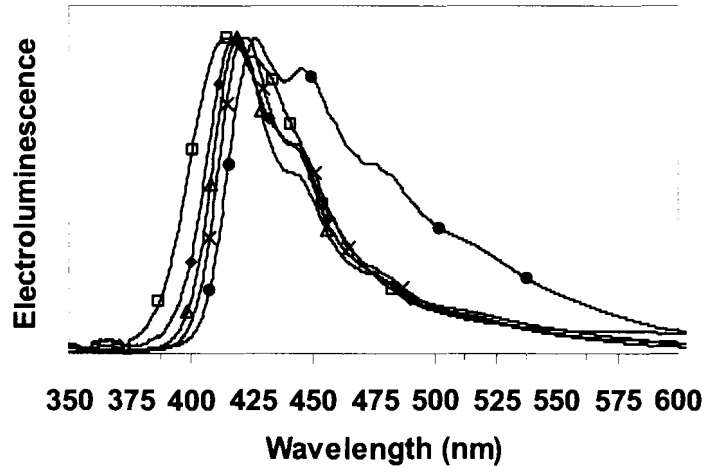

Figure 3.18: Electroluminescence of PFT copolymers: PFT-0.05C (□), PFT-0.20C (◆), PFT-0.35C (△), PFT-0.5C (×), PDHF (●).

Quantum yields of electroluminescence were generally quite low (external efficiencies: 1×10^{-4} for PDHF). With the addition of a 15 nm thick electron transport / injection layer (triphenyltriazine) between the polymer and the cathode,[11] the efficiency increased: the external quantum efficiency of PDHF was 1.3×10^{-3}; for PFT-0.5C, 7×10^{-3}; PFT-0.35C, 5.3×10^{-3}; PFT-0.20C, 1.1×10^{-2}; and PFT-0.05C, 1.1×10^{-3}. Copolymer content has a pronounced effect on the quantum yields of electroluminescence. Too high a DHF content decreases the quantum efficiency. However, with ≤ 5% DHF content, the quantum efficiency also drops. Furthermore, the host (PFT) efficiency was low ($<1\times10^{-4}$), with a high turn-on voltage of ~11V. The low efficiency indicates that resistance to charge injection into the host is significant, and the device efficiency is injection limited at DHF contents ≤ 5%. Nonetheless, between 20-50% DHF content, the polymers exhibit a pronounced enhancement (up to 10 fold) in quantum efficiency. This enhancement has been observed in other host-guest based polymers, and was attributed to isolation of the emitting states.[12]

3.2.2.2.4 Spectral Stability

An important attribute of blue-emitting luminescent polymers is spectral stability. The two leading theories for colour instability in poly(fluorene)s are fluorenone formation[6] and aggregation[7]. The host-guest system presented here is a model system to investigate this effect since aggregation is reduced and the emitters are isolated. Thus films were annealed, and electroluminescence recorded at various current densities. These two experiment methods are depicted in Figure 3.19. Upon annealing the films at 140 °C for 2 hours, a broad

luminescence band evolves at ~560 nm. The same band is observed in the electroluminescence recorded at different current densities. Instability in these poly(fluorene)s is therefore attributed to fluorenone formation, which may be minimized in combination with modified fluorene monomers and polymers.[6,13]

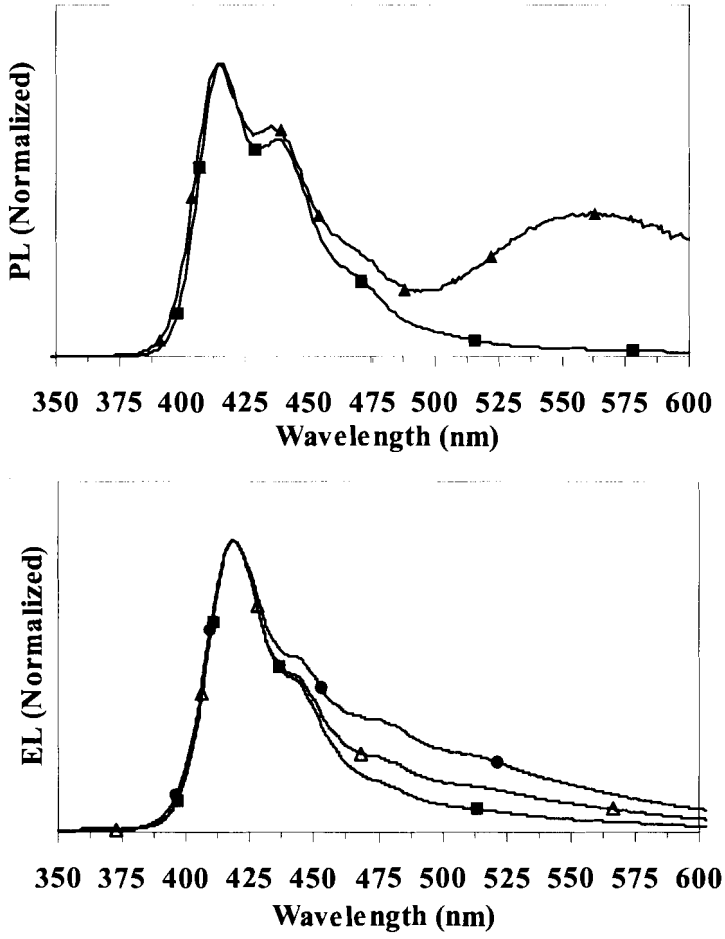

Figure 3.19: (a) Photoluminescence of PFT-0.1C before (■) and after annealing (▲). (b) Electroluminescence of PFT-0.35C at various current densities (25 mA/cm^2: ■, 50 mA/cm^2: △, 125 mA/cm^2: ●).

3.3 Conclusion

It was found that the optical properties were significantly tuned with the use of various dibromothiophene isomers in PFTs. The quantum yields of photoluminescence were quite low, possibly due to a non-emissive eximer formation.

Host-guest type systems were also investigated with use of polymer blends and copolymers. The emission colour depended on the concentration of the guest. For instance, cyan-blue to green was observed in Part 1, and blue-violet to light blue was observed in Part 2. These differences are attributed to aggregation (or the lack of) of the emitting species. Furthermore, quantum yields of luminescence were analyzed, and it was found that copolymers showed greater values rather than polymer blends. This effect is ascribed to a lack of molecular dispersion in polymer blends.

In Part 2, both polymer blends and copolymers provided blue-violet emission, thus presenting a facile alternative route for increasing the blue colour purity in blue emitting PLEDs. Furthermore, electroluminescent efficiencies increased 10-fold. The polymer's photo- and electro- luminescent properties mimicked PDHF with the additional attributes that the luminescent yields were much higher, and red-tailing was absent.

3.4 Experimental

3.4.1 Synthesis

General synthesis of poly(9,9-dihexylfluorene-alt-thiophene)s: Polymers were prepared by Suzuki polycondensation according to previously reported methods.[1] To a flask containing a degassed solution of 3,4-dibromothiophene (0.26g, 1 mmol), 9,9-dihexylfluorene-2,7-bis(trimethyleneborate) (0.53g, 1 mmol) and 2 ml of an aqueous solution of 2.4M K_2CO_3 in freshly distilled THF (10 ml) was added 3 mol % of $Pd(PPh_3)_4$ (0.036g, 0.03 mmol). The mixture was heated for 24-72 hours at 80°C in a sealed tube, diluted with $CHCl_3$, and washed with water. The organic phase was dried with $MgSO_4$ and the solvent was partially removed under reduced pressure. The remaining polymer solution was precipitated into a methanol solution. The polymer was collected and dissolved in chloroform, and further purified *via* column chromatography (neutral activated alumina, 60-325 mesh, Fisher Scientific). Weight average molecular weights (M_w) ranged from 5800-35,600 Daltons and PDI values were 1.2-2.6.

Poly((2,5-thienylene)-2,7-(9,9-dihexylfluorene)), PFT-2,5: 400MHz ^1H NMR, PPM (CD_2Cl_2): δ=7.65-7.4 (6H, fluorene), 7.10 (2H, thiophene), 2.25 (4H, β-CH_2), 1.05 (12H, CH_2), 0.71 (10H, CH_2 and CH_3). FTIR, cm^{-1} (KBr): 3105 (C-H stretch, aromatic), 2950 (CH_3 asymmetric stretch), 2929 (CH_2 in-phase vibration), 2858 (CH_2 out-of-phase vibration), 1465 (C=C stretch, ring), 823 (C-H out-of plane bending). Molecular weight (GPC): M_w = 7500 , PDI = 1.7

Poly((2,4-thienylene)-2,7-(9,9-dihexylfluorene)), PFT-2,4: 500MHz ^{1}H NMR, PPM (CD_2Cl_2): δ 7.82-7.71 (6H, fluorene), 7.5 (2H, thiophene), 2.25 (4H, β-CH_2), 1.05 (12H, CH_2), 0.71 (10H, CH_2 and CH_3). FTIR, cm^{-1} (KBr): 3062 (C-H stretch, aromatic), 2950 (CH_3 asymmetric stretch), 2929 (CH_2 in-phase vibration), 2860 (CH_2 out-of-phase vibration), 1463 (C=C stretch, ring), 815 (C-H out-of plane bending). Molecular weight (GPC): M_w = 6300, PDI = 1.5

Poly((3,4-thienylene)-2,7-(9,9-dihexylfluorene)), PFT-3,4: 400MHz ^{1}H NMR, PPM (CD_2Cl_2): δ 7.7-7.1 (8H, fluorene and thiophene), 1.7 (4H, β-C*H*$_2$), 1.05 (12H, C*H*$_2$), 0.70 (6H, C*H*$_3$) 0.55 (4H, C*H*$_2$). FTIR, cm^{-1} (KBr): 3058 (C-H stretch, aromatic), 2950 (CH_3 asymmetric stretch), 2929 (CH_2 in-phase vibration), 2856 (CH_2 out-of-phase vibration), 1465 (C=C stretch, ring), 823 (C-H out-of plane bending). Molecular weight (GPC): M_w = 8100, PDI = 1.31.

Poly(9,9-dihexylfluorene), PDHF: 400MHz ^{1}H NMR, PPM (CD_2Cl_2) δ 7.88-7.37 (6H), 2.16 (4H), 1.13 (12H), 0.81-0.75 (10H). FTIR, cm^{-1} (KBr): 3064 (C-H stretch, aromatic), 2958 (CH_3 asymmetric stretch), 2931 (CH_2 in-phase vibration), 2860 (CH_2 out-of-phase vibration), 1458 (C=C stretch, ring), 813 (C-H out-of plane bending). Molecular weight (GPC): M_w = 35, 601, PDI = 2.56.

The NMR spectra of the hybrid copolymers were a combination of signals from PFT-3,4 and -2,5 signals for PFT-A series and PFT-3,4 and PDHF signals for PFT-C series.

3.4.2 Materials

3,4-dibromothiophene (99%), 2,5-Dibromobromothiophene (95%), 9,9-dihexylfluorene-2,7-bis(trimethyleneborate) (97%) and tetrakis(triphenyl-

phosphine)palladium (0) ($Pd(PPh_3)_4$) (99%) were purchased from Sigma-Aldrich Canada Ltd. and used as received. 2,4-dibromothiophene (97%) was purchased from Spectrum, and used as received. PEDOT (electronic grade Baytron® P VP CH 8000) was purchased from H.C. Stark, and used as received. Tetrahydrofuran was distilled prior to use.

3.4.3 Measurements

^1H NMR spectra were recorded in CD_2Cl_2 on a 400 MHz Bruker AMX400 spectrometer. Chemical shifts were recorded in parts per million (ppm) and referenced to CH_2Cl_2 (δ 5.32). Molecular weights were measured by gel permeation chromatography (GPC) (Waters Model 1515 isocratic pump) equipped with μ-Styrgel columns against polystyrene standards. Polymers (2mg/ml) were eluted with tetrahydofuran (THF) using a flow rate of 1mL/min and monitored with a UV-vis detector (Waters 2487). UV-vis absorption spectra were measured with a Cary 3E (Varian) spectrophotometer. Photoluminescence spectra were recorded with a Photon Technology International QuantumMaster model QM-1 equipped with an extra sample compartment containing an integrating sphere. For precise comparisons, both solution and solid-state absolute quantum yield of luminescence efficiencies (±10%) were obtained using an integrating sphere, as previously reported.[14] The excitation wavelength was 320 nm for all polymers, except for PDHF (370 nm). Solutions were de-oxygenated with pre-purified nitrogen prior to the fluorescence measurements and the sample compartment was flushed with nitrogen for thin film measurements. Fluorescent spectra of the thin films, spin cast from $CHCl_3$ on

quartz, had an optical density of ~0.5 (3-5 mg/0.5 ml of solvent; corresponding thickness' were approximately 0.3 μm). Spectra were recorded 22.5° normal to the incident light.

Polymer LEDs were based on the following structure: indium tin oxide (ITO) anode/ PEDOT (140 Å thick) / polymer / magnesium:silver alloy (9:1) cathode (~1200 Å). The PEDOT layer was deposited at a rate of 2000 RPM, after filtering through a 0.45μm PVDF filter on an ozone pre-cleaned patterned ITO substrate. The polymer films were prepared by dissolving 8 mg of polymer in 1 ml of toluene, filtering through a 0.2 μm PTFE filter and spin coating (2000 RPM). A Mg:Ag cathode was formed by co-evaporation of Mg and Ag at a rate of 4 Å/s and 0.4 Å/s, respectively. Deposition rates were controlled individually by quartz crystal monitors.

3.5 References

1. (a) P. Blondin, J. Bouchard, S. Beaupre, M. Belletete, G. Durocher, M. Leclerc, *Macromolecules* **2000**, *33*, 5874. (b) M. Ranger, M. Leclerc, *Can. J. Chem.* **1998**, *76*, 1571. (c) M. Ranger, M. Leclerc, *Macromolecules* **1999**, *32*, 3306.

2. A. Charas, J. Morgado, J.M.G. Martinho, L. Alcácer, F. Cacialli, *Synth. Met.* **2002**, *127*, 251.

3. (a) B. Liu, Y-H. Niu, W-L Yu, Y. Cao, W. Huang, *Synth. Met.* **2002**, *129*, 129. (b) B. Liu, W-L. Yu, Y-H. Lai, W. Huang, *Macromolecules* **2000**, *33*, 8945.

4. (a) K. -Y. Peng, S. -A. Chen, W. -S. Fann, *J. Am. Chem. Soc.* **2001**, *123*, 11388.

5. M. Grell, W. Knoll, D. Lupo, A. Meisel, T. Miteva, D. Heher, H. -G. Nothofer, U. Scherf, A. Yasuda, *Adv. Mater.* **1999**, *11*, 671.

6. J. H. Lee, D. H. Hwang, *Chem. Commun.* **2003**, 2836.

7. (a) K. -H. Weinfurtner, H. Fujikawa, S. Tokito, Y. Taga, *Appl. Phys. Lett.* **2000**, *76*, 2502. (b) M. Grell, D. D. C. Bradley, G. Ungar, J. Hill, K. S. Whitehead, *Macromolecules* **1999**, *32*, 5810. (c) G. Zeng, W. -L. Yu, S. -J Chua, W. Huang, *Macromolecules* **2002**, *35*, 6907.

8. (a) C. Yang, M. Abley, S. Holdcroft, *Macromolecules* **1999**, *32*, 6889. (b) A. J. Cadby, C. Yang, S. Holdcroft, D. D. C. Bradley, P. A. Lane, *Advanced Materials* **2002**, *14*, 57 (c) B. Xu, S. Holdcroft, *J. Am. Chem. Soc.* **1993**, *115*, 8447.

9. C. H. Chen, C. W. Tang, *Appl. Phys. Lett.* **2001**, *79*, 3711.

10. V. Bulović, M. A. Baldo, S. R. Forrest, in Materials Science, Organic Electronic Materials Conjugated Polymers and Low Molecular Weight Organic Solids, Farchioni, R., Grosso, G., Eds., Springer: New York, 2001; Vol. 41, p 404.

11. (a) S. Holdcroft, Y. Li, G. Vamvounis, H. Aziz, Z. D. Popovic, in Chromogenic Phenomena in Polymers: Tunable Optical Properties. Proceedings of the American Chemical Society Symposium on Chromogenic Polymers, S. Jenekhe, Ed.; Chapter 17. (b) Z. P. Popovic, H. Aziz, N. X. Hu, A. Ioannidis, P. N. M. dos Anjos, *J. Appl. Phys.* **2001**, *89*, 4673.

12. C. Ego, D. Marsitzky, S. Becker, J. Zhang, A. C. Grimsdale, K. Müllen, D. J. MacKenzie, C. Silva, R. H. Friend, *J. Am. Chem. Soc.* **2003**, *125*, 437 (c) Q. Hou, Y. Xu, W. Yang, M. Yuan, J. Peng, Y. Cao, *J. Mater. Chem.* **2002**, *12*, 2887. (d) M. S. Liu, J. Luo, A. K. -Y. Jen, *Chem. Mater.* **2003**, *15*, 3496.

13. (a) C. -H. Chou, C. -F. Shu, *Macromolecules* **2002**, *35*, 9673. (b) J. H. Lee, D. H. Hwang, *Chem. Commun.* **2003**, 2836. (c) M. Grell, W. Knoll, D. Lupo, A. Meisel, T. Miteva, D. Heher, H. -G. Nothofer, U. Scherf, A. Yasuda, *Adv. Mater.* **1999**, *11*, 671. (d) K. Hosoi, T. Mori, T. Mizutani, T. Yamamoto, N. Kitamura, *Thin Solid Films* **2003**, *438-439*, 201. (e) G. Klärner, J. -I. Lee, V. Y. Lee, E. Chan, J. -P. Chen, A. Nelson, D. Markiewicz, R. Siemens, J. C. Scott, R. D. Miller, *Chem. Mater.* **1999**, *11*, 1800.

14. L. -O. Pålsson, A. P. Monkman, *Adv. Mater.* **2002**, *14*, 757.

Chapter 4.

Synthesis and Luminescent Properties of Poly(thiophene)s and Poly(fluorene-*co*-thiophene)s bearing Tetrahydropyran Groups

Sections of this Chapter have been reproduced in part with permission from:

- *European Polymer Journal* **2004** *40*, 2659-2664

4.1 Introduction

Spatially-controlled deposition of π-conjugated polymers[1a] is an important aspect in the development of full colour displays[1b] and integrated circuitry.[1c] Soft- and photo-lithography has been successfully demonstrated with the use of acid sensitive tetrahydropyran (THP) groups as a cleavable functional group. Spatially-controlled deprotection of the THP group yields pendent hydroxyl groups which results in an insoluble hydrogen bonded polymer network.[2] This work has been discussed in detail in Section 1.5. Structure-property relationships – particularly those pertaining to photophysical properties - of THP-containing conjugated polymers is of interest because of their potential use in high-resolution, full-colour polymeric LED based displays.[3]

4.2 Results and Discussion

4.2.1 Regio-Regular Poly(3-alkylthiophene)s

The solid state quantum yield of photoluminescence (Φ_{pl}) of regio-regular poly(3-alkylthiophene)s is too low[4-5] - due to molecular aggregation - to be of practical interest for organic display devices. However, the extent of molecular aggregation can be lowered by the attachment of bulky substituents.[6] Recently, Bolognesi *et al* report that molecular aggregation of polythiophenes may be minimized – and hence solid state luminescence substantially increased- by attaching bulky tetrahydropyran groups (THP) to *regio-random* polythiophenes via alkyl spacers.[3a] R*egio-regular* analogs with hexyl spacers, tend to aggregate,

resulting in poor solid state luminescence properties.[3a] However, it is documented that phenyl groups attached directly to regio-regular poly(3-phenylthiophene)s are strongly luminescent due to the increased interlayer distance imposed.[6] It is postulated therefore that π-π intermolecular interactions in THP–bearing *regio-regular* polythiophenes can be reduced if shorter alkyl chain spacer lengths are employed.

In this part, structure-property relationships of *regio-regular* THP-bearing poly(3-alkylthiophene)s are investigated. In particular, aggregation phenomena are addressed by investigating the influence of the alkyl chain length with respect to their photo-physical and electro-optical properties (Series 1, Figure 4.1). In order to obtain a greater understanding on the effect of supramolecular organization on the optical properties, the effect of co-polymerizing a THP-bearing thiophene, 3-(2-(2-tetrahydropyranyloxy)ethyl)thiophene), with 3-alkylthiophenes of various alkyl chain length (Series 2, Figure 4.1), and with various proportions of 3-hexylthiophene (Series 3, Figure 4.1) are reported and discussed.

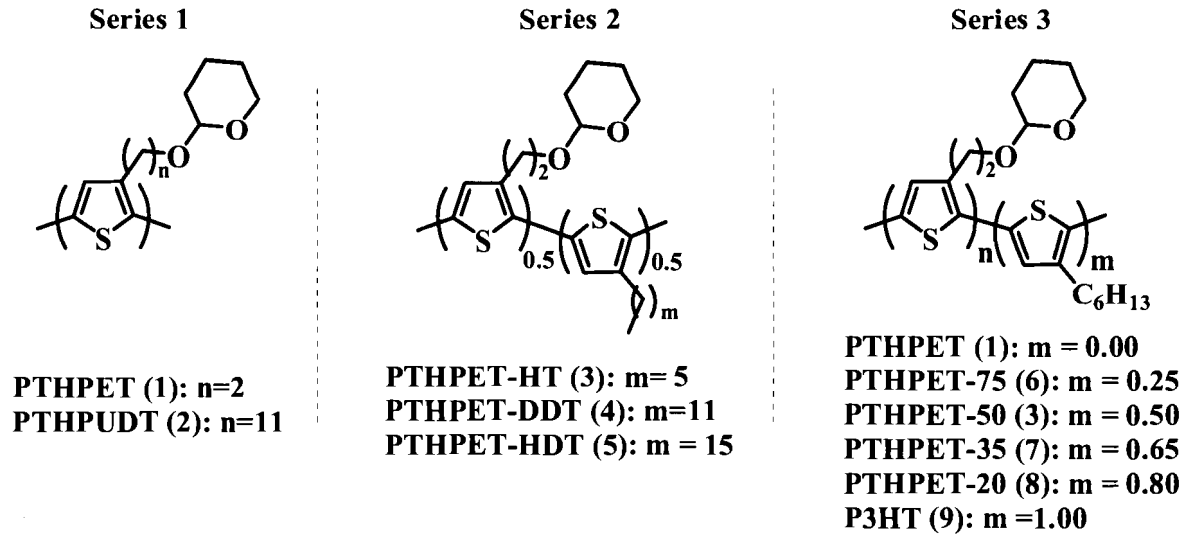

Figure 4.1: Molecular structures of polymers investigated.

4.2.1.1 Effect of Alkyl Chain Spacer Length

The effect of the alkyl spacer length of THP-bearing polythiophenes was investigated using poly[3-(2-(2-tetrahydropyranyloxy)ethyl)thiophene)] PTHPET and poly[3-(11-(2-tetrahydropyranyloxy)undecyl)thiophene] PTHPUDT, which possessed 2 and 11 carbon alkyl chains, respectively. Figure 4.2 shows their absorption and emission spectra in THF solution. Solution absorption spectra exhibited maxima at 440 and 449 nm for PTHPET and PTHPUDT, respectively. Emission spectra of polymer solutions are structured, with two peaks appearing at 569 and 604 nm for PTHPET, and 573 and 614 nm for PTHPUDT. The slightly red-shifted optical properties indicate that the effective conjugation length for PTHPUDT is slightly greater than PTHPET. Quantum yields of luminescence were similar to each other (39 ± 4%).

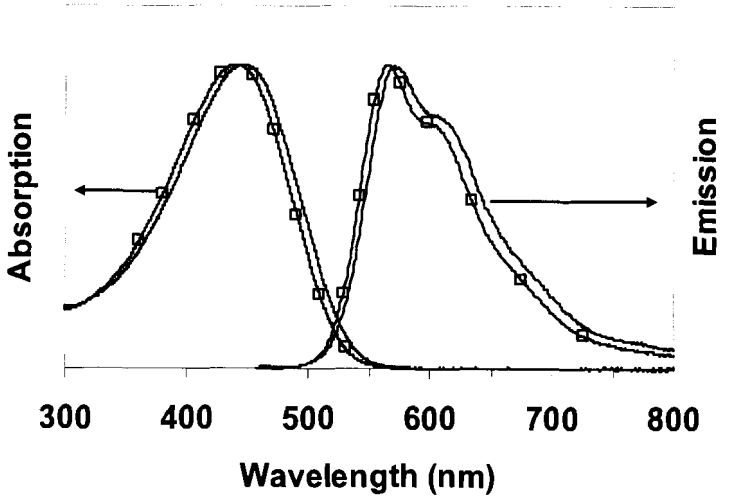

Figure 4.2: Solution absorption and emission spectra of **1** (□) and **2**

Solid-state absorption spectra of spin coated polymers on glass substrates revealed PTHPUDT to be significantly red-shifted compared to PTHPET, as shown in Figure 4.3. The absorption spectrum of PTHPET is featureless, centered at 472 nm, while PTHPUDT is red shifted, exhibiting peaks at 517 nm. Fine structure is attributed to a combination of Davydov splitting and the inherent excitonic band structure – which results from aggregation of the polymer backbone.[7]

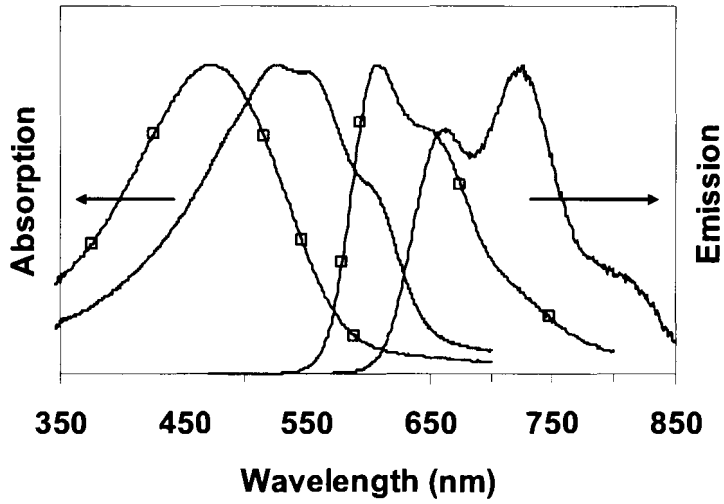

Figure 4.3: Solid state absorption and emission spectra of PTHPET (□) and PTHPUDT.

Structured emission, characterized by two peaks, was observed for PTHPET and PTHPUDT in the solid state. Spectra were significantly red shifted, with respect to their solution values; exhibiting peaks at 607 and 661 nm for PTHPET, and 666 and 727 nm (with a shoulder at 817 nm) for PTHPUDT. Solid state quantum yields of luminescence for PTHPET and PTHPUDT were 12 % and 2.7%, respectively. The extra distance of separation between the bulky THP functional group and the polymer backbone provided by the undecyl group of PTHPUDT relieves interannular steric constraints and allows aggregation of the main chain- thus lowering photoluminescence (PL).

Electroluminescence (EL) of these two polymers was investigated using a device structure consisting of ITO/polymer/triphenyl-triazine(TPT)/Mg:Ag [9b]. Electroluminescence spectra (Figure 4.4) were similar to their corresponding solid state emission spectra, indicating that the excited state structure – whether obtained photonically or electrically - is the same. The external quantum yields of

EL were 0.36% for PTHPET and negligible (~0.02%) for PTHPUDT: values which correspond to their PL efficiency.

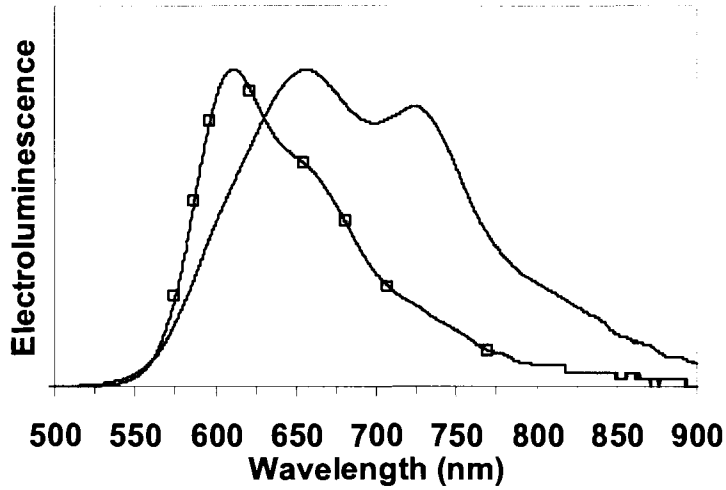

Figure 4.4: Electro-luminescence spectra of PTHPET (□) and PTHPUDT

4.2.1.2 Effect of Copolymers Containing THPET and 3-Alkylthiophenes

It is clear from the above observations that solid-state optical properties of THP-bearing polythiophenes are dependant on the alkyl spacer length. It is speculated that longer alkyl chain derivatives reduce PL by promoting local order and intermolecular π-π aggregation. In order to investigate this further, two additional sets of polymers were prepared and investigated: one based on random copolymers of 3-(2-(2-tetrahydropyranyloxy)ethyl)thiophene) and 3-alkylthiophenes (namely, 3-hexylthiophene (PTHPET-HT), 3-dodecylthiophene (PTHPET-DDT) and 3-hexadecylthiophene (PTHPET-HDT) (Series 2, Figure 4.1); and the other based on random copolymers of 3-(2-(2-tetrahydro-pyranyloxy)ethyl)thiophene) containing various amounts of 3-hexylthiophene

(Series 3, Figure 4.1).

Solution absorption spectra of PTHPET-HT, PTHPET-DDT, and PTHPET-HDT were very similar, as shown in Figure 4.5, as were their emission spectra. Absorption spectra are structureless, centered at 440 nm, while the emission spectra are characterized by a maximum at 570 nm and a shoulder at 608 nm. The effective conjugation length, in either the ground or excited state, is therefore not related to the alkyl chain length of the constituent 3-alkylthiophene. However, quantum yields of luminescence measured in THF decreased from 41% to 33% as the alkyl chain length increased. The origin of this difference may be attributed to aggregation of the polymer backbone induced by differences in polymer-solvent interactions, non-emissive excimer formation and/or differences in re-organizational energy losses. For aggregation, however, the absorption spectrum should be different and therefore, the latter two theories are more plausible.

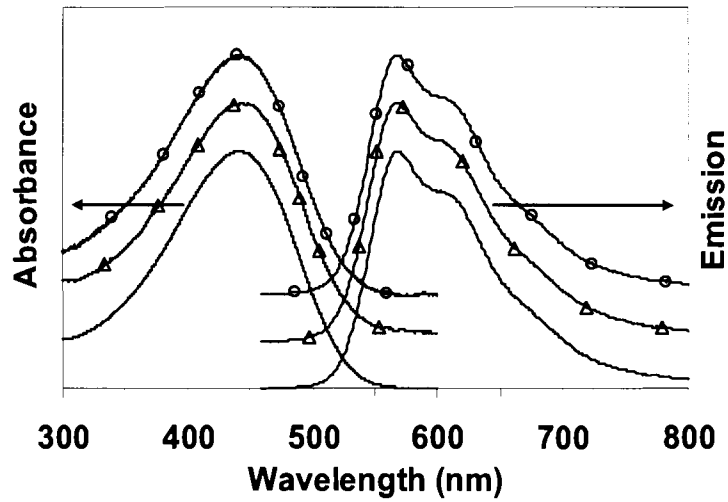

Figure 4.5: Solution absorption and emission spectra of PTHPET-HT, PTHPET-DDT (△) and PTHPET-HDT (○). Spectra are offset for clarity.

Absorption and emission spectra recorded on thin films of PTHPET-HT, PTHPET-DDT, and PTHPET-HDT are shown in Figure 4.6. Unlike solution spectra, a significant dependence of alkyl chain length on the spectral properties is observed. On traversing series 2 (PTHPET-HT → PTHPET-HDT), the absorption maximum increased in wavelength and became more structured: PTHPET-HT exhibited a featureless spectrum centered at 495 nm; PTHPET-DDT, an absorption maximum at 514 nm and shoulder at ~588 nm; and PTHPET-HDT, a structured absorption band having peaks at 520, 553 and 594 nm. Molecular aggregation is apparently more pronounced as the alkyl chain length of the 3-alkylthiophene increases. This is consistent with regioregular homopolymers of 3-alkylthiophenes, where longer side chains are observed to promote side chain ordering and π-stacking of the main chain.[8] Solid state emission spectra show a similar trend: emission maxima red-shifted from 623 to 730 nm as the alkyl chain length increases. Quantum yields of luminescence are 7.2% for PTHPET-HT, 2.4% for PTHPET-DDT, and 1.6% for PTHPET-HDT suggesting that local ordering of the chains – which increases with alkyl chain length - quenches emission in the solid state.

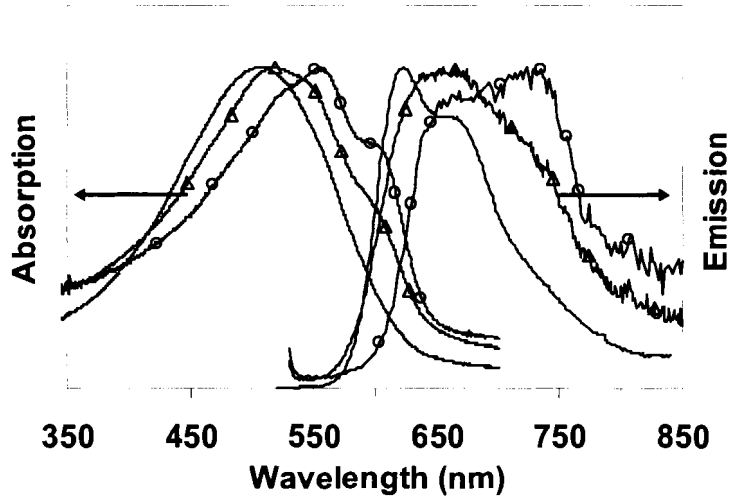

Figure 4.6: Solid state absorption and emission spectra of PTHPET-HT, PTHPET-DDT (△) and PTHPET-HDT (○)

4.2.1.3 Effect of Copolymers Containing PTHPET With Various Ratios of 3-Hexylthiophene

In order to further isolate and investigate the effect of π-π intermolecular interactions on THP-bearing polymers, copolymers of the highly luminescent moiety 3-(2-(2-tetrahydropyranyloxy)ethyl)thiophene) and various ratios of 3-hexylthiophene were investigated (Series 3, Figure 4.1). The optical properties of polymer solutions correlate with the amount of the 3-hexylthiophene incorporated, as illustrated in Figure 4.7: the absorption maximum marginally increases from 440, to 441, to 442, to 443, to 445 nm, to 448 nm as 3-hexylthiophene content increases. Emission spectra show a similar trend: structured luminescence is observed with a maximum ranging from 569 nm (PTHPET) to 576 nm (P3HT). There is a negligible effect on the composition of this series on solution photoluminescence quantum yields, which range from 39% to 41%, implying only minor differences exist in the emitting species.

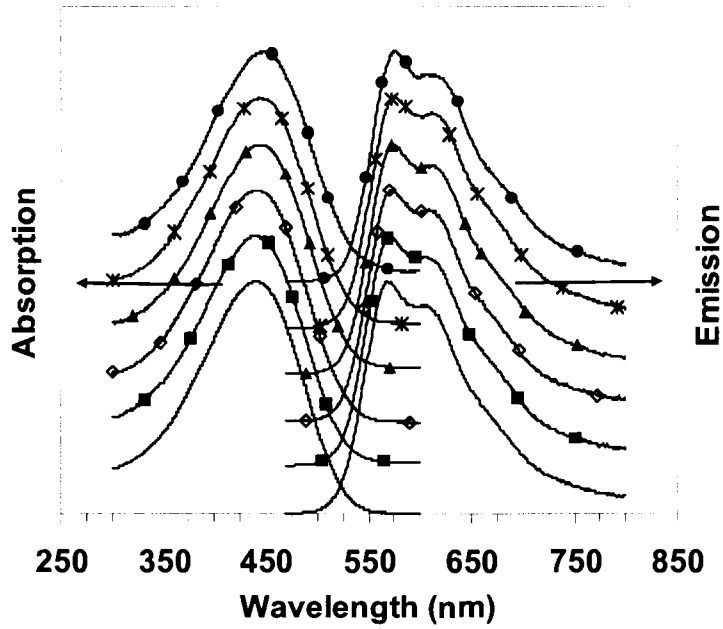

Figure 4.7: Solution absorption and emission spectra of series 3: PTHPET, PTHPET-75 (■), PTHPET-50 (◇), PTHPET-35 (▲), PTHPET-20 (∗), P3HT (●). Spectra are offset for clarity.

Solid state optical properties were more affected by polymer composition than in solution, as shown in Figure 4.8. With increasing 3-hexylthiophene content (PTHPET - P3HT), the absorption maximum - and by inference to the extent of π-conjugation- incrementally increases from 472, to 476, to 508, to 513, to 518, and to 520 nm. Quantum yields of luminescence decrease with 3-HT content from 12 to 2.9 % for polymers PTHPET to P3HT. Data for other polymers are plotted in Figure 4.9. As the 3-HT content increases the polymers are able to π-stack to a greater extent, increasing non-radiative pathways, commensurate with an increasing coplanar arrangement.

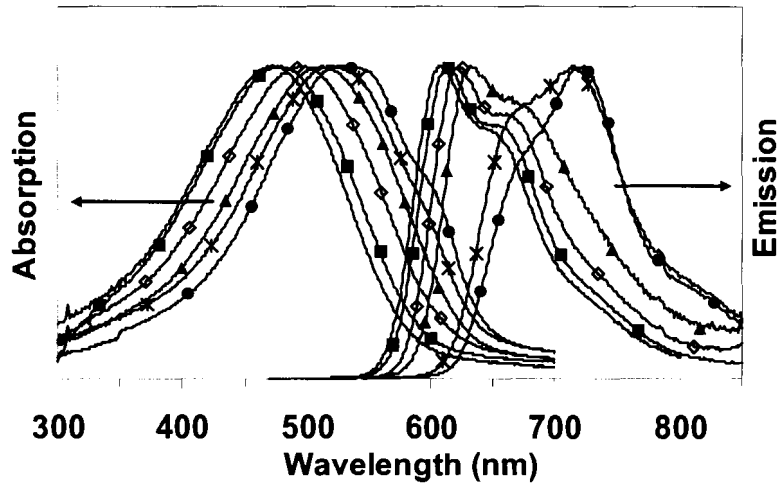

Figure 4.8: Solid state absorption and emission spectra of series 3: PTHPET, PTHPET-75 (■), PTHPET-50 (◇), PTHPET-35 (▲), PTHPET-20 (∗), P3HT (●)

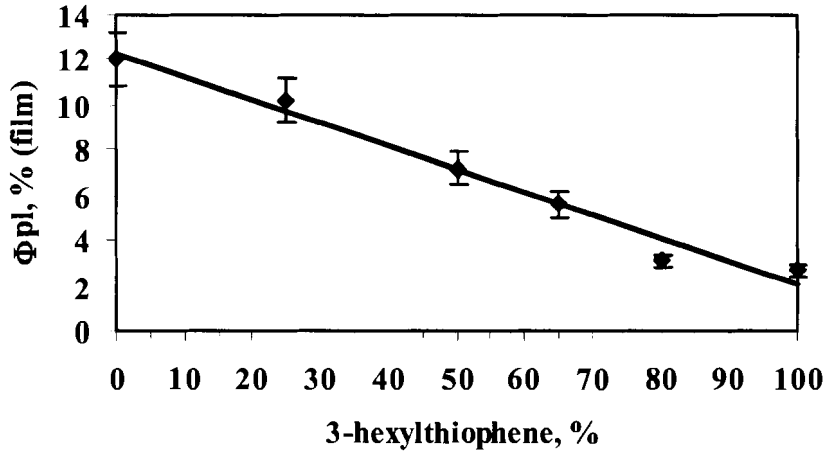

Figure 4.9: Solid state quantum yields of luminescence of series 3

4.1.2.4 Photo-Physics of Deprotected PTHPET

The emission properties of these polymers in the deprotected state is an important characteristic for display applications. Poly[3-(2-(2-tetrahydro-pyranyloxy)ethyl)thiophene)] (PTHPET) is a good model for investigating highly luminescent imaged conjugated polymers. Figure 4.10 depicts the emission from

PTHPET in protected and deprotected forms. Upon deprotection, a large red shift in the emission is observed, accompanied with a large decrease in the quantum yield of luminescence (from 12% to 2%). This further confirms the steric influence of the THP moiety on the interlayer distance, since after deprotection, the Φ_{pl} decreases drastically. For this reason, it is desirable to obtain a polymer that is luminescent after deprotection, which is the topic of discussion in Part 2 (Section 4.2.2).

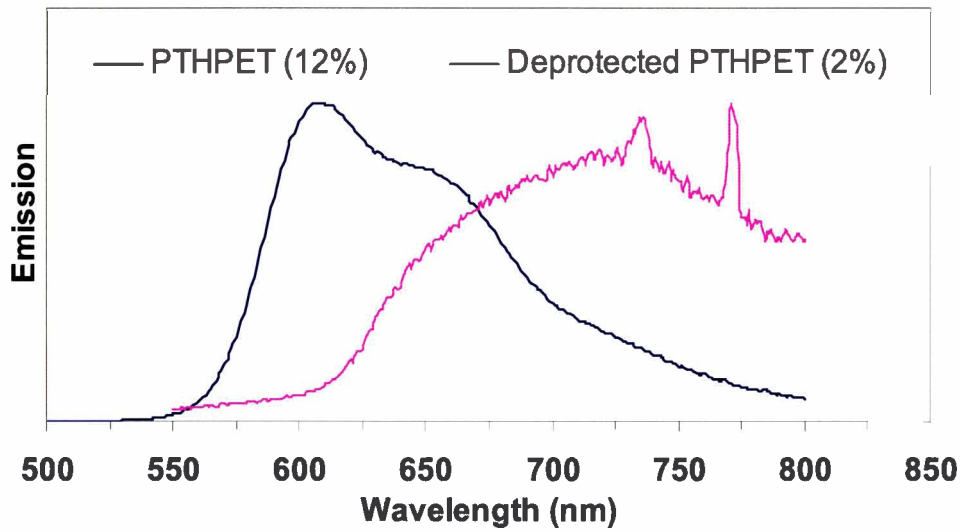

Figure 4.10: Solid state emission spectra of PTHPET (blue) and deprotected (magenta) PTHPET with their corresponding Φ_{pl} of luminescence.

4.2.2 Poly(fluorene-co-thiophene)s

The focus of this section is to obtain enhanced solid state emission from deprotected THP containing conjugated polymers. Since poly(thiophene)s generally have low quantum yields of luminescence in the solid state, investigation of other polymers such as poly(fluorene-*co*-thiophene)s (PFTs) bearing tetrahydropyran (THP) moieties will be investigated. Poly(fluorene-*co*-thiophene)s are good candidates for strong emitters, for the reasons discussed in

Chapter 3. Specifically, PFTs with THP moieties attached to thiophene for two different alkyl chain spacer lengths are discussed (Section 4.2.2.1), and the possibility of a host-guest copolymer (Section 4.2.2.2) is also investigated.

4.2.2.1 Effect of Alkyl Chain Spacer Length in THP-Bearing PFTs

4.2.2.1.1 Synthesis

Three polymers were studied; namely, poly(9,9-dihexylfluorene-alt-2-(2-thiophene-3-ethoxy)tetrahydropyran) (PFT-C_2THP), poly(9,9-dihexylfluorene-alt-3-(11-(2-tetrahydropyranyloxy)undecyl)thiophene) (PFT-C_{11}THP), and poly(9,9-dihexyfluorene-alt-3-hexylthiophene) (PFT-HT). The chemical structures for these polymers are illustrated in Figure 4.11. PFT-HT was synthesized for comparison purposes, to understand the effect of the THP moiety.

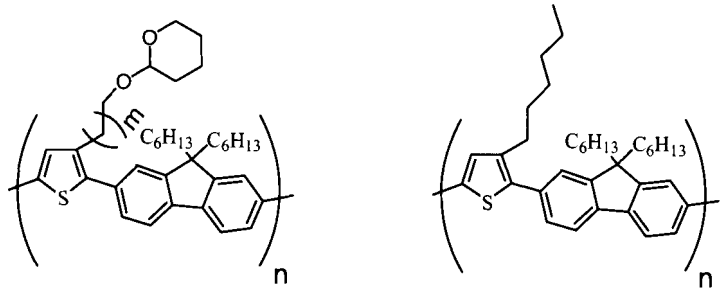

PFT-C2THP, m = 1
PFT-C11THP, m = 10

PFT-HT

Figure 4.11: Structures of polymers investigated.

The polymers were synthesized via a Suzuki polycondensation reaction of the appropriate dibromothiophene with 9,9-dihexylfluorene-2,7-bis(trimethylene-borate) in the presence of $Pd(PPh_3)_4$ in THF, as illustrated in Scheme 4.1. The polymer molecular weights (M_w) were in the range of 10,000 – 15,000 daltons.

Caution was exercised when synthesizing THP containing PFTs, due to the possibility of deprotection. This tendency was reduced by using a lower polymerization temperature (40°C) for Suzuki reactions, and the use of a diboronic ester rather than a diboronic acid. ^{1}H NMR resonances appearing between 4.67 and 3.5 ppm for PFT-C_2THP, 4.5 and 3.35 ppm for PFT-C_{11}THP corresponding to the THP groups gives clear evidence that the polymer remained protected. Infrared analysis indicated the absence of a broad OH band, also confirming the polymer remained protected.

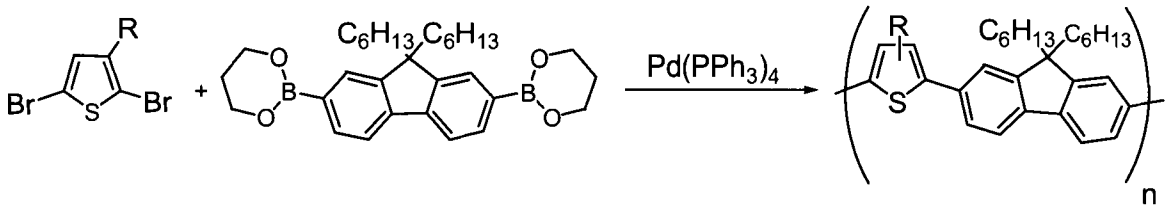

Scheme 4.1: Synthesis of THP containing PFTs

4.2.2.1.2 Thermal Properties

Thermal gravimetric analysis (TGA) was performed on these polymers, in order to obtain information on their deprotection temperature and their thermal sensitivity to acid. The calculated percentage of THP in the polymer is 15.4% for PFT-C_2THP and 12.5% for PFT-C_{11}THP. Thermal gravimetric analysis curves for these polymers are presented in Figure 4.12 in *absence* of acid, leading to 16.3% mass loss for PFT-C_2THP at 215°C, and 11.2% mass loss observed for PFT-C_{11}THP at 215°C, while no weight loss was observed for PFT-HT. The similarity in weight loss to their calculated values further confirms the polymer structure.

Furthermore, it was found that the deprotection temperature was similar in polymers PFT-C_2THP and PFT-C_{11}THP, indicating that the polymer structure plays little role on the thermal deprotection when acid was *not* present.

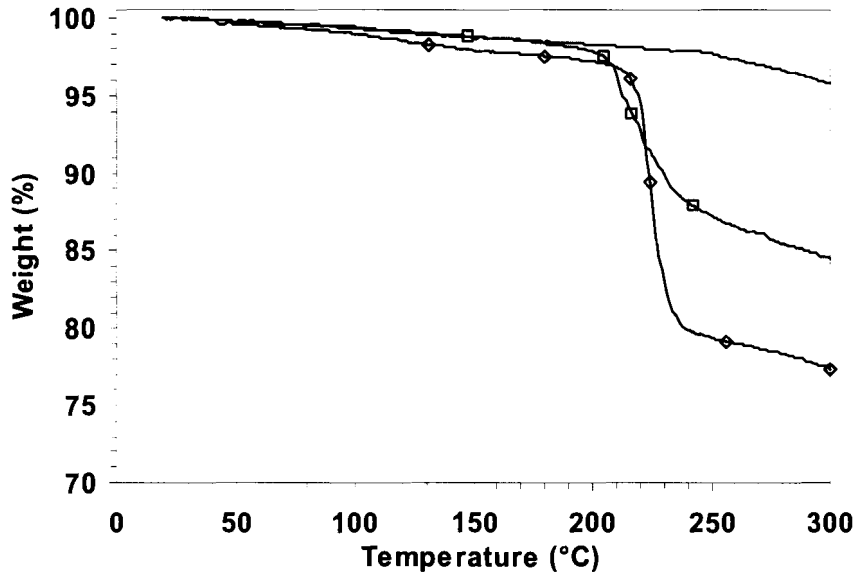

Figure 4.12: TGA of PFT-HT, PFT-C_2THP (◇) and PFT-C_{11}THP (□)

Figure 4.13 depicts the TGA traces of PFT-C_2THP and PFT-C_{11}THP in the presence of camphor sulphonic acid. It was found that thermolytic elimination of THP is much more efficient for polymer PFT-C_2THP, rather than PFT-C_{11}THP. This effect has also been observed for the poly(thiophene)s discussed in Section 4.2.1.1.[2] The differences in the acid sensitive deprotection were attributed to differences in polymer morphology, structure and molecular weight.

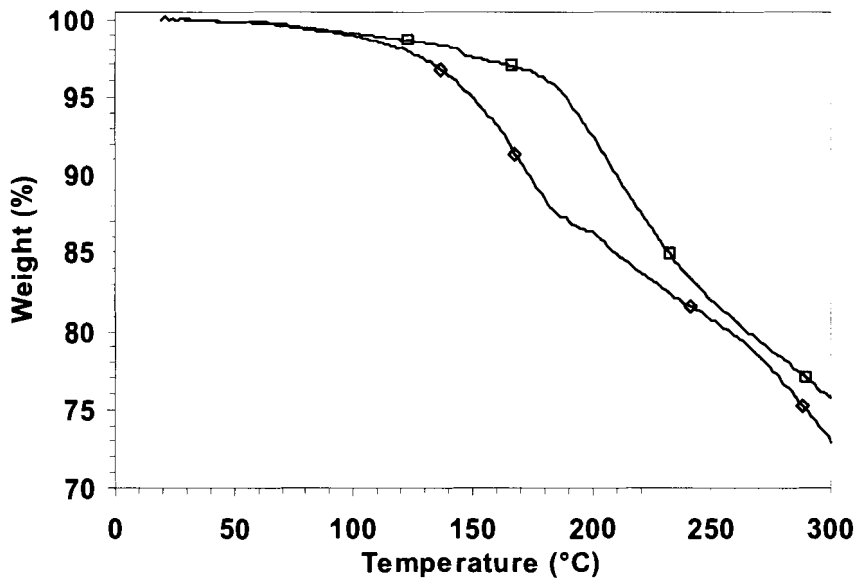

Figure 4.13: TGA of PFT-C_2THP (◇) and PFT-C_{11}THP (□) in the presence of Acid

4.2.2.1.3 Photophysical Properties

The photophysical properties of the PFTs in solution are illustrated in Figure 4.14. The absorption and emission characteristics were similar. The absorption maximum for PFT-HT is 397 nm, for PFT-C_2THP is 398 nm and for PFT-C_{11}THP is 395 nm. Emission maximum for PFT-HT is 462 nm, and 461 nm for both PFT-C_2THP and PFT-C_{11}THP. The similarity indicates that the mean conjugation length is not affected by the steric interactions of the THP moiety on the polymer backbone. Furthermore, the quantum yield of luminescence of the polymers was independent of the alkyl chain length (0.55).

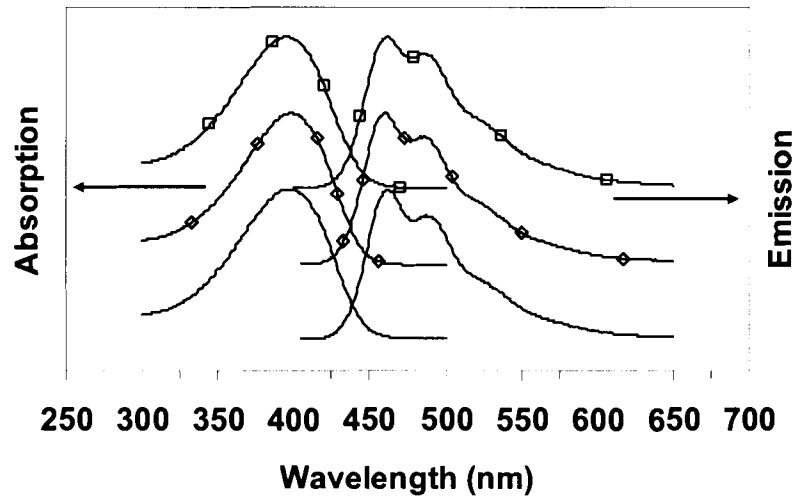

Figure 4.14: Solution optical properties of PFT-HT, PFT-C_2THP (◇) and PFT-C_{11}THP (□). Spectra are offset for clarity.

The photophysical properties of the PFTs in their solid state are illustrated in Figure 4.15. The polymers absorption maxima were 406 nm, 414 nm and 413 nm for PFT-HT, PFT-C_2THP and PFT-C_{11}THP, respectively. The increase of the absorption maximum may be attributed to the aggregation and/or planarization of the polymer backbone. The emission from these polymers is structured, appearing at 477 nm and 491 nm for PFT-HT; 476 nm and 485 nm for PFT-C_2THP; and 500 nm and 530 nm for PFT-C_{11}THP. Quantum yields of luminescence are also affected by the polymer structure. These values are 0.19 for PFT-C_2THP, 0.16 for PFT-C_{11}THP, and 0.12 for PFT-HT. Therefore, the excited state of these polymers is effected by the THP-backbone distance: smaller interlamellar distances decrease excimer formation and increases the Φ_{pl}.

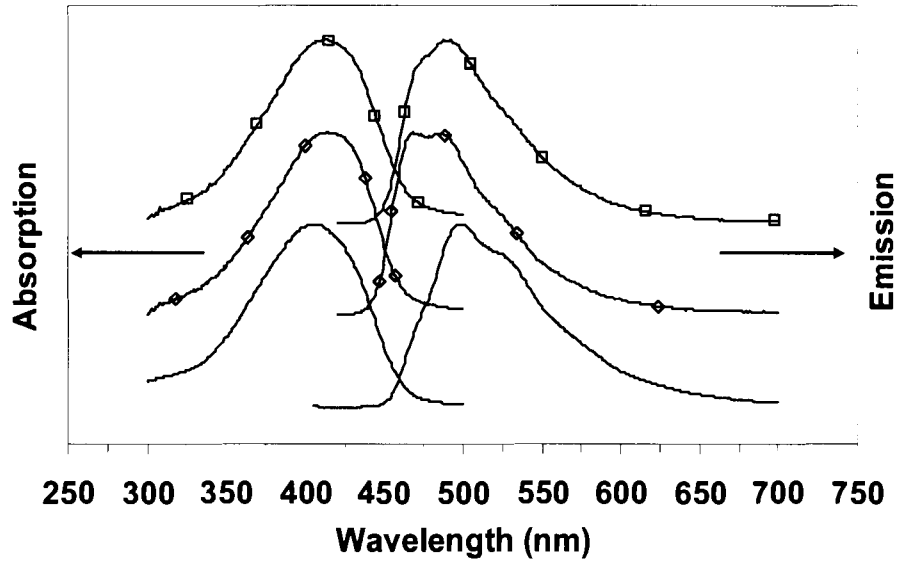

Figure 4.15: Solid state optical properties of PFT-HT, PFT-C_2THP (◇) and PFT-C_{11}THP (□). Spectra are offset for clarity.

4.2.2.1.4 Electroluminescent Properties

Light emitting diodes fabricated employing THP-bearing PFT polymers, discussed herein, have the following device structure: ITO anode, poly-3,4-ethylenedioxythiophene polystyrenesulfonate (PEDOT) (140 nm) hole injection layer, PFT polymer, electron transport/injection layer (15 nm), Mg:Ag (9:1; 100nm) cathode, Ag (300nm) encapsulation layer. The electroluminescence spectra are illustrated in Figure 4.16. Structured electroluminescence emission is observed for PFT-HT, PFT-C_2THP and PFT–C_{11}THP. Emission wavelengths for PFT-HT occur at 475 nm and 494 nm with a shoulder at 538 nm; at 470 and 495 nm for PFT-C_2THP; at 501 nm, 540 nm and a shoulder appearing at ~475 nm for PFT-C_{11}THP. Electroluminescence maxima closely correspond to their solid

state PL maxima, however the relative intensities of the different vibrational modes are different.

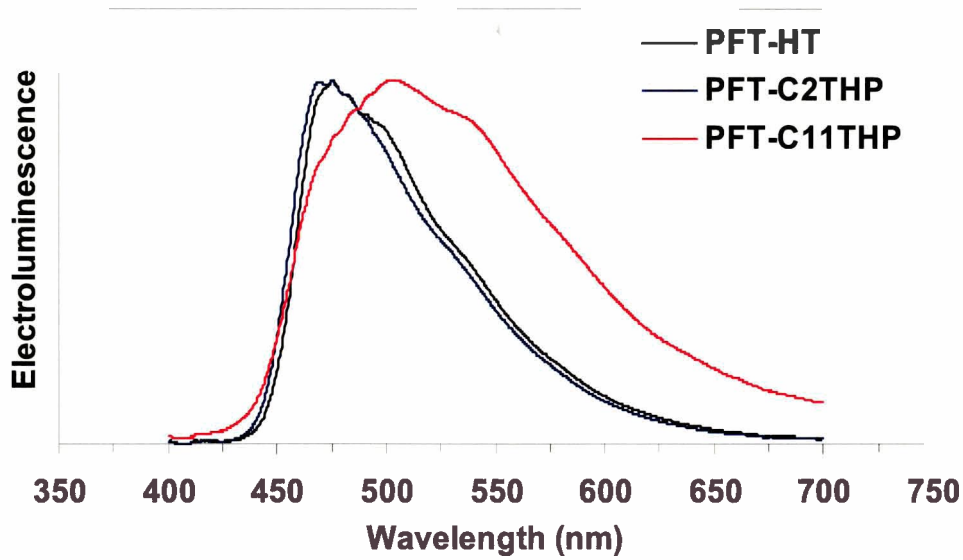

Figure 4.16: Electroluminescence spectra of THP bearing PFT polymers

External efficiencies of the device corresponding to PFT-HT, PFT-C_2THP and PFT-C_{11}THP are 0.22 %, 0.56 % and 0.09 %. This trend correlates with their solid state photoluminescence efficiency, where the least aggregated polymer gives the highest efficiencies. With the aim to further increase the efficiency, a host-guest copolymer containing THP moieties is investigated, where the emitters species are isolated from one another.

4.2.2.2 Host-Guest Copolymers Bearing THP Functionality

4.2.2.2.1 Host-Guest Polymer Design

A host-guest design of a THP-bearing PFT may be useful to increase further the quantum yield of luminescence. Upon deprotection, the guest should

remain isolated, giving the opportunity for enhanced emission efficiency of deprotected polymers. This model is illustrated in Figure 4.17.

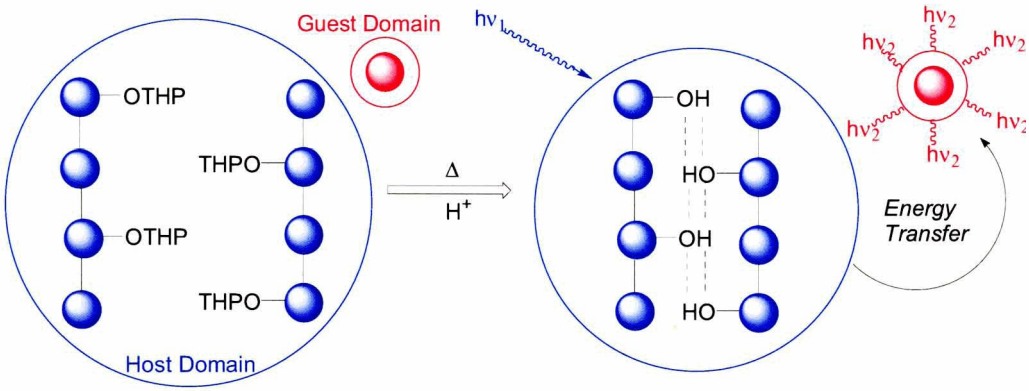

Figure 4.17: Host-guest design using a THP-containing host and a non-aggregating isolated emitter.

PFT-C_2THP was chosen as the host, since it undergoes acid sensitive thermal deprotection, and poly(9,9-dihexylfluorene-alt-2,2'-bithiophene) (PFTT, illustrated in Figure 4.18) was chosen as the guest due to its greater conjugation length, lower band gap and chemical stability. The optical properties of PFT-C_2THP and PFTT are illustrated in Figure 4.19. Considerable overlap between the emission of PFT-C_2THP and the absorption of PFTT (both solution and solid state), makes this a potential host-guest copolymer system.

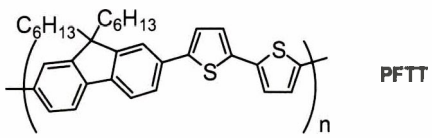

Figure 4.18: Chemical structure of PFTT

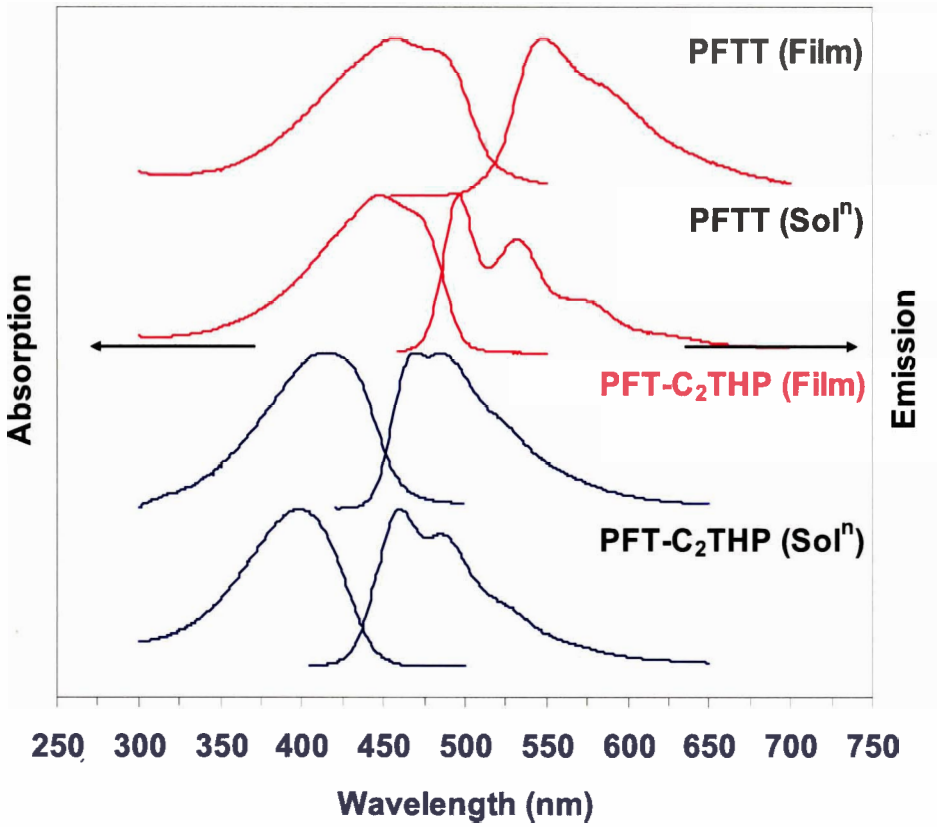

Figure 4.19: Optical properties of PFT-C_2THP and PFTT in solution and a film.

4.2.2.2.2 Synthesis of host-guest co-polymer

Synthesis of this copolymer system was performed by Suzuki polycondensation, similar to that described in Section 4.2.2.1.1. This reaction is illustrated in Scheme 4.2. The guest concentration chosen was 5%. The molecular weight (Mw) of this polymer was 10,000 Daltons.

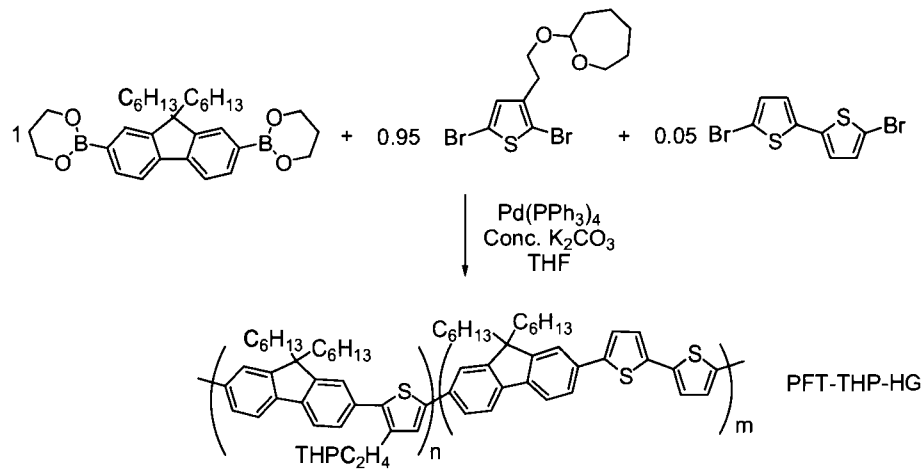

Scheme 4.2: Synthesis of host-guest copolymer system bearing THP-moieties (PFT-THP-HG)

4.2.2.2.3 Thermal Properties of Host-Guest Polymer

Figure 4.20 displays TGA of the PFT-THP-HG polymer in neat form and in the presence of acid. When the neat PFT-THP-HG was heated to 300°C, a sharp change in weight is observed at 200°C. The theoretical weight percentage of the THP moiety represents 14.8% for PFT-THP-HG. According to TGA, the actual weight loss is 13.7% between 190°C and 227 °C. In the presence of acid, thermolytic elimination of the THP group is less distinct, and occurs at a much lower temperature at ~130°C. Deprotection of this polymer is therefore acid sensitive.

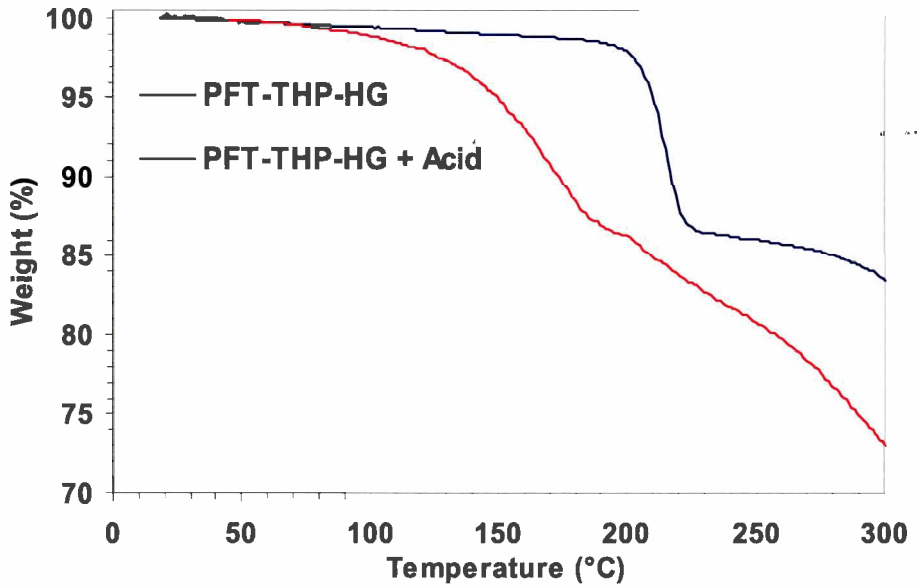

Figure 4.20: TGA of neat PFT-THP-HG and in the presence of acid.

4.2.2.2.4 Photophysical Properties of Host-Guest Polymer

Figure 4.21 depicts the absorption and emission characteristics of PFT-THP-HG in solution and solid state. The solution absorption appears at 405 nm with a negligible shoulder attributed to the PFTT moiety. The solution emission clearly shows a band from 430 to 470 nm which is attributed to the PFT-C_2THP segment and a band from 470 to 630 nm which is attributed to the PFTT segment, revealing incomplete energy transfer. The quantum yields of luminescence in solution (tetrahydrofuran) for PFT-THP-HG is 0.48, for PFTT 0.47, and for PFT-C_2THP 0.55. Since these values are within experimental error of each other, no conclusion can be drawn.

In the solid state, the absorption maximum increased to 414 nm, a similar value to PFT-C_2THP. Structured emission is observed at 500, 530 and 573 nm,

with no emission in the PFT-C_2THP region, indicating that complete energy transfer to the PFTT segments occurs in the solid state. The solid state quantum yield of luminescence for PFT-THP-HG is 0.38. The solid state emission from PFT-THP-HG has a value similar to PFTT solution (0.47). In addition, the film spectrum of PFT-C_2THP and the solution spectrum of PFTT are similar (Figure 4.22), suggesting that the emitting species are isolated and not aggregated.

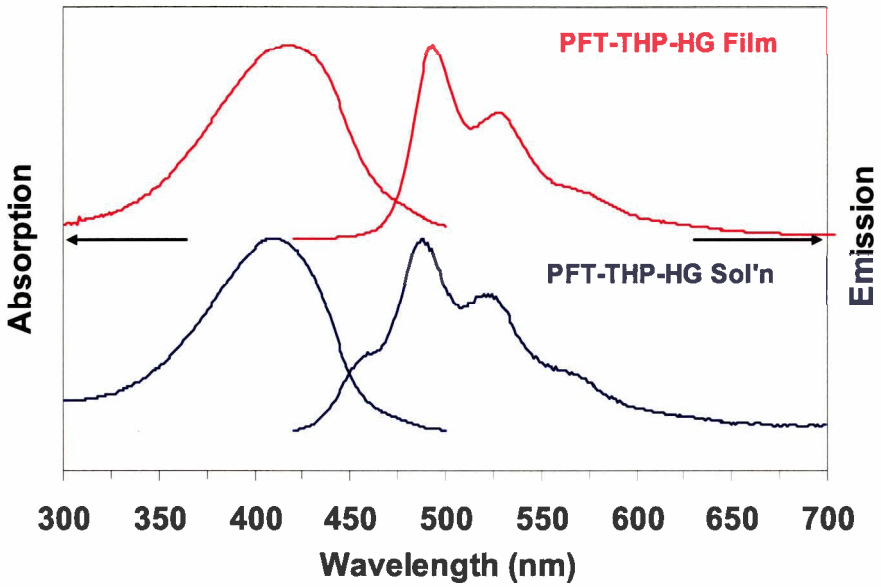

Figure 4.21: Solution (blue) and solid state (red) optical properties of PFT-THP-HG.

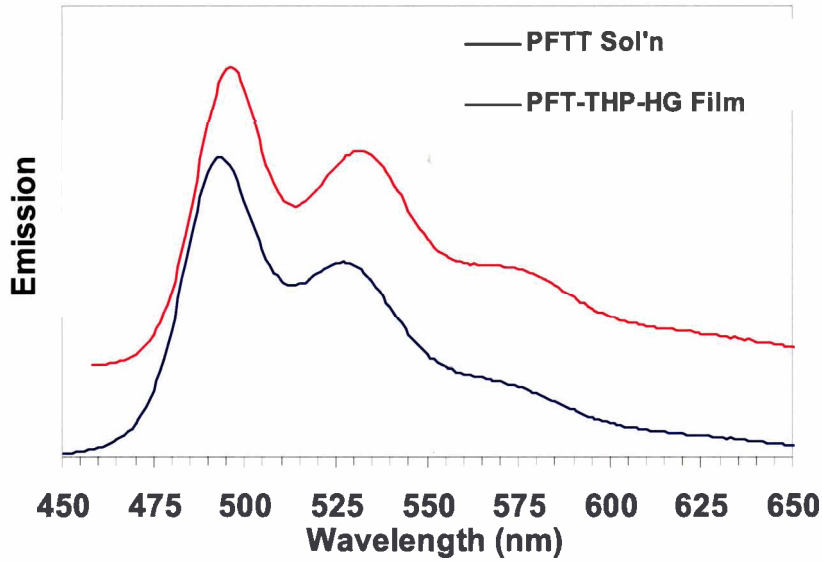

Figure 4.22: Comparison of PFTT solution emission (red) and PFT-THP-HG solid state emission (blue).

4.2.2.2.5 Electroluminescent Properties of Host-Guest Polymer

The electroluminescence of PFT-THP-HG was studied using the device structure mentioned in section 4.2.2.1.4. The electroluminescence spectrum of PFT-THP-HG is illustrated in Figure 4.23. Structured electroluminescence was observed at 499, 534 and 580 nm. The quantum yield of electroluminescence of this device was 1% (external). This yield is twice the value of PFT-C_2THP, indicating that isolation of the emitters has a dramatic influence on the efficiency of the device.

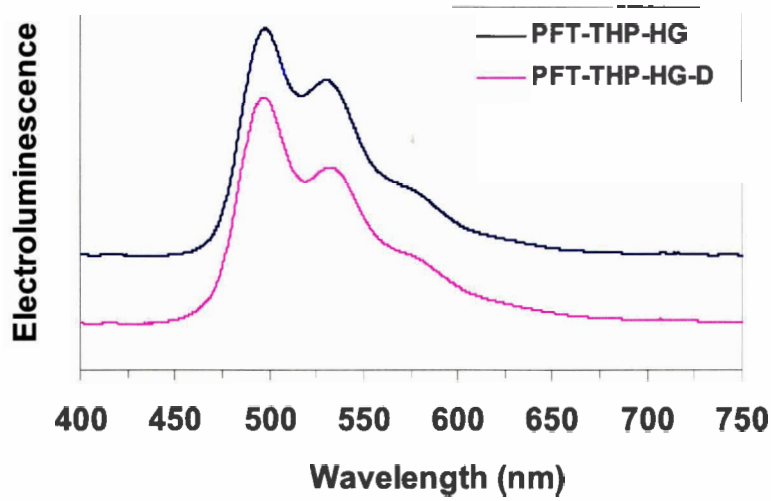

Figure 4.23: Electroluminescence of PFT-THP-HG in protected form (Blue) and deprotected form (PFT-THP-HG-D, Magenta)

4.2.2.3 Photo-Physical Properties of Deprotected Polymers

To study the thermolytic deprotection of these THP bearing polymers, six polymer films were studied: PFT-HT, PFT-C_2THP and PFT-THP-HG with and without acid. PFT-C_{11}THP was not studied, since thermal deprotection was much higher in the presence of acid. These polymers were analyzed after spin casting, and after thermal annealing at 150°C. In the presence of acid, PFT-C_2THP and PFT-THP-HG undergoes thermolytic elimination of the THP, while in the absence of acid, the polymer remains in protected form (refer to Figure 4.12, Figure 4.13 and Figure 4.20). The results are summarized in Table 4.1.

The emission spectra of the PFT films are depicted in Figure 4.24. The presence of acid did not have an effect on the polymers optical properties after casting. Upon heating these polymers to 150°C, the polymers absorption characteristics slightly blue shifted, and the emission characteristics were

negligibly affected. The quantum yields of luminescence decreased slightly, possibly due to aggregate formation or chemical defects. Electroluminescence of PFT-THP-HG in deprotected form (PFT-THP-HG-D) is shown in Figure 4.23. This polymer has similar emission characteristics to PFT-THP-HG in the protected form and to PFTT in solution, indicating that the emitter remains isolated even after deprotection.

Polymer	Film, as cast			Film, annealed at 150°C		
	λ_{abs}	λ_{em}	Φ_{pl}	λ_{abs}	λ_{em}	Φ_{pl}
PFT-HT	406	477, 491	0.12	405	474, 488	0.10
PFT-HT[a]				405	474, 488	0.11
PFT-C_2THP	414	476, 485	0.19	409	474, 488	0.14
PFT-C_2THP[a]				407	474, 488	0.16
PFT-THP-HG	414	500, 530	0.38	411	504, 534	0.36
PFT-THP-HG[a]				412	502, 534	0.35

Table 4.1: Optical Properties of PFT Polymers. [a)] in the presence of camphor sulphonic acid.

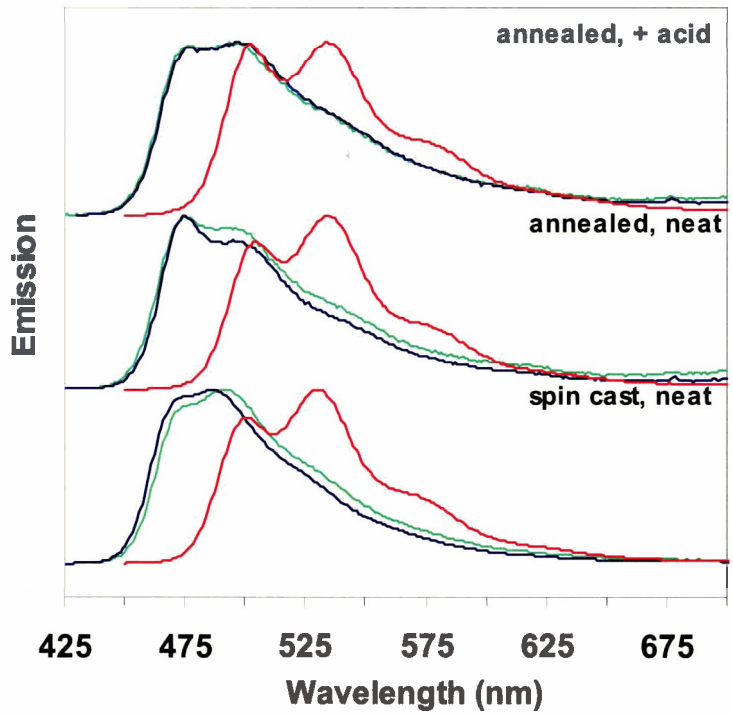

Figure 4.24: Solid state emission spectra from PFT-HT (green), PFT-C_2THP (blue), and PFT-THP-HG (red), after spin cast, annealed in neat form, and annealed in the presence of acid.

4.3 Conclusions

The following conclusions are drawn regarding the composition of THP-bearing polythiophenes: poly[3-(2-(2-tetrahydropyranyloxy)ethyl)thiophene)] exhibits a solid state photoluminescence that is almost 10 times higher than non-THP-bearing analogs because of the higher degree of steric interaction between juxtaposed bulky groups, and the resultant twisting of the main chain and inhibition of π-stacking. The steric hindrance between the adjacent THP-substituted thiophene monomer units is relieved by 1) increasing the length of the alkyl spacer between the THP moiety and the polythiophene backbone; or 2) the insertion of 3-alkylthiophenes, *via* copolymerization. With respect to the latter, for a given 3-alkylthiophene content, relief from hindrance increases with the percent

composition of the non-THP-bearing component; and for a given alkyl chain length, relief from hindrance increases with the length of alkyl chain. As steric interactions are reduced, the degree of coplanarity increases, together with the extent of π-stacking; solid state luminescence, however, decreases.

In an effort to increase the quantum yield of luminescence in the deprotected form of THP-bearing conjugated polymers, alternating poly(fluorene-*co*-thiophene)s were studied. Similar to polythiophenes, shorter alkyl chain spacers resulted in greater emission quantum yield of luminescence due to increased steric interaction on the polymer backbone. Furthermore, introducing host-guest copolymer design proved useful to obtain even greater solid state quantum yields of luminescence after deprotection.

Although these PFT copolymers have promising properties, successful development was not achieved due to similar solubility of the protected and deprotected polymer. It is postulated that poly(fluorene-*co*-thiophene)s with additional THP moieties will form stronger H-bonding interactions and therefore result in greater differences in solubilities between protected and deprotected forms. This is a topic of current interest –refer to Chapter 5.

4.4 Experimental

4.4.1 Synthesis

2,5-Dibromo-3-(2-hydroxy)ethylthiophene (10): In the absence of light, a solution of NBS (7.12 g, 40 mmol) in DMF (20 mL) was added dropwise to a solution of 3-(2-hydroxyethyl)-thiophene (2.56 g, 20 mmol) (Aldrich) in DMF (20

mL). After stirring for 3 h, the reaction mixture was quenched with ice-water and extracted with ether. Combined organic phases were washed with water, dried over magnesium sulfate, and concentrated under vacuum. Distillation of the crude product gave 5.61 g of desired product. 400MHz ^{1}H NMR, PPM (CD_2Cl_2): δ 6.91 (s, 1H, thiophene), 3.78 (t, *J* = 6.6 Hz, 2H, β-C*H*$_2$), 2.78 (t, *J* = 6.6 Hz, 2H, α-C*H*$_2$), 1.80 (s, 1H, O*H*). ^{13} C NMR δ 140.2, 132.0, 111.1, 109.8, 33.3, 62.1. Elemental analysis: Calcd: C, 25.17%; H, 2.11%. Found: C, 25.09%; H, 2.16.

2,5-Dibromo-3-(2-(2-tetrahydropyranyl-2-oxy)ethyl)thiophene (11): To a solution of 2,5-dibromo-3-(2-hydroxy)-ethylthiophene (4.29g, 15 mmol) and freshly distilled dihydropyran (2.52 g, 30 mmol) in 80 mL of dry chloroform, cooled to 0 °C, was added 29 mg (0.15 mmol) of p-toluene-sulfonic acid monohydrate under N_2. After stirring for 10 min at 0 °C, by 2 h at room temperature, the mixture was poured into ice-water and extracted with chloroform. The organic phase was combined, washed with saturated sodium hydrogen carbonate solution and water, and dried over magnesium sulfate. The crude product obtained following removal of solvent was chromatographed on silica gel (Silica Gel 60, EM Science) with chloroform to afford 5.12 g of the desired monomer. 400MHz ^{1}H NMR, PPM (CD_2Cl_2): δ = 7.25 (s, 1H), 4.60 (s, 1H), 3.91-3.48 (m, 4H,), 2.84 (t, *J* = 6.9 Hz, 2H), 1.82-1.49 (m, 6H). ^{13}C NMR: 140.5, 132.1, 110.5, 109.3 (4C, thienyl ring), 98.9, 62.3, 31.0, 25.8, 19.8, 30.4 , 66.2. MS: 371, M+1. Elemental analysis: Calcd: C, 35.68%; H, 3.78%. Found: C, 35.72%; H, 3.76.

11-Bromo-1-(2-tetrahydropyanyloxy)undecane (12): To an ice cooled solution of 11-bromo-1-undecanol (19g, 75 mmol) and dihydropyran (60ml, 0.66 mole) in 220 ml of Dichloromethane was added *p*-toluenesulfonic acid (1.0g, 5.4 mmol) under nitrogen. After stirring for 10 min at 0°C followed by 1.5 hours at ambient temperature, the mixture was poured into an ice-water mixture and extracted 3-4 times with dichloromethane. Organic phases were combined, washed with saturated $NaHCO_3$ solution followed with water and dried over anhydrous $MgSO_4$. Evaporation of the solvent under reduced pressure and the resultant oil was purified via column chromatography with dichloromethane to afford 20g, 79% yield of the title compound. 400MHz ^1H NMR, PPM (CD_2Cl_2): δ 4.57 (m, 1H), 3.87-3.46 (m, 4H), 3.40 (t, J = 7.9 Hz, 2H), 1.86-1.28 (m, 24H). MS: 337, M^+.

3-(11-(2-tetrahydropyranyloxy)undecyl)thiophene (13): To a flame dried 2-neck flask with a fitted condenser and anti-pressure funnel and stir bar, was added 20 ml of diethylether, magnesium (2.4g, 0.1 mole) and iodine (trace) under nitrogen. To this suspension, 11-bromo-1-(2-tetrahydropyanyloxy)undecane (15g, 45 mmol) in ether (20 ml) was added dropwize and after activation of the magnesium to maintain a light reflux. After complete addition of 11-bromo-1-(2-tetrahydropyanyloxy)undecane, the solution was refluxed for 4 hours to ensure complete Grignard formation. 3-bromothiophene (7.3 g, 45 mmol) was then added dropwize to the solution in the presents of $Ni(dppp)Cl_2$ (0.65g, 1.2 mmol) catalyst. After complete addition of the thiophene, the reaction was left to reflux for 15 hours. The reaction was then quenched with an ice-water bath and extracted 3-4 times with ether and the combined extracts were washed with a

saturated solution of $NaCO_3$, followed by water 2 times. Evaporation of the solvent under reduced pressure resulted in an oil and was purified via flash chromatography with hexane to afford 9g (59% yield). 400MHz ^1H NMR, PPM (CD_2Cl_2): δ 7.24 (m, 1H), 6.95 (m, 2H), 4.5 (t, *J* = 3.6 Hz, 1H), 3.8 (m, 1H), 3.68 (m, 1H), 3.44 (m, 1H), 3.33 (m, 1H), 2.6 (t, *J* = 9.2, 2H), 1.8-1.27 (m, 24H). MS: 339, M^+.

2,5-Dibromo-3-(11-(2-tetrahydropyranyloxy)undecyl)thiophene (14): In the absence of light, a solution of NBS (3.9g, 22 mmol) in 30 ml of DMF was added slowly to a solution of 3-(11-(2-tetrahydropyranyloxy)undecyl)thiophene (3.5g, 10 mmol) in DMF (30 ml). After stirring for 3 hours at room temperature, the reaction mixture was poured into water and extracted 3 times with ether. The combined organic phases were washed with water and dried with anhydrous $MgSO_4$. Evaporation of the solvent under reduced pressure and the oil was purified via column chromatography using hexane/ether (95:5) solution to afford the title compound (3.0 g, 60% yield). 400MHz ^1H NMR, PPM (CD_2Cl_2): δ 6.8 (s, 1H), 4.5 (t, J = 4 Hz, 1H), 3.85 (m, 1H), 3.7 (m, 1H), 3.5 (m, 1H), 3.34 (m, 1H), 2.5 (t, J = 8Hz, 2H), 1.8-1.3 (m, 24H). ^{13}C NMR δ 143.65, 131.53, 110.48, 108.15, 99.09, 67.80, 62.42, 31.18, 30.10, 29.93, 29.91, 29.88, 29.85, 29.74, 29.68, 29.40, 26.61, 25.95, 20.06.

Poly(9,9-dihexyfluorene-alt-3-hexylthiophene) (PFT-HT, 15): To a degassed solution (with nitrogen) of 2,5-dibromo-3-hexyl-thiophene (0.197g, 0.6 mmol), 9,9-dihexylfluorene-2,7-bis(trimethyleneborate) (0.303g, 0.6mmol) and a 1 ml of an aqueous solution of 2.4M K_2CO_3 in THF (6 ml) was added 3 mol % of $Pd(PPh_3)_4$ (0.020g, 0.02 mmol) to a vial and sealed. The solution was heated for 24 hours at

40°C. The solution was then diluted with $CHCl_3$ and washed with water (2 times). The organic phase was dried with $MgSO_4$ and most of the solvent was removed under reduced pressure. The remaining polymer solution (~2ml) was then precipitated into methanol to afford a yellow product. After filtration, 0.260 g (86% yield) of polymer was obtained. Flash chromatography with $CHCl_3$ was performed to remove catalyst residues, followed by precipitation. 400MHz ^1H NMR, PPM (CD_2Cl_2): δ 7.82-7.58 (m, 4H), 7.56-7.46 (m, 2H), 7.36 (s, 2H), 2.8-2.6 (m, 2H), 2.0 (s, 4H), 1.7-0.7 (m, 33H). ^{13}C NMR δ 152.2, 151.6, 143.8, 142.7, 140.4, 138.2, 133.7, 128.4, 126.2, 124.8, 123.8, 120.5, 120.1, 55.6, 40.8, 32.1, 31.9, 31.5, 30.1, 30.0, 29.7, 29.6, 24.2, 23.0, 23.0, 14.2. FTIR (KBr), cm^{-1}: 3100 (C-H stretch, aromatic), 2929 (CH_2 in-phase vibration), 2860 (CH_2 out of phase vibration), 1460 (C=C stretch, ring), 819 (C-H out of plane bending). GPC: Mw 13, 872, PDI 2.60.

Poly(9,9-dihexylfluorene-alt-2-(2-thiophene-3-ethoxy)tetrahydropyran) (PFT-C_2THP, 16): To a degassed solution (with nitrogen) of 2,5-dibromo-3-(2-hydroxy)ethylthiophene (0.204g, 0.55 mmol), 9,9-dihexylfluorene-2,7-bis(trimethyleneborate) (0.277g, 0.55 mmol) and an 1 ml of an aqueous solution of 2.4M K_2CO_3 in THF (6 ml) was added 3 mole % of $Pd(PPh_3)_4$ (0.0187g, 0.00162 mmol) to a vial and sealed. The solution was heated for 72 hours at 40°C. The solution was then diluted with $CHCl_3$ and washed with water (2 times). The organic phase was dried with $MgSO_4$ and most of the solvent was removed under reduced pressure. The remaining polymer solution (~2ml) was then precipitated into methanol to afford a bright yellow product. After filtration, 0.256 g (86 % yield) of polymer was obtained. Flash chromatography with $CHCl_3$ was

performed to remove catalyst residues, followed by precipitation. 400MHz ^{1}H NMR, PPM (CD_2Cl_2) δ 7.8-7.5 (m, 6H), 7.46 (s, 1H), 4.67 (m, 1H), 4.1 (m, 1H), 3.8(m, 2H), 3.5 (m, 1H), 3.0 (br, s, 2H), 2.1 (s, 4H), 1.9-0.49 (m, 28H). ^{13}C NMR δ 142.28, 140.56, 139.58, 136.76, 133.56, 128.50, 126.35, 124.76, 124.10, 120.09, 98.94, 67.69, 62.21, 55.69, 40.71, 31.87, 31.08, 30.049, 25.93, 24.22, 22.95, 19.87, 14.14. FTIR (KBr), cm^{-1}: 3150 (C-H stretch, aromatic), 2929 (CH_2 in-phase vibration), 2860 (CH_2 out of phase vibration), 1465 (C=C stretch, ring), 1135, 1133, 819 (C-H out of plane bending). IR (deprotected): 3458 (OH stretching), 3150 (C-H stretch, aromatic), 2929 (CH_2 in-phase vibration), 2860 (CH_2 out of phase vibration), 1465 (C=C stretch, ring), 819 (C-H out of plane bending). GPC: M_w 9395, PDI 2.36.

Poly(9,9-dihexylfluorene-alt-3-(11-(2-tetrahydropyranyloxy)undecyl)thiophene) (PFT-C_{11}THP, 17): To a degassed solution (with nitrogen) of 2,5-dibromo-3-(11-(2-tetrahydropyranyloxy)undecyl)thiophene (0.285g, 0.57 mmol), 9,9-dihexylfluorene-2,7-bis(trimethyleneborate) (0.288g, 0.57 mmol) and an 1 ml of an aqueous solution of 2.4M K_2CO_3 in THF (6 ml) was added 3 mole % of $Pd(PPh_3)_4$ (0.0199g, 0.00172 mmol) to a vial and sealed. The solution was heated for 72 hours at 40°C. The solution was then diluted with $CHCl_3$ and washed with water (two times). The organic phase was dried with $MgSO_4$ and most of the solvent was removed under reduced pressure. The remaining polymer solution (~2ml) was then precipitated into methanol to afford a yellow product. After filtration, 0.336 g (88 % yield) of polymer was obtained. Flash chromatography with $CHCl_3$ was performed to remove catalyst residues, followed by precipitation. 400MHz ^{1}H NMR, PPM (CD_2Cl_2) δ 7.9-7.5 (m, 6H), 7.3 (m, 1H),

4.5 (m, 1H), 3.8(m, 1H), 3.65 (m, 1H), 3.43 (m, 1H), 3.35 (m, 1H), 2.8 (br, s, 2H), 2.1 (s, 4H), 1.8-0.6 (m, 46H). ^{13}C NMR: 153.7, 153.1, 145.3, 144.3, 142.1, 139.8, 135.3, 130.0, 127.7, 126.3, 125.4, 123.3, 122.0, 121.6, 99.1, 42.3, 33.4, 33.0, 32.7, 31.7, 28.2, 27.5, 25.8, 24.5, 21.6, 15.7. FTIR (KBr), cm^{-1}: 3127 (C-H stretch, aromatic), 2933 (CH_2 in-phase vibration), 2860 (CH_2 out of phase vibration), 1465 (C=C stretch, ring), 1139, 1037, 823 (C-H out of plane bending). GPC: Mw 15, 395, PDI 2.21.

Poly(9,9-dihexylfluorene-alt-2-(2-thiophen-3-ethoxy)tetrahydropyran)-co-(9,9-dihexylfluorene-alt-bithiophene) (PFT-THP-HG, 18): To a degassed solution (with nitrogen) of 2,5-dibromo-3-(2-hydroxy)ethylthiophene (0.488g, 1.32 mmol), 9,9-dihexylfluorene-2,7-bis(trimethyleneborate) (0.70g, 1.39 mmol), 5,5'-dibromo-2,2'-bithiophene (0.023g, 0.07mmol) and an 3 ml of an aqueous solution of 2.4M K_2CO_3 in THF (15 ml) was added 3 mole % of $Pd(PPh_3)_4$ (0.048g, 0.00418 mmol) to a vial and sealed. The solution was heated for 72 hours at 40°C. The solution was then diluted with $CHCl_3$ and washed with water (2 times). The organic phase was dried with $MgSO_4$ and most of the solvent was removed under reduced pressure. The remaining polymer solution (~2ml) was then precipitated into methanol to afford a bright yellow product. After filtration, 0.6 g (80 % yield) of polymer was obtained. Flash chromatography with $CHCl_3$ was performed to remove catalyst residues, followed by precipitation. 400MHz ^1H NMR, PPM (CD_2Cl_2) δ 7.8-6.8 (m, 6H), 7.46 (s, 1H), 4.67 (m, 1H), 4.1 (m, 111), 3.8 (m, 2H), 3.5 (m, 1H), 3.0 (br, s, 2H), 2.1 (s, 4H), 1.9 0.49 (m, 28H). FTIR (KBr), cm^{-1}: 3102 (C-H stretch, aromatic), 2930 (CH_2 in-phase vibration), 2850 (CH_2 out of phase vibration), 1465 (C=C stretch, ring), 823 (C-H out of plane

bending). GPC: Mw 9871, PDI 3.2.

Poly(9,9-dihexylfluorene-alt-2,2'-bithiophene) (PFTT, 19): 5,5'-dibromo-2,2'-bithiophene (0.193g, 0.597mmol), 9,9-dihexylfluorene-2,7-bis(trimethylene-borate) (0.300g, 0.597mmol) and 1.38M K_2CO_3 (2ml, aqueous) were all dissolved in THF (10 ml, degassed with N_2). To this solution, 3 mole % of $Pd(PPh_3)_4$ (0.021g, 0.018mmol) was added and the glass vial was sealed. The solution was heated for 48 hours at 80°C. The solution was then diluted with $CHCl_3$ and washed with water (two times). The organic phase was dried with $MgSO_4$ and most of the solvent was removed under reduced pressure. The remaining polymer solution (~2ml) was then precipitated into methanol and produced an orange solid. After filtration, 0.431 g (72% yield) of polymer was obtained. Flash chromatography with $CHCl_3$ was performed to remove catalyst residues, followed by precipitation. 400MHz ^1H NMR, PPM (CD_2Cl_2) δ 7.8-7.6 (m, 6H), 7.45-7.2 (m, 4H), 2.1 (m, 4H), 1.7-0.5 (s, 26H). FTIR (KBr), cm^{-1}: 3120 (C-H stretch, aromatic), 2930 (CH_2 in-phase vibration), 2845 (CH_2 out of phase vibration), 1460 (C=C stretch, ring), 819 (C-H out of plane bending). GPC: Mw 16, 000, PDI: 1.61.

4.4.2 Materials

Poly(3-alkylthiophene)s (polymers **1-9,** Figure 4.1) were prepared with Grignard cross coupling methods by Dr. J. Yu, according to the general method described by McCullough et al.[2a, 9] Polymers were regio-regular, possessing at least 95% head-to-tail coupling, as determined by NMR spectroscopy. Weight average molecular weights ranged from 22,100 to 10,100 Daltons with a polydispersity (PDI) ranging from 1.39 to 1.85.

3-Bromothiophene, 3-(2-hydroxyethyl)thiophene, *N*-bromosuccinimide (NBS), 11-bromo-1-undecanol, dihydropyran, *p*-toluenesulfonic acid, tetrakis(triphenylphosphine)palladium (0) ($Pd(PPh_3)_4$), potassium carbonate (K_2CO_3) and 9,9-dihexylfluorene-2,7-bis(trimethyleneborate) were purchased from Sigma-Aldrich Canada Ltd. and used as received. Solvents (diethylether, THF, Toluene, $CHCl_3$) were distilled prior to use. 2,5-dibromo-3-hexylthiophene was synthesized according to literature procedures.[10]

PEDOT (electronic grade Baytron® P VP CH 8000) was purchased from H.C. Stark, and used as received. Indium tin oxide (ITO) coated glass was purchased from Delta technologies LTD. Electronic grade triphenyltriazene electron transport material (ETM) was provided by Dr. N.-X. Hu and J. Coggan. Cathode and encapsulation materials were electronic grade and used as received.

4.4.3 Measurements

^1H NMR and ^{13}C NMR spectra were recorded in CD_2Cl_2 on a 400 MHz Bruker AMX400 spectrometer, the chemical shifts were recorded in parts per million (ppm), referenced to CH_2Cl_2 (δ 5.36). Molecular weights were measured by gel permeation chromatography (GPC) (Waters Model 1515 isocratic pump) equipped with μ-Styragel columns against polystyrene standards. Polymers were eluted with tetrahydrofuran (THF) using a flow rate of 1mL/min and monitored UV-vis detection (Waters 2487). UV-vis absorption spectra were measured with a Cary 3E (Varian) spectrophotometer. Photoluminescence spectra were recorded with a Photon Technology International QuantumMaster model QM-1

equipped with an extra sample compartment containing an integrating sphere, which was used to measure absolute quantum yields of luminescence efficiencies (±10%) of solutions and thin films.

Solutions were de-oxygenated with high pre-purified nitrogen prior to fluorescence measurements and the sample compartment flushed with nitrogen for thin film measurements. Fluorescent spectra of thin films, spin cast from $CHCl_3$ on quartz or glass, possessed an optical density of ~0.5. Spectra were recorded 22.5° normal to the incident light. PLEDs were based on the following structure: indium-tin-oxide (ITO) anode/ polymer/ electron transport layer (~300Å Thick, 3Å/s)/ magnesium:silver alloy (9:1) cathode (~1200 Å). The polymer films were prepared by dissolving 4 mg of polymer in 0.5 mL of chloroform, filtering through a 0.2 μm Teflon filter and spin coating (2000 RPM) on an ozone pre-cleaned patterned ITO substrate. A Mg:Ag cathode was formed by co-evaporation of Mg and Ag at a rate of 4Å/s and 0.4Å/s, respectively. Deposition rates were controlled individually by quartz crystal monitors.

4.5 References

1. (a) S. Holdcroft, *Adv Mater* **2001**,*13*,1753 and references therein. (b) C. D. Müller, A. Falcou, N. Reckefuss, M. Rojahn, V. Wiederhirn, P. Rudati, H. Frohne, O. Nuyken, H. Becker, K. Meerholz, *Nature* **2003**, *421*, 829. (c) H. Sirringhaus, T. Kawase, R. H. Friend, T. Shimoda, M. Inbasekaran, W. Wu, E. P. Woo, *Science* **2000**, *290*, 2123.

2. (a) J. Yu, S. Holdcroft, *Macromolecules* **2000**, *33*, 5073. (b) J. Yu, M. Abley, C. Yang, S. Holdcroft, *Chem. Commun.* **1998**, 1503. (c) J. Yu, S. Holdcroft, *Chem. Mater.* **2002**, *14*, 3705. (d) J. Yu, S. Holdcroft, *Chem. Mater.* **2001**, *13*, 526. (e) J. Yu, S. Holdcroft, *Chem. Commun.* **2001**, 1274.

3. (a) A. Bolognesi, A. G. Schieroni, C. Botta, M. Marinelli, R. Mendichi, R. Rolandi, A. Relini, O. Inganäs, M. Theandher, *Synth. Met.* **2003**, *139*, 303. (b) A. Bolognesi, R. Mendichi, A. Schieroni, D. Villa, O. Ahumada, *Macromol. Chem. Phys.* **1997**, *198*, 3277. (c) K. A. Murray, S. C. Moratti, D. R. Baigent, N. C. Greenham, K. Pichler, A. B. Holmes, R. H. Friend, *Synth. Met.* **1995**, *69*, 395.

4. (a) B. Xu, S. Holdcroft, *Macromolecules* **1993**, *26*, 4457. (b) H. Mao, B. Xu, S. Holdcroft, *Macromolecules* **1993**, *26*, 1163.

5. Y. Li, G. Vamvounis, S. Holdcroft, *Macromolecules* **2002**, *35*, 6900.

6. S. Vaidyanathan, H. Dong, M. E. Galvin. *Synth. Met.* **2004**, *142*, 1.

7. J. K. Politis, J. C. Nemes, M. D. Curtis, *J. Am. Chem. Soc.* **2001**, *123*, 2537.

8. C. Yang, F. P. Orfino, S. Holdcroft, *Macromolecules* **1996**, *29*, 6510.

9. R. D. McCullough, R. D. Lowe, M. Jayaraman, D. L. Anderson, *J. Org. Chem.* **1993**, *58*, 904.

10. R. S. Loewe, S. M. Khersonsky, R. D. McCullough, *Adv. Mater.* **1999**, *11*, 250.

Chapter 5.

Prospective Future Projects

5.1 Controlled Nanophase Separation in Blended Films

The control of nanophase separation in conjugated polymers is an ideal attribute for many applications, including thin film transistors,[1a] solar cells[1b] and LEDs.[1c] Blending two (or more) post-functionalized 3,4-disubstituted poly(thiophene)s offers a convenient approach to produce phase separated nanostructures, since the degree of polymerization of the polymers is the same and the polymer structures are similar. This concept is illustrated in Figure 5.1, where the phase separation should incrementally increase with differences in the degree of substitution between the two polymers in the blend. That is, small differences in the degree of substitution between the polymers should result in little phase separation of the polymer blends with enhanced emission efficiency. On the other hand, greater differences in the degree of substitution between the polymers should lead to greater phase separation, and possibly greater solar cell performance. These films are currently being analyzed by atomic force microscopy at the University of South Australia by Ms. Sandra Thompson. Preliminary results show the phase separation can indeed be controlled.

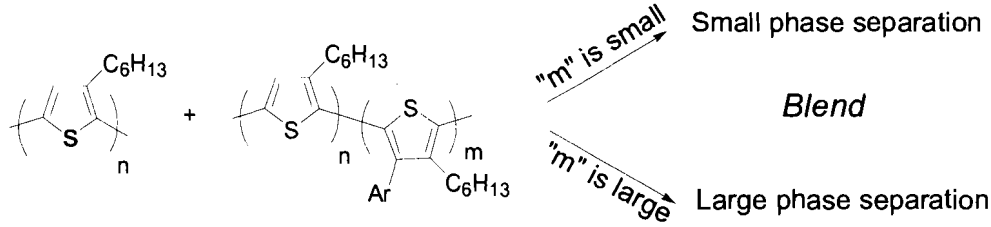

Figure 5.1: Polymer blends concept

5.2 Tetrahydropyran-Bearing Conjugated Polymers

High solid state luminescence efficiency was obtained from THP-bearing PFTs. However, spatial controlled deposition of the luminescent conjugated polymers was not obtained, probably due to small differences in solubility between the protected and the deprotected forms. Therefore, additional hydrogen bonds, after deprotection, may aid in the solubility difference. With this in mind, luminescent polymers containing THP groups on the fluorene unit is designed, which will address this theory, as illustrated in Figure 5.2.

This experiment was performed by Mrs. Xu Han, and micron resolution has been obtained.

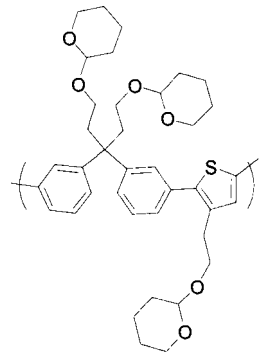

Figure 5.2: Alternating PFT decorated with tetrahydropyrans.

5.3 References

1. (a) C. D. Dimitrakopoulos, D. J. Mascaro, *Adv. Mater.* **2002**, *14*, 99. (b) J. Christoph, J. Brabec, N. S. Sariciftci, J. C. Hummelen, *Adv. Funct. Mater.* **2001**, *11*, 15. (c) L. Akcelrud, *Prog. Polym. Sci.* **2003**, *28*, 875.